Aus der Klinik für Pädiatrie mit Schwerpunkt Neurologie

der Medizinischen Fakultät Charité der Humboldt-Universität zu Berlin

Dissertation

Establishment of a two-dimensional electrophoresis map of human mitochondrial proteins

zur Erlangung des akademischen Grades

Doctor medicinae (Dr. med.)

vorgelegt der Medizinischen Fakultät Charité

der Humboldt-Universität Berlin

von

Jing XIE

geboren am 06.01.1970

aus Beijing (China)

Dekan der Medizinischen Fakultät Charité

Prof. Dr. J. W. Dudenhausen

Gutachter: 1. Prof. Dr. med. Markus Schülke-Gastenfeld

2. Prof. Dr. med. Thomas Meitinger

3. Prof. Dr. med. E. Wilichowski

DATUM DER PROMOTION: 15. 12. 2003

CONTENTS

ZUSAMMENFASSUNG

Mitochondriopathien sind Multisystemerkrankungen die durch verschiedene Defekte in den Energie (ATP) produzierenden Stoffwechselwegen der Mitochondrien verursacht sind. Will man Mitochondriopathien auf molekularer Ebene diagnostizieren, stößt man auf folgende Schwierigkeiten: (A) Ungefähr 1000 Gene sind an der Biogenese des Mitochondriums beteiligt. Die Dysfunktion jedes einzelnen dieser Gene kann potentiell zur Mitochondriopathie führen. (B) Mitochondriale Proteine werden durch zwei Genome, durch die mitochondriale und durch die nukleäre DNA kodiert. (C) Die klinischen Symptome der Patienten weisen selten auf die molekulare Diagnose, da der Phänotyp oft nur auf einem sekundären Energiemangel beruht. In der Regel besteht keine sichere Genotyp-Phänotyp-Relation.

Mit den gegenwärtig zur Verfügung stehenden Methoden lassen sich bei nur 20% der Patienten Mutationen finden. Wir wollten daher eine neue Screening-Methode entwickeln, mit deren Hilfe wir hoffen, die Aufspürungsrate für mitochondriale Mutationen zu erhöhen. Die Gesamtheit der Proteine einer Organelle oder einer ganzen Zelle (ihr "Proteom") stellt das Verbindungsglied zwischen Geno- und Phänotyp dar. Aus diesem Grunde wollten wir das mitochondriale Proteom von gesunden Kontrollpersonen und von Patienten mit Mitochondriopathien untersuchen. Protein-Muster, die zwischen diesen beiden Gruppen abweichen, könnten die Aufmerksamkeit auf Gene und Proteine richten, die an der Entstehung des Krankheits-Phänotyps beteiligt sind. Um solch eine vergleichende Studie durchzuführen, muß zunächst eine Referenzkarte des normalen mitochondrialen Proteoms erstellt werden. In meinem Dissertationsprojekt habe ich diese grundlegende Arbeit durchgeführt und zahlreiche Proteine auf der Proteomkarte menschlicher Mitochondrien identifiziert, die aus Epstein-Barr-Virus-transformierten lymphoblastoiden Zellen gewonnen worden waren. Ich wählte diese Zellsorte als Untersuchungsmaterial, da sie nicht nur einfach von Patienten gewonnen werden, sondern auch potentiell permanent wachsen kann. Dies erlaubt die Züchtung einer hohen Zellzahl ohne übermäßigen Aufwand. Ich optimierte ein Protokoll zur Zentrifugation in einem hybriden Gradienten, mit dem genug gereinigte Mitochondrien aus 10^8 Zellen gewonnen werden konnten. Für die Referenzkarte benutzte ich die lymphoblastoide Zellline einer gesunden Kontrollperson.

Die Methode der Wahl zur Proteinidentifikation in Proteom-Projekten ist die zweidimensionale Proteinelektrophorese gekoppelt mit der MALDI-TOF-Massenspektrometrie. Ich entdeckte mehr als 400 Punkte in meinem silbergefärbten zweidimensionalen Gel und analysierte die 141 stärksten Punkte nach in-gel Trypsin-Verdau

und anschließender MALDI-TOF-Massenspektrometrie in einem Verfahren, das als “Peptide Mass Fingerprinting” (Peptidmassen-Fingerabdruck) bezeichnet wird. Mit Hilfe entsprechender Datenbanken konnte ich schließlich 115 verschiedene Proteinpunkte (entsprechen 95 verschiedenen Proteinen) identifizieren. 90 dieser Punkte (entsprechend 74 verschiedenen Proteinen) waren sicher mitochondrialer Herkunft und sind Komponenten aller wesentlichen im Mitochondrium lokalisierten Stoffwechselwege. 16 der 74 identifizierten mitochondrialen Proteine gehören zur Atmungskette. Obwohl 18 mitochondriale Proteine in der Datenbank SWISS-PROT als “Membran-assoziiert” annotiert sind, identifizierte ich nur vier Proteine mit sicheren Transmembrandomänen. Ich entdeckte keine der 13 durch die mitochondriale DNA kodierten Proteine, die alle stark hydrophobe Membranproteine sind. Andere Forscher sind bei dem Versuch diese Proteine zu identifizieren, auf die gleichen Schwierigkeiten gestoßen.

Mit meiner Dissertationsarbeit habe ich unsere eigene Datenbank und Referenzkarte des mitochondrialen Proteoms lyphoblastoider Zellen erstellt. Diese Daten ermöglichen nun die Analyse des mitochondrialen Proteoms von Patienten. Meine weiteren Untersuchungen auf diesem Gebiet werden sich nun auf die genetische Variabilität des Proteoms gesunder Kontrollpersonen und auf das Proteom der Patienten mit Mitochondriopathien beziehen.

Schlüsselwörter: Mitochondrien, Proteom, Dichtegradientenzentrifugation, zweidimensionale Proteinelektrophorese, Proteinidentifikation, MALDI-TOF Massenspektrometrie, Peptidmassen-Fingerabdruck.

ABSTRACT

Mitochondrial disorders are multisystem diseases that can be caused by any defect in the energy (ATP) generating pathways in the mitochondria. The difficulty in diagnosing mitochondrial diseases on the molecular level arises from several obstacles: (A) About 1000 genes are involved in the biogenesis of mitochondria. The dysfunction of each of them may potentially cause mitochondriopathy. (B) The mitochondrial proteins are encoded by two genomes: the mitochondrial DNA and the nuclear DNA. (C) The clinical symptoms of the patients rarely suggest a molecular diagnosis since in most cases, the phenotype is a secondary phenomenon to energy depletion. Generally there is no genotype-phenotype relation.

Based on current diagnostic methods in only 20% of the patients a mutation can be found. We therefore wanted to develop a new screening method by which we hope to increase the identification rate. Since the numerous proteins of an organelle or of a whole cell (its "proteome") connect the genotype with the phenotype, we set out to study the proteome of the mitochondrion in healthy individuals and in patients with mitochondrial diseases. Deviating protein patterns between the two individuals could direct the attention to disease-specific proteins and genes, which might be involved in the expression of a disease-phenotype. In order to perform such a comparison I first had to establish a normal reference map. In my dissertation project I performed this basic task and identified numerous mitochondrial proteins on the proteome-map of human mitochondria, which had been extracted from lymphoblastoid cells. I selected Epstein-Barr-Virus-transformed lymphoblastoid cells as samples not only because they are easily obtained from patients, but also due to their potential permanent growth. This approach allows the cultivation of high cell numbers without excessive expenditure of work and cost. I optimized a protocol for hybrid gradient centrifugation, by which enough mitochondria can be purified from 10^8 cells. I used a cultured lymphoblastoid cell line from a normal control patient and isolated mitochondria from it by using hybrid gradient centrifugation. In proteomics the combination of the high-resolution two-dimensional electrophoresis and matrix assisted laser desorption/ionization–time–of–flight–mass spectrometry (MALDI-TOF-MS) is currently the method of choice for protein identification. I detected more than 400 spots in a silver-stained two-dimensional gel. I analyzed the 141 strongest spots of it by trypsin in gel digestion and subsequent MALDI-TOF mass spectrometry in a process termed "peptide mass fingerprinting". After database search, I finally identified 115 protein spots (corresponding to

95 different proteins), 90 of which (corresponding to 74 different proteins) are of confirmed mitochondrial origin. These identified proteins are components of the main biological pathways located in the mitochondrion. 16 of the 74 identified mitochondrial proteins belong to the respiratory chain. Despite the fact that 18 mitochondrial proteins are annotated in the SWISS-PROT-database as “membrane associated proteins”, only four of them have clear transmembrane domains. None of the proteins encoded by the mitochondrial DNA could be detected. All of them are hydrophobic membrane proteins. A similar difficulty in resolving these proteins was encountered by other research groups.

With my dissertation I established our own database and reference map of the mitochondrial proteome of lymphoblastoid cells. These data will facilitate the analysis of the mitochondrial proteome in patients. My future research based on this dissertation will mainly focus on the genetic variation of the proteome of healthy individuals and on patients with mitochondrial diseases.

Keywords: mitochondria, proteome, density gradient centrifugation, two-dimensional protein electrophoresis, protein identification, MALDI-TOF mass spectrometry, peptide mass fingerprinting.

LIST OF ABBREVIATIONS

A (mA)	ampère (milliampère)
ADP	adenosine diphosphate
ATP	adenosine triphosphate
bp	base pair
BSA	bovine serum albumin
°C	degree Celsius
CHAPS	3-[(3-cholamidopropyl)-dimethylammonio] -propan-sulfonate
cm	centimeter
CoA	coenzyme A
Complex I	NADH:ubiquinone oxidoreductase
Complex III	ubiquinol:cytochrome c oxidoreductase
Complex IV	cytochrome c oxidase
Complex V (F_0F_1ATPase)	adenosine triphosphate synthase
CPEO	chronic progressive external ophthalmoplegia
1D	first dimension
2D	second dimension
Da (kDa)	dalton (kilodalton)
DIDMOAD	diabetes insipidus, diabetes mellitus, optic atrophy and deafness
DMSO	dimethylsulfoxide
DNA	desoxyribonucleic acid
DTT	1,4-dithiothreitol
EBV	Epstein-Barr-virus
EDTA	ethylenediaminetetraacetic acid
EMBL	European Molecular Biology Laboratory
$FADH_2$	reduced flavin adenine dinucleotide
g (mg, ng)	gram (milligram, nanogram)
g	gravity (used in centrifugation)
h	hour
IEF	isoelectric focussing

kbp	kilobase pairs
l (ml, µl)	liter (milliliter, microliter)
LHON	Leber's hereditary optic neuropathy
M (mM)	molar (millimolar)
MALDI-TOF	matrix assisted laser desorption/ionisation – time of flight
MALDI-QTOF	matrix assisted laser desorption/ionisation – quadrupole/time of flight
MELAS	mitochondrial encephalomyopathy with lactic acidosis and stroke-like episodes
MERRF	myoclonicus epilepsy with ragged-red fibres
min	minute
MOPS	3-morpholinopropanesulfonic acid
MW	molecular weight
mtDNA	mitochondrial DNA
NADH	reduced nicotinamide adenine dinucleotide
No.	number
PDH	pyruvate dehydrogenase
PDHc	pyruvate dehydrogenase complex
pI	isoelectric point
Q_1	selection cell (in MALDI-QTOF-MS)
Q_2	collision cell (in MALDI-QTOF-MS)
RNA	ribonucleic acid
rpm	rotations per minute
rRNA	ribosomale RNA
SDH	succinate: ubiquinone oxidoreductase
SDS	sodium dodecylsulfate
SDS-PAGE	sodium dodecylsulfate-polyacrylamide gel electrophoresis
sec	second
TEMED	N,N,N',N'-tetramethylethylenediamine
TFA	trifluoroacetic acid
TIM	translocases of the inner membrane
TOM	translocases of the outer membrane
TOF	time-of-flight
Tris-base	tris(hydroxylmethyl)-amoniomethane

Tris-HCl	trizma hydrochloride
tRNA	transfer RNA
v/v	volume per volume
V (mV)	volt (millivolt)
w/v	weight per volume

LIST OF INTERNET SITES

Internet site name	Internet address
Blast 2 sequences	http://www.ncbi.nlm.nih.gov/blast/bl2seq/bl2.html
GenBank	http://www.ncbi.nlm.nih.gov/
Genome Database (GDB)	http://gdbwww.gdb.org/
Human Mitochondrial Genome Database (mtDB)	http://www.genpat.uu.se/mtDB/
Human Mitochondrial Proteins Database	http://bioinfo.nist.gov:8080/examples/servlets/Descrition.html
LocusLink	http://www.ncbi.nlm.nih.gov/LocusLink/
MASCOT	http://matrixscience.com
Mendelian Inheritance and the MITOCHONDRION (MitoDat)	http://srdata.nist.gov/mitdb/
MITOMAP	http://www.mitomap.org/
MITOP	http://mips.gsf.de/cgi-bin/proj/medgen/filter_cat.pl?h+fun
MS-Fit	http://Prospector.ucsf.edu
NCBI	http://www.ncbi.nlm.nih.gov/
Neuromuscular Disease Center	http://www.neuro.wustl.edu/neuromuscular/mitosyn.html
Online Mendelian Inheritance in Man (OMIM)	http://www.ncbi.nlm.nih.gov/omim/
PepSea	http://195.41.108.38/PepSeaIntro.html
PeptideMass	http://www.expasy.ch/tools/peptide-mass.html
PeptIdent	http://www.expasy.ch/tools/peptident.html
PeptideSearch	http://www.mann.embl-heidelberg.de/GroupPages/ Page-Link/peptidesearchpage.html
ProFound	http://129.85.19.192/profound_bin/WebProFound.exe
Protein Data Bank (PDB)	http://nist.rcsb.org/pdb/
SOSUI	http://sosui.proteome.bio.tuat.ac.jp/sosuiframe0.html
Swiss-Prot/ TrEMBL	http://www.expasy.ch/cgi-bin/sprot-search-ful

1 INTRODUCTION

1.1 Introduction to mitochondria

1.1.1 Mitochondrial morphology, biogenesis and composition

Mitochondria are essential cell organelles in the cytoplasm which have a double-membrane. They are thought to have arisen about 1.5 billion years ago and to originate from a symbiotic association between oxidative bacteria and glycolytic proto-eukaryotic cells [Margulis, 1974]. "Modern" mitochondria retain a number of features that reflect their endosymbiotic origin. These include the double membrane structure and a bacteria-like circular mitochondrial genome with mitochondria-specific transcription, translation, and protein assembly systems [Margulis, 1974; Gray *et al*., 1999; Lopez *et al*., 2002].
Mitochondria are made up of two highly specialized membrane systems. These are the inner and the outer membranes. In the center of the mitochondrion and between the membranes there are two aqueous compartments: the matrix and the inter-membrane space [Frey *et al*., 2000]. The two membrane systems contain carrier proteins and channels that regulate the exchange of substrates between the compartments. The inner membrane is especially rich in proteins, e.g. the high molecular weight multi-protein-complexes of the respiratory chain are located at the inner mitochondrial membrane. The total number of different proteins or polypeptides making up a mitochondrion is estimated to be around 1000 [Lopez *et al.*, 2002].

1.1.2 Functions of the mitochondria

Mitochondria serve many important functions for the cell. These are the oxidative ATP-production, the degradation of fatty acids, the modulation of intracellular calcium homeostasis and a major role in cell signaling and apoptosis, as well as biosynthesis (e.g. heme-groups, nucleotides, and amino acids) and degradation (e.g. urea cycle) of metabolites [Lopez *et al.*, 2002]. Below I describe the functions of the mitochondria shortly:

1.1.2.1 Oxidative phosphorylation

The oxidative phosphorylation takes place in the mitochondrion and is the main pathway of oxidative ATP-production in animals, plants and many forms of microbial life (e.g. yeast). One mole ATP hydrolyzes into one mole ADP and inorganic phosphate with concomitant release of 3054 Joules. This free energy can be made available to all cellular compartments that take up ATP. Most mammalian cells rely on the ATP produced this way for survival and anabolism [Grossman *et al.*, 1996]. The respiratory chain-oxidative phosphorylation system consists of five multi-subunit enzyme complexes [Smeitink *et al*., 2001]. Mitochondrial complexes I, III and IV function as proton pumps to generate an electro-chemical gradient across the inner membrane. This proton gradient is then utilized by the ATP-synthase (complex V) to generate ATP from ADP and inorganic phosphate.

1.1.2.2 β-Oxidation

The carnitine-dependent transport of fatty acids and their β–oxidation is another important metabolic pathway located in the mitochondrion. Most of the fatty acids to be oxidized for energy production by intra-mitochondrial β-oxidation have to be transported from the cytosol into the mitochondrion. For transport, the fatty acids are first esterified with Coenzyme A (CoA) for "activation", and are then coupled to carnitine to transverse the mitochondrial dou-

ble membrane. All enzymes of the β-oxidation are mitochondrial enzymes [Stryer, 1995; Kerner *et al.*, 2000]. Acetyl-CoA, NADH, and $FADH_2$, which are generated in each round of fatty acid oxidation, will later be channeled either into the citric acid cycle or directly into the respiratory chain to produce ATP.

1.1.2.3 Citric acid cycle

The citric acid cycle, also named the "Krebs' cycle" or "tricarboxylic acid cycle", is located in the mitochondrion too. This is the final common pathway for different metabolites such as carbohydrates, fatty acids and amino acids. The details of this cycle are shown in Fig. 1-1. The compounds with a high redox-potential [reduced nicotinamide-adenine-dinucleotide (NADH) and reduced flavin-adenine-dinucleotide ($FADH_2$)], which are generated in this cycle, are later delivered to the respiratory chain of the mitochondrion in order to generate ATP.

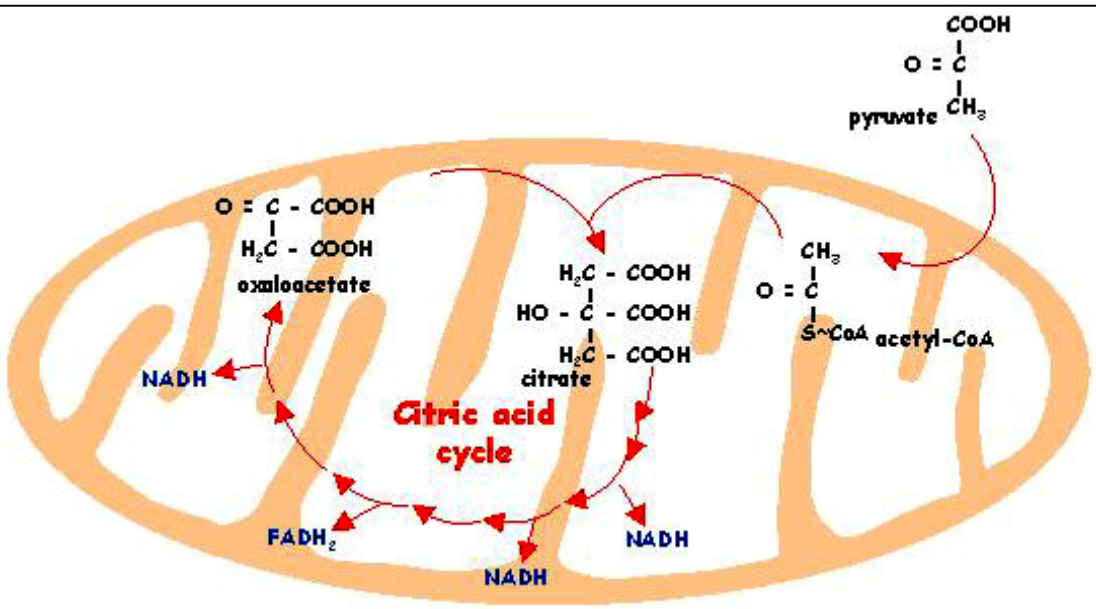

Fig. 1-1: *The citric acid cycle* is the final common pathway for the oxidation of fuel molecules. Most fuel molecules enter the cycle as acetyl-CoA. The cycle starts with the fusion of oxaloacetate and acetyl-CoA to citrate. Citrate then undergoes a series of isomerisation-, oxidation-, and decarboxylation-steps that finally regenerate oxaloacetate. The free energy of these intermittent steps is used for the reduction of three molecules NAD^+ and one molecule FAD^+. The NADH- and $FADH_2$-molecules thus generated, are subsequently delivered to the respiratory chain of the mitochondrion to generate ATP.

1.1.2.4 Urea cycle

The urea cycle has a role in the degradation of amino acids. It is partially located in the mitochondria of liver cells. In this pathway ammonia is detoxified, which is a by-product of amino acid catabolism. The cycle comprises four reactions and enzyme systems. The first reaction, the formation of citrulline from ammonia and ornithine, takes place in the matrix of the mitochondrion. Citrulline is then exported from the mitochondrion to the cytosol, where the other steps of the urea cycle take place [Krebs *et al.*, 1932; Katunuma *et al.*, 1966]. The details of this cycle are shown in Fig. 1-2.

1.1.2.5 Heme biosynthesis

Heme, which is needed as a prosthetic group in several important proteins such as hemoglobin, myoglobin and cytochrome C, is partly synthesized in the mitochondrion. The condensation of succinyl-CoA and glycine to δ–aminolevulic acid is the key-step of the heme-synthesis and takes place in the mitochondrion. δ–Aminolevulic acid is then delivered into the cytosol where coproporphyrinogen III is formed after a series of reactions. This molecule later returns into the mitochondrion to be converted into heme. The details of this process are depicted in Fig. 1-3.

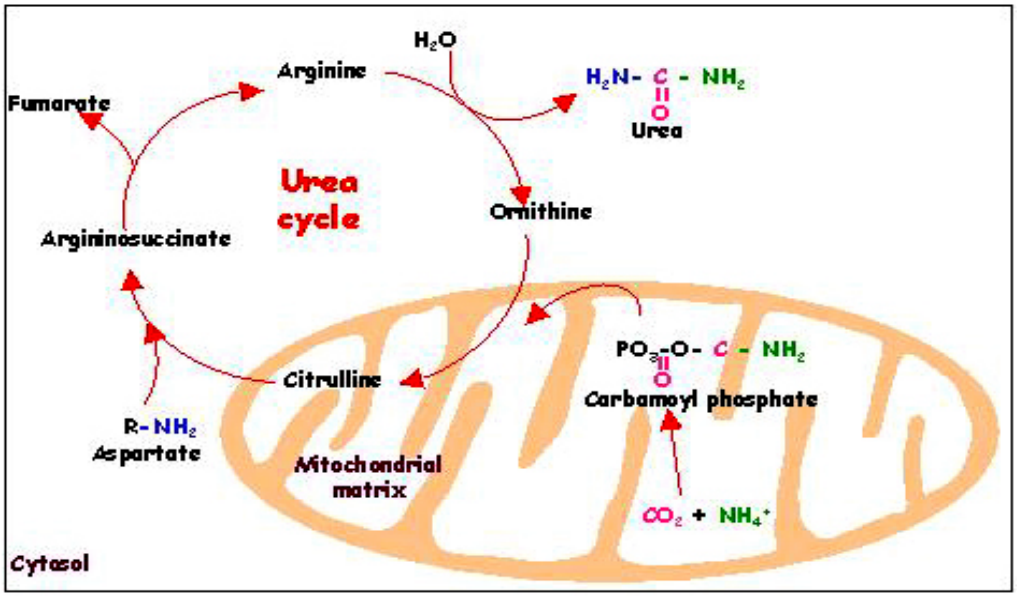

Fig. 1-2: *The urea cycle* is part of the degradation pathway of amino acids. It converts the NH_4^+ generated by amino acid degradation into urea. The first reaction of the urea cycle — the condensation of ornithine and carbamaylphosphate - takes place in the mitochondrial matrix. Citrulline is then exported into the cytosol.

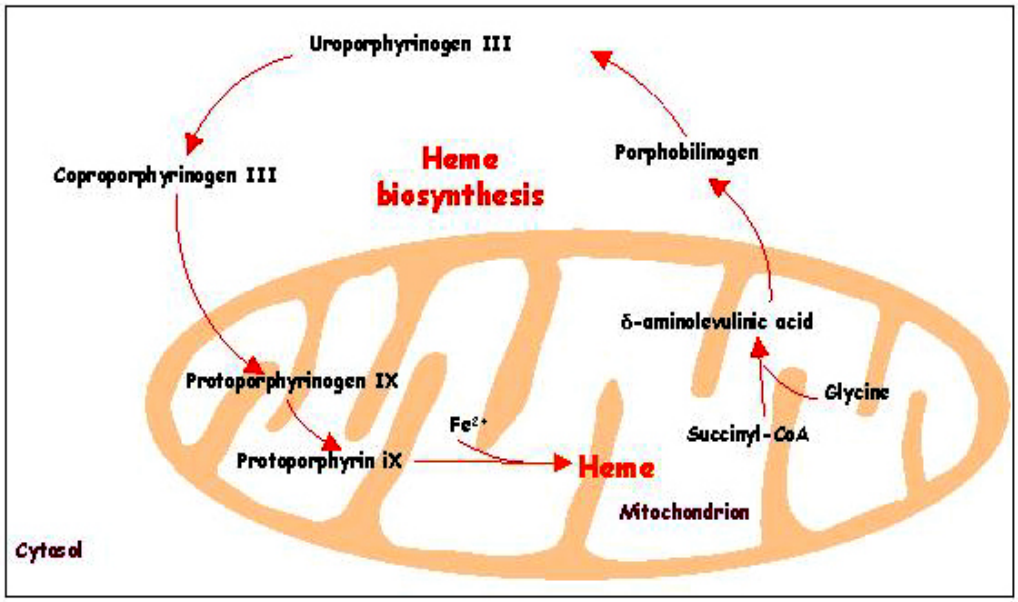

Fig. 1-3: *The heme biosynthesis* occurs partly in the mitochondrion and partly in the cytoplasm. The first step (the condensation of succinyl-CoA and glycine to δ–aminolevulic acid) and the final two steps (production of heme) take place in the mitochondrion. Most of the intermediate steps take place in the cytoplasm.

1.1.2.6 Apoptosis

In recent years mitochondria have been discovered to be able to initiate apoptosis by the release of several mediators like cytochrome c and apoptosis-inducing factor. These mediators activate the caspase family proteases which result in apoptosis [Osiewacz, 1997; Green *et al*., 1998].

Beyond that there are still other biochemical pathways located in the mitochondrion such as pathways for iron metabolism and for calcium signaling. Recent findings also indicate that mitochondria appear to be responsible for functional age-related impairments of human tissues and organs [Osiewacz, 2002] and may influence cellular mechanisms and pathways located in the cytosol such as insulin secretion [Green *et al.*, 1998].

1.1.3 Mitochondrial genetics

Each mitochondrion contains up to 10 copies of mitochondrial DNA (mtDNA). The mtDNA, which was completely sequenced in 1981 [Anderson *et al.*, 1981], is a 16.56 kbp circular and double-stranded molecule. It encodes 13 polypeptides, 12S and 16S rRNA and 22 transfer-RNAs. All of these products are essential for the formation of a functional mitochondrion. All 13 polypeptides encoded by the mtDNA are components of the respiratory chain complexes. However, the total number of polypeptide subunits of all five mitochondrial respiratory complexes exceeds 88 [Lestienne, 1992; "Neuromuscular Disease Center" (see list of internet sites)]. Four of five enzyme complexes of the respiratory chain-oxidative phosphorylation system are encoded by both the nuclear DNA and the mtDNA. Only complex II (succinate: ubiquinone oxidoreductase; SDH) is made up exclusively of four nuclear encoded polypeptides. Seven of the 43 subunits of complex I (NADH: ubiquinone oxidoreductase), one of the eleven subunits of complex III (ubiquinol: cytochrome c oxidoreductase), three subunits of 13 subunits of complex IV (cytochrome c oxidase; COX), and two membrane components of complex V (adenosine triphosphate (ATP) synthase) are encoded by the mtDNA [Pesole *et al.*, 2000].

The genetics of vertebrate mtDNA is characterized by these unique features:

- **Maternal inheritance**: This means that only the mtDNA of the oocyte can be transmitted to the offspring [Giles *et al.*, 1980]. With very rare exceptions the sperm mtDNA does not contribute to the fetus [Gustafson *et al.*, 2002].
- **Heteroplasmy and threshold effect**: The term heteroplasmy means that two populations of mtDNA - the wild type and the mutation type - coexist in an individual, in an organ or even in a single cell. Since deleterious mtDNA-mutations usually affect only parts of the mtDNA copies, the disease phenotype will only be expressed if the number of the mutant gene copies surpasses a certain threshold.
- **High mutation rate**: mtDNA is thought to be vulnerable due to its compact structure, its lack of histone protection, its insufficient repair mechanisms and its exposure to reactive oxygen species generated along the respiratory chain. This vulnerability results in a high mutation rate, about 10-20 fold higher than that of the nuclear DNA [Osiewacz, 1997; Zeviani *et al.*, 1998; DiMauro, 2000].

Therefore, in inherited mitochondrial diseases the genetic defect might reside in the mitochondrial DNA or in the nuclear DNA. For example, in the former case the inheritance pattern

is maternal, while it might be autosomal or X-chromosomal recessive or autosomal dominant in the later case.

1.1.4 Mitochondrial disorders

1.1.4.1 Definition of mitochondrial disorders

Traditionally, the term "mitochondrial disorders" describes defects in the energy-generating apparatus of the mitochondrion, i.e. the respiratory chain coupled to the oxidative phosphorylation [Bauer *et al.,* 1999]. Mitochondrial disorders comprise a heterogeneous group of clinical phenotypes, which can result from mutations in the mtDNA, the nuclear DNA or both. Abnormalities of the electron transport and the oxidative phosphorylation system are probably the most common causes of mitochondrial disorders [Schapira *et al.,* 1999]. However, mitochondrial diseases can also result from defects in metabolic pathways located only partially in the mitochondria (e.g. the pyruvate-dehydrogenase-complex deficiency). Mitochondrial disorders may manifest themselves at any time of life, from infancy to late adulthood. They may affect virtually any tissue either alone or in combination. Tissues with high energy-requirements such as heart, muscles, brain, kidney and endocrine organs are most commonly affected [Lopez, 2002].

1.1.4.2 Classification of mitochondrial disorders

The first mitochondrial disease that was understood at the molecular level was Leber's hereditary optic neuropathy (LHON) with a mutation in a mtDNA encoded subunit of complex I [Wallace *et al.,* 1988] and the Kearns-Sayre syndrome with a large deletion in the mtDNA [Holt *et al.,* 1988]. The current classification of mitochondrial disorders is based on the kind and the location of the genetic defect (mtDNA versus nuclear DNA).

1.1.4.2.1 Mutations in the mtDNA

- *Large-scale duplications or deletions of the mtDNA*: three main clinical syndromes are associated with large-scale rearrangements of the mtDNA. They are :

  Kearns-Sayre syndrome (OMIM 530000): this is a mitochondrial encephalomyopathy defined by the triad of progressive external ophthalmoplegia (PEO), pigmentary retinopathy and conduction block of the heart plus either the increase of cerebral spinal fluid protein (above 100 mg/dl) or cerebellar ataxia.

  CPEO: this is a syndrome with chronic progressive external ophthalmoplegia that manifests itself mostly in adult patients. Since the etiology is not homogenous, several gene defects could lead to CPEO, such as mtDNA-deletions (OMIM 157640) or mutations in nuclear genes [*POLG* (OMIM 174763) and *ANT1* (OMIM 103220)].

  Pearson syndrome (OMIM 557000): also termed Pearson's bone marrow-pancreas syndrome, it is a rare disorder of early infancy. It is characterized by sideroblastic anemia with pancytopenia and exocrine pancreatic insufficiency.

Additionally, large-scale rearrangements of mtDNA were occasionally reported in patients with hypoparathyroidism, growth hormone deficiency and infertility [Folgero *et al*., 1993; Wilichowski *et al.,* 1997; Boles *et al*. 1998]. Somatic mtDNA deletions have also been detected in various tumors [Polyak *et al.,* 1998; Leonard *et al.,* 2000a].

- *Point mutations of the mtDNA*: can be subdivided into missense mutations that affect **(A) the rRNA or tRNA-genes** and that **(B) one of the 13 protein-encoding genes**.

  A) tRNA- and rRNA-mutations have a global effect on mitochondrial protein synthesis. Until now, approximately 69 different mutations in 18 out of the 22 tRNA-genes of the mtDNA have been reported [MITOMAP]. Some of the mutations are associated with neurological syndromes such as the mitochondrial encephalomyopathy with lactic acidosis and stroke-like episodes (=MELAS syndrome; caused by a $tRNA^{Leu(UUR)}$ mutation; OMIM 540000) and myoclonic epilepsy with ragged-red fibres (=MERRF syndrome; caused by a $tRNA^{Lys}$ mutation; OMIM 545000). Patients with mtDNA-mutations have a wide phenotypic variability. The "classic" 3243A>G point mutation in the mitochondrial encoded $tRNA^{Leu(UUR)}$, which is known mainly as the "MELAS-mutation" might also cause other clinical symptoms such as cardiomyopathy, CPEO, myoclonic epilepsy and maternally inherited diabetes with deafness. On the other hand, the MELAS syndrome can also be caused by several other nucleotide exchanges within mitochondria encoded tRNA-genes, such as mutations at the mtDNA-nucleotides 3252, 3256, 3271, and 3291 [MITOMAP].

  B) Point-mutations of the mtDNA that affect genes which encode polypeptides. These mutations may cause:

  Leber's hereditary optic neuropathy (**LHON**; OMIM 535000): it is characterized by bilateral, acute or sub-acute loss of central vision due to optic atrophy. A total of 17 mtDNA-mutations is known to be associated with LHON [Wallace *et al.,* 1999]. However, the primary LHON mutations affect subunits of complex I.

  Neuropathy, ataxia, and retinitis pigmentosa (**NARP**; OMIM 551500): this maternally inherited, adult-onset syndrome is caused by a point mutation at position 8993 in the mtDNA-encoded ATP synthase 6 subunit gene.

1.1.4.2.2 Mutations in the nuclear DNA

The second group of mitochondrial disorders is due to mutations in nuclear genes. These mutations may affect structural subunits of the respiratory chain, their assembly, the replication of the mtDNA and the transport of polypeptides through the mitochondrial double membrane [Zeviani *et al.,* 1999; Leonard *et al*., 2000b; Sue *et al*., 2000; Orth *et al*., 2001]. These gene defects can be grouped as follows:

- *Mutations in structural genes*: The most common mitochondrial disorder of this group is **Leigh syndrome**, i.e. infantile sub-acute necrotizing encephalomyelopathy that is thought to be caused by a severe failure of energy production in the developing brain. Several different defects of mitochondrial enzyme complexes including pyruvate dehydrogenase complex (PDHc) and respiratory chain complexes I, II, IV, and V can lead to Leigh syndrome. Other diseases such as **hereditary spastic paraplegia** (progressive weakness and spasticity of the lower limbs; OMIM 602783) with mutations in the *PARAPLEGIN*-gene also fall into this group.
- *Mutation in assembly genes*: SURF1, SCO1 and 2 and COX10 are assembly proteins of complex IV [Tiranti *et al*., 1998; Petruzzella *et al*., 1998; Papadopoulou *et al*., 1999]. Mutations in these genes can lead to **Leigh syndrome** and in some cases to **hypertrophic cardiomyopathy**.
- *Mutations in genes involved in mitochondrial nucleotide metabolism*: Mutations in these genes (*ANT1*, *TP*, *TWINKLE*) disturb the mtDNA-replication leading to multiple deletions

of the mtDNA. Such patients suffer from a **mitochondrial neurogastrointestinal encephalomyopathy** (MNGIE; OMIM 603041) or the **autosomal dominant progressive external ophthalmoplegia** (adPEO; OMIM 103220).

- *Mutations in genes involved in mitochondrial iron hemostasis*: **Friedreich's ataxia**, an autosomal recessive disease with cerebral ataxia, peripheral neuropathy and hypertrophic cardiomyopathy (OMIM 229300) is due to the deficiency of frataxin, which is a mitochondrial protein functioning in the iron-metabolism. Additionally the **X-linked sideroblastic anaemia with ataxia** (OMIM 301310) that is caused by the defects of the *ABC7*-gene (ATP-binding cassette, transporter 7) also belongs to this group.
- *Mutations in transmembrane transport proteins*: The only known disease of this type is the **X-linked deafness-dystonia (Mohr-Tranebjaerg) syndrome** that is caused by a mutation of a mitochondrial protein (TIM8) that functions as a transporter for peptides through the mitochondrial double membrane.

1.1.4.3 Diagnosis of mitochondrial disorders

The diagnosis of mitochondrial disorders has to rely on the sum of clinical, morphological, biochemical, and molecular genetic investigations since there is no explicit relation between genotype and phenotype. Atypical clinical pictures can be observed quite frequently in mitochondrial disorders. With the exception of typical syndromes like MELAS or MERRF, histological studies of muscle biopsy specimens are usually recommended in suspected cases. Characteristic changes include the presence of paracrystalline mitochondrial inclusions, mitochondria with abnormal size and shape, ragged-red-fibres (RRFs) in muscle, fat deposits and histochemically focal enzyme deficiencies (e.g. patchy COX-deficiency or SDH-deficiency) [Zeviani *et al.,* 1998; Parker, 2000]. In most cases, however, biochemical analysis have to be performed in order to formulate a diagnosis [Letellier *et al.*, 2000]. Using enzymatic tests, the activities of pyruvate dehydrogenase complex (PDHc), carnitine-palmitoyl-transferase and all complexes of the respiratory chain-oxidative phosphorylation system can be determined in muscle homogenate. Single enzyme activities can also be measured in cultured fibroblasts and in blood cells (lymphocytes and platelets). But only the molecular genetic analysis can verify the diagnosis of a mitochondrial disorder. In the case of a maternal inheritance pattern the investigations will focus on the analysis of the mtDNA. Otherwise, the biochemical results may narrow possible candidate genes to screen for mutations. For example, in the case of an isolated complex I deficiency, one would at first sequence the structural subunits of complex I in which mutations have been described before.

1.1.5 Characteristics of mitochondrial proteins and preproteins

It is estimated that the mitochondrial proteome consists of approximately 1000 distinct proteins [Lopez *et al.,* 2002]. With the exception of 13 proteins, which are encoded by the mtDNA, most mitochondrial proteins are encoded by nuclear genes, including most of the mitochondrial OXPHOS proteins, the metabolic enzymes, the DNA and RNA polymerases, the ribosomal proteins, and the mtDNA regulatory factors [Grivell *et al.*, 1988; Wallace, 1999]. These proteins are synthesized at the encoplasmatic reticulum and are later imported into the mitochondrion. Fig. 1-4 depicts this principle of the transportation of the preproteins through the double membrane. Before being transported into the mitochondrion, proteins are synthesized as preproteins, i.e. precursors that contain transit sequences either as amino-terminal targeting pre-sequences, or as targeting and sorting information sequences within the mature proteins. The cytosolic preproteins are imported through the translocases of the outer membrane (TOM) when their targeting information is recognized by the receptors of TOM. They are then sorted either directly to the outer membrane, the inter-membrane space or to the

translocases of the inner-membrane (TIM). Preproteins with a typical amino-terminal targeting sequence engage the TIM17/TIM23 complex that guides preproteins into the matrix. In the matrix the targeting sequences are removed by the matrix-processing-protease, and the remaining polypeptide chains are folded by chaperones into mature proteins. Preproteins, which lack a targeting sequence, engage with the TIM22 complex to be inserted into the inner membrane [Millar *et al.*, 1994; Shore *et al.*, 1995; Hanson *et al.*, 1996; Koehler, 2000].

1.2 Proteome analysis

1.2.1 Definition of proteome analysis

The term “proteome” was first advocated by Marc Wilkins in 1996 as a linguistic equivalent to “genome” which indicates all chromosomes and their genes of any cell type of a given organism. The proteome was defined as the entire protein complement expressed by a cell type, tissue or an organism [Wilkins *et al.*, 1996]. Genome research usually refers to sequencing the total genomic DNA of an organism and mapping all genes within these sequences. In contrast, the aim of proteome research focuses on the structural and functional analysis of the proteome and the interaction of proteins with one another. This includes the isolation, identification and characterization of all proteins encoded by the genome of an organism.

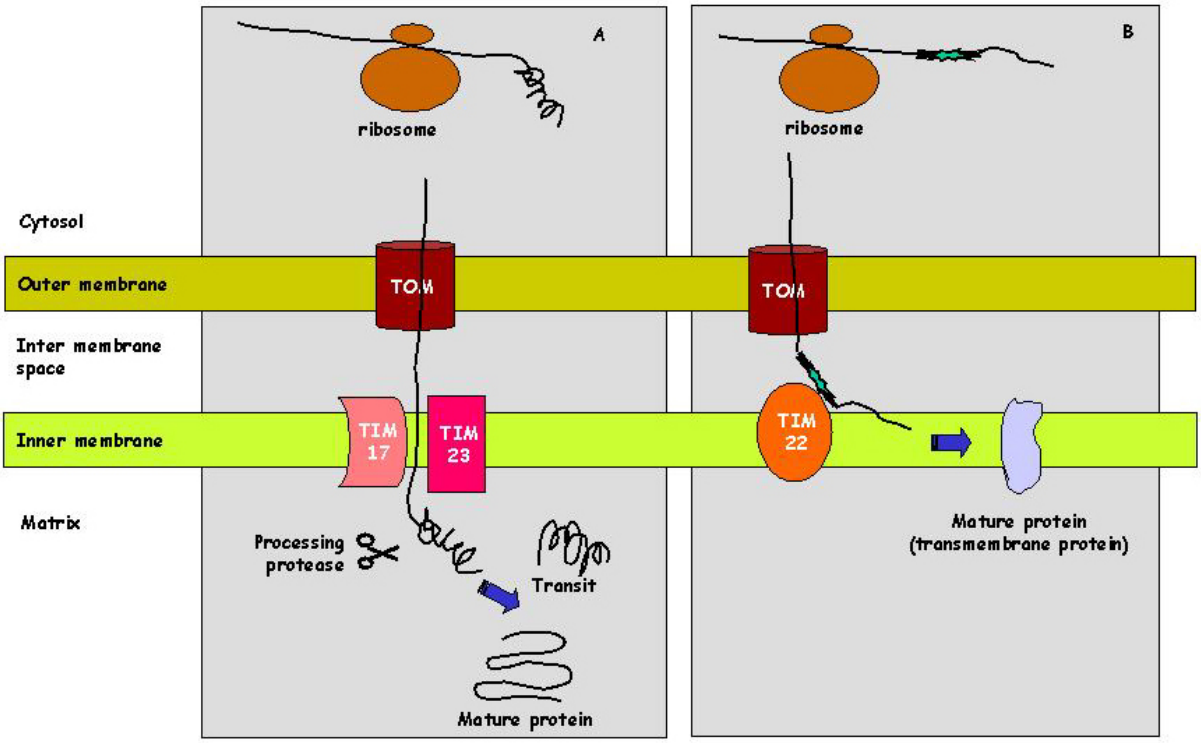

Fig. 1-4: *Preprotein import pathways into the mitochondrion*. Before being transported into the mitochondrion, proteins are synthesized as preproteins in the cytosol. They are then imported through the translocases of the outer membrane (TOM). Preproteins with a typical amino-terminal targeting sequence engage with the inner-membrane (TIM) complex 17+23 (pathway A) to be imported into the matrix. In the matrix the targeting sequences are removed by the matrix-processing protease to form the mature proteins. Preproteins, which lack a targeting sequence, engage with the TIM22 complex (pathway B) to be inserted into the inner membrane.

Proteome analysis could lead the way to explain the function of an organism dynamically rather than statically. This is important since the protein compositions and concentrations change from cell type to cell type, even within sub-cellular compartments. Moreover, they

also differ between various stages of development [Abbott, 1999]. Proteome analysis can also offer the opportunity to examine entire pathways, or multiple enzymatic pathways simultaneously [Lopez *et al.*, 2000]. High throughput two-dimensional protein electrophoresis [Klose, 1975; O'Farrell, 1975] coupled with peptide mass fingerprinting analysis by MALDI-TOF mass spectrometry [Karas *et al.*, 1988] have become the most powerful techniques for proteome analysis.

1.2.2 Previous work on the proteome

Using two-dimensional protein electrophoresis in order to establish a whole proteome map was first done by Boucherie *et al*. (1995) in yeast. The work was extended in 1999 [Perrot *et al*., 1999]. They identified more than 400 proteins on their reference proteome map. Similar results have been reported by Garrels *et al.* (1997), Shevchenko *et al.* (1996b) and Maillet *et al.* (1996). Lopez *et al.* (2000) established a 2D-electrophoresis map of the mitochondrial proteome of rat liver that included ca. 70 proteins by using high–throughput automated equipment in combination with mini-spin affinity columns. Analysis of the human mitochondrial proteome has first been done by Rabilloud *et al.* (1998). They investigated human mitochondrial proteins from placenta using 2D-electrophoresis and MALDI-TOF mass spectrometry, complemented by protein sequencing and immunodetection. They detected ca. 1500 spots on a silver-stained reference gel and finally identified 46 proteins [Rabilloud *et al.*, 1998]. Most recently, Fountoulakis *et al.* (2003) identified approximately 185 different proteins in mitochondria isolated from a cultured neuroblastoma cell line (IMR-32) using similar methods.

1.3 The aim of my study

Despite the advent of high throughput sequencing, with the exception of typical syndromes like MELAS, MERRF and LHON, most cases of mitochondrial diseases are difficult to diagnose on the molecular level.

The difficulties in making a molecular diagnosis are:

- **Pleiotropy**: Mutations in one gene cause different phenotypes.
- **Heterogenity**: Mutations in different genes cause similar phenotypes. Often there is no fixed relationship between genotype and phenotype.
- **Two sources of encoding genes**: The gene defect may reside in two different genomes, the nuclear and the mitochondrial genome.
- **Genetic variability**: Any dysfunction of about 1000 different gene products located in the mitochondrion can potentially lead to mitochondrial diseases.
- **Neutral polymorphisms**: The high mutation rate of the mtDNA causes large numbers of neutral changes without pathogenic significance (polymorphisms). The high number of these polymorphisms complicates the work of genetic analysis.

Until now less than 20% of mitochondrial diseases can be diagnosed on the molecular level. Therefore, new tools should be established in order to increase the identification rate of mitochondrial diseases. Since the proteome bridges the genotype with the phenotype, we hypothesize that mutations in mitochondrial genes encoded by the mtDNA or nuclear DNA cause changes on the proteome level. These changes might be primary (e.g. a mutated protein is absent or has different running characteristics) or secondary (e.g. other proteins that are up- or down-regulated to compensate for a mutated protein).

However, to lay a basis for these proteome analyses we first have to establish what is “normal”. Furthermore we have to choose a model system that guaranties purification of a sufficient amount of mitochondria from patients.

Since lymphocytes generally express the functional defects of mitochondrial enzymes, we chose to work on immortalized lymphoblastoid cell lines since they can be cultivated permanently in order get sufficient material for analysis.

The aim of the present study is to establish a method to purify mitochondria from as little as possible patient material (cultured lymphoblastoid cells) and to establish a reference map for the mitochondrial proteome of lymphoblastoid cells.

The reference map and database can be later used to compare deviating protein patterns between healthy and diseased individuals. This might direct the attention to disease-specific proteins and genes and open new ways to diagnose mitochondrial diseases on proteome level or with a combined genetic-proteomic approach.

2 THEORY OF EMPLOYED METHODS

2.1 Mitochondrial isolation

In order to study mitochondrial proteins, mitochondria have to be isolated first and purified from proteins of other cell compartments. Such a sub-fractionation allows the detection of those proteins which would be invisible in total cell lysates for their low-abundance [Lopez *et al.,* 2000]. We selected Epstein-Barr-Virus (EBV) transformed lymphoblastoid cell line samples because they have several advantages compared to other biopsy specimens: they are easily obtained from patients and can grow permanently in liquid, non-adherent cell cultures. This allows the cultivation of large cell numbers without excessive work.

The initial step in purifying mitochondria is to rupture the cell membrane. There are various methods to disrupt cells in order to release their mitochondria. They can be ground, subjected to osmotic shock or to ultrasonic vibration or they can be forced through a small orifice. There are two "classic" methods for mitochondrial isolation:

- **Nitrogen cavitation:** this method is based on the increased solubility of nitrogen in water under high pressure and its abrupt reversal after pressure release. Under high pressure, nitrogen penetrates quickly though the cell membranes into the cytoplasm and cell organelles. When the pressure is released quickly, nitrogen bubbles form, thus disrupting the cell membrane. Nitrogen cavitation is a gentle method for cell disruption without shearing. This allows efficient recovery of intact mitochondria [Gottlieb *et al.,* 2000]. However, the high cost for the equipment and varying results from one experiment to another limit its use.

- **Potter-Elvehjem glass-Teflon pestle homogenizer:** this is a method that disrupts cells mechanically using a motor-driven teflon pestle within a tightly fitted glass-tube [Alberts *et al.*, 1994]. The shearing forces between the glass wall of the tube and the pestle disrupt the cells. However, if this is done too often or using a too tightly fitted pestle, the mitochondria might be disrupted as well. Therefore, an optimum has to be established in regard to the type of cells, type of pestle and number of repetitive homogenizing cycles. The results of the disruption (e.g. the intactness of the mitochondria) should be checked by electron microscopy.

The second step of mitochondrial isolation is to retrieve mitochondria from the mixture of subcellular components. Both differential-velocity centrifugation and density-gradient centrifugation are commonly used for this purpose.

- **Differential-velocity centrifugation:** the different sedimentation rates of various cellular components make it possible to separate them by (ultra)-centrifugation in a sucrose solution. "Classic" cell sub-fractionation yields four major fractions: the nuclear, the mitochondrial, the microsomal (i.e. endoplasmatic reticulum, Golgi-apparatus, plasma membrane) and the cytosolic fraction [de Duve *et al.*, 1955]. The nuclei can be pelleted at low speed centrifugation (1000 g), the mitochondria at medium speed (20,000 g), the microsomal fraction at high speed (100,000 g), and the ribosomes at very high speed (150,000 g) [Almeida *et al.*, 1997; Martin *et al.*, 1998; Harvey *et al.*, 1999]. This method, however, does not yield totally pure organelle fractions. Therefore, it is coupled to a second purification step by equilibrium density-gradient centrifugation.

- **Density gradient centrifugation:** this method separates cellular components according to their density. The impure organelle fraction is layered on top of a gradient solution and then centrifuged for a determined time to allow each particle to migrate to an equilibrium position where the density of the surrounding liquid is equal to the density of the particle. The commonly used density gradients can be grouped as continuous and discontinuous density gradients. Typical continuous gradients are made of sucrose, glycerol or Percoll medium [Sims, 1990; Roberti *et al.*, 1997]. The discontinuous gradients are poured as discontinuous Percoll gradients [Rajapakse *et al*., 2001] or as Percoll/metrizamide hybrid gradients [Madden *et al.*, 1987; Strack *et al.*, 2001] in order to separate mitochondria from other organelles by accumulating them at a certain inter-phase after centrifugation.

2.2 Determination of the protein concentration

Mitochondrial proteins can be separated into two main groups [Klose, 1999a]: the *hydrophilic proteins* including the proteins of the matrix and of the inter-membrane space; the *hydrophobic proteins* such as transmembrane proteins of the inner- and outer-membrane. Since only proteins in solution can be analyzed, several detergents and ultrasonication are used to solubilize the hydrophobic (membrane) proteins [Harvey *et al.*, 1999].
To measure the total protein content of a sample, several protein assay methods are routinely used.

- **Lowry protein assay**: The most commonly used one is the Lowry protein assay and its modified protocols [Lowry *et al.*, 1951]. The method is based on the characteristics of the Folin phenol reagent, which changes color when it is reduced. However, the Lowry procedure is less preferable than other methods since it is subjected to more interference by a wide variety of chemicals and even proteins.
- **Bradford protein assay**: An accurate alternative is the Bradford assay that is based on the specific binding of Coomassie blue G-250 dye to proteins. Coomassie blue G-250 absorbs light at a wavelength of λ=595 nm. The protein concentration of the sample can thus be determined photometrically by comparing its absorption to a series of protein standards known to exhibit a reproducible linear absorption profile. Bovine serum albumin (BSA) or immunoglobulin G (IgG) are the most commonly used standard proteins [Bradford, 1976; Stoscheck, 1990].
- **Bicinchoninic acid (BCA) protein assay**: In recent years a modification of the Bradford assay is used widely that uses bicinchoninic acid (BCA) instead of Coomassie blue G-250 for the colorimetric detection. In alkaline medium Cu^{2+} is reduced to Cu^{+} by proteins. The Cu^{+}-ions can be detected colorimetrically with high sensitivity and selectivity by a reagent containing BCA. The purple-colored reaction product exhibits a strong absorption at λ=562 nm that is linear with the protein concentration [Smith *et al.*, 1985].

2.3 Two-dimensional electrophoresis techniques

Methodical approaches to separate proteins electrophoretically by two different principles in order to improve resolution can be traced back to 1956 when Smithies and Poulik developed a two-dimensional (2D) electrophoresis technique combining filter paper electrophoresis (first dimension) and starch gel electrophoresis (second dimension) [Smithies *et al.*, 1956]. In the following years, a number of other 2D-electrophoresis methods were developed by combining various electrophoretic techniques. The current modern 2D-electrophoresis technique was developed independently by Klose (1975) and O'Farrell (1975). They combined isoelectric focussing (first dimension) with SDS-polyacrylamide gel electrophoresis (second dimension). This method separates proteins firstly according to their isoelectric points (*pI*) and secondly according to their molecular weights (*MW*). Each protein can then be attributed a *pI* and a

MW. The 2D-electrophoresis method allows the visualization of thousands of protein-spots at a time, even up to total of 10,000-15,000 protein spots in a single large gel [Klose *et al.*, 1995]. Fig. 2-1 shows the principle of the 2D-electrophoresis method.

2.3.1 First dimension: isoelectric focussing

Through isoelectric focussing (IEF) proteins are separated according to their isoelectric points (*pI*). The *pI* depicts the pH-value at which the net charge of the protein is zero. The mobility of a protein in an electric field depends on the sum of its positive and negative charges. When the net charge of the protein is zero, the protein stops migrating in the electric field. It focusses where the pH of the gel equals the *pI* of the protein. A pH gradient can be established by adding a mixture of ampholytes with different isoelectric points to a polyacrylamide gel. The protein mixture can then be loaded either on the anodic or on the cathodic end of the gel. Since some very basic proteins may not migrate into the gel if the proteins were loaded on the cathodic end of the gel, we choose to load our samples on the acid side of the IEF-gel [Klose, 1975, 1995].

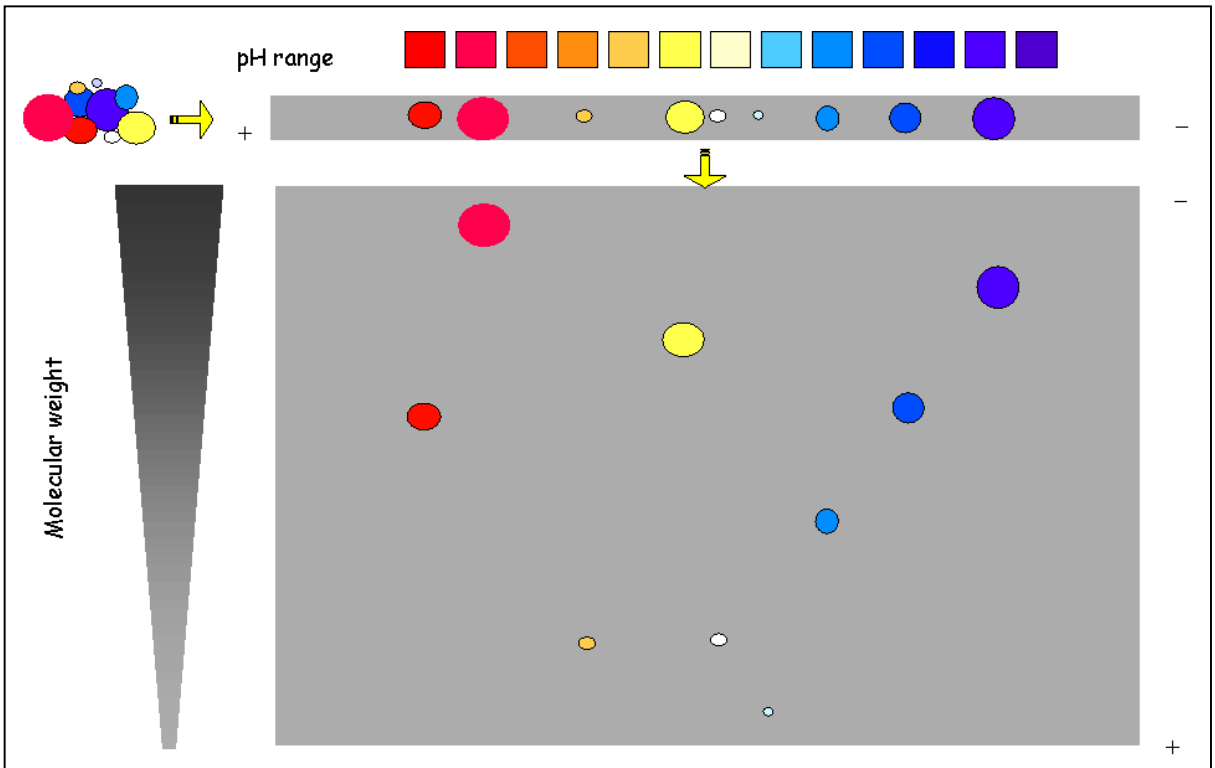

Fig. 2-1: *Principle of 2D-electrophoresis*. In 2D-electrophoresis a complex protein mixture can be separated by two biochemical principles. In the first dimension isoelectric focussing (IEF) the proteins are separated according to their isoelectric points (*pI*), e.g. proteins run in an electric field as long as the surrounding pH differs from their *pI*. If they reach their *pI*, their net charge is zero and they stop running in the electric field. In the second dimension, proteins are separated according to their molecular weights (*MW*) in a SDS-polyacrylamide gel.

2.3.2 Second dimension: sodium dodecylsulfate (SDS)-polyacrylamide gel electrophoresis

The SDS-polyacrylamide gel electrophoresis (SDS-PAGE) utilizes SDS as an anionic detergent. SDS forms complexes with proteins and dissociates them into their individual subunits. This combination leads to two results: the ratio of SDS/protein remains sufficiently constant

(1.4 g SDS per gram protein). Thus the complexes have a high anionic charge density which is much higher than the charge density of an individual protein. Therefore the charge difference between proteins can be ignored. Due to the same charge/protein ratio at pH 8.4, all SDS-protein complexes migrate to the cathode if an electrical field is applied. Secondly, since all SDS-protein complexes have a similar cylindrical form with a constant diameter (about 1.8 nm) but different lengths, the sizes of the proteins are directly proportional to their molecular weights. Thus the electrophoretic mobility of the SDS-protein complexes depends only on their molecular weight, i.e. the mobility of the proteins is little influenced by any individual protein feature such as charge or conformation [Weber *et al.*, 1969; Laemmli, 1970].

2.3.3 Staining

To visualize the protein spots on the gel, the gel has to be stained. If the protein abundance is high (i.e. more than 100 ng), the gel can be dyed with Coomassie brilliant blue. For the detection of lesser protein amounts different silver staining protocols have been developed [Rabilloud, 1990 and 1992; Swain *et al.*, 1995; Klose *et al.*, 1995]. Compared to the commonly used Coomassie brilliant blue staining, silver staining is more sensitive and has an improved detection limit of 1-10 ng. Moreover, the sensitivity of silver staining can be improved further by the use of several sensitizers. These sensitizers act via different chemical mechanisms: increasing the binding of silver (sulfosalicylic acid), creating latent images of spots by precipitation of micro-granules of silver sulfide (sodium thiosulfate, dithiothreitol), promoting silver reduction (glutaraldehyde) and complexing free unbound silver cations (chelators). On the other hand, the silver staining techniques treat proteins with the strong oxidizing agent Ag^+ that may cause oxidative damage to the proteins. This can lead to chemical modification or destruction, and subsequent protein microanalysis will be rendered impossible. Several sensitizing pre-treatments of the gel with glutaraldehyde, chromic acid, sodium thiosulfate or thimerosal could even result in covalent modifications of the proteins. Shevchenko *et al.* (1996a) have tried to solve this problem by modifying the ”classic” silver-staining protocols. They omitted the fixation and sensitization treatment with glutaraldehyde that is known to attach covalently to the protein through Schiff base formation with the α- and ε-amino groups. Additionally they carried out the silver nitrate treatment at 4°C in order to minimize oxidation.

2.3.4 Reproducibility

Reproducibility means that if the same sample is run on two or more different two-dimensional gels, each spot on one gel must have its corresponding spot on another gel. Reproducibility is influenced by many factors ranging from sample preparation, stability of electrophoresis conditions and temperature to gel staining and drying [Klose, 1975; O’Farrell, 1975]. Occasionally, some single spots can change their positions within well-reproduced patterns. This phenomenon can be caused by some proteins with specific variable sensitive properties. The problem may be solved by using optimum conditions, i.e. running the same sample twice, side by side and by using the same batches of solutions at each step [Klose, 1995]. The reproducibility of the 2D-electrophoresis is reliable enough that it can be used to detect genetic variations by demonstrating the qualitative and quantitative changes of protein spots [Klose, 1995; Klose *et al.*, 2002].

2.4 Protein identification methods

In order to connect the information from proteome analysis to the corresponding genes, it is necessary to identify the protein spots. Mass spectrometry is becoming more and more impor-

tant in the field of protein analysis. It is proving useful for identification of proteins separated by two-dimensional protein electrophoresis. The particular advantage of mass spectrometry is that it generally requires a limited amount of material. Sometimes even femtomoles are sufficient [Perrot *et al.*, 1999]. The most commonly used technique for protein identification by mass spectrometry is called "peptide mass fingerprinting". This involves the generation of peptides from a protein by a proteolytic enzyme such as trypsin. The masses of the ensuing peptides are determined by mass-spectrometry and are matched against a theoretical list of peptide fragments calculated from databases of known protein sequences [Pennisi, 1997; ExPaSy database]. As peptide mass fingerprinting has a higher sample throughput than amino acid sequencing, it is especially suitable for rapid protein identification. (Fig 2-2)

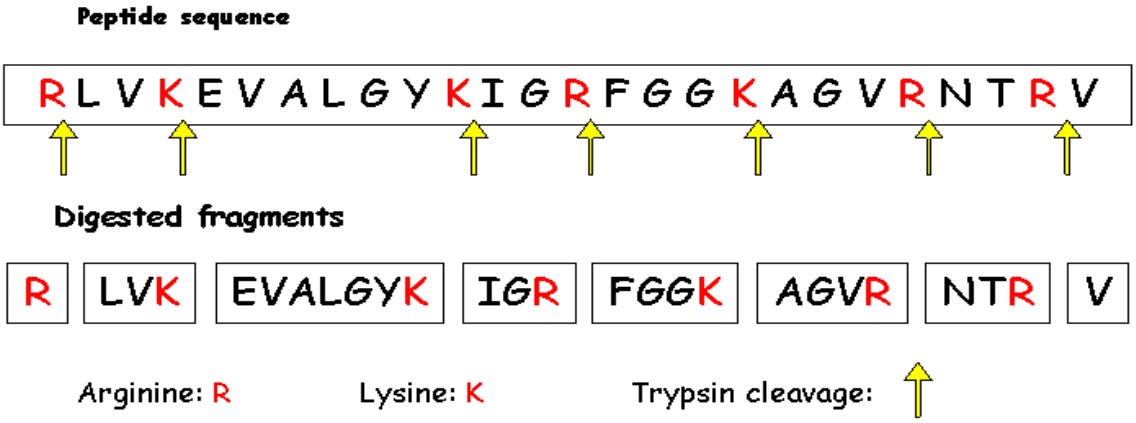

Fig. 2-2*: Principle of peptide mass fingerprinting by trypsin digestion.* Trypsin cleaves at the carboxylic side of arginine and lysine residues. The sizes of the peptide fragments obtained after trypsin digestion, represent the peptide mass fingerprint and are characteristics of each protein.

2.4.1 Matrix-assisted laser desorption/ionization time-of-flight mass spectrometry

Peptide mass fingerprinting by matrix-assisted laser desorption/ionization time-of-flight (MALDI-TOF) mass spectrometry is one tool for protein identification [Fernandez *et al.*, 1998]. The principle of this technique is depicted in Fig. 2-3. After in-gel digestion, the protein is cut into several peptide fragments by proteases, such as trypsin or chymotrypsin. This peptide-mixture is mixed with a matrix of 2,5-dihydroxybenzoic acid or α-cyano-4-hydroxycinnamic acid and is let to crystallize. Subsequently the surface of the peptide/matrix mixture is evaporated and ionized by the photons of a high-energy laser beam. The ions are then accelerated in an electric field and fly towards a target. The speed and therefore the time of flight depends on the mass/charge ratio. The time of flight can thus be used to exactly measure the molecular weight of each peptide fragment up to the precision of 0.1 Dalton. At first this method was a rather unspecific identification tool but rapidly improved with the advent of machines that were able to measure also high molecular weight fragments with sufficient accuracy. New matrix preparations and higher sensitivity led to higher sequence coverage [Fernandez *et al.*, 1998]. In favorable cases a mass coverage of over 90% of the peptide fragments can be achieved. The high accuracy in mass determination is made possible by the "delayed extraction" method [Jensen *et al.*, 1996]. Until now, bio-macromolecules with molecular masses up to 300 kDa can be identified by peptide mass fingerprinting [Nielsen *et al.*, 2002]. This technique has been developed to an extent that high throughput analyses are possible, and it has a firm place for protein identification in proteomic projects (see section 2.4.3).

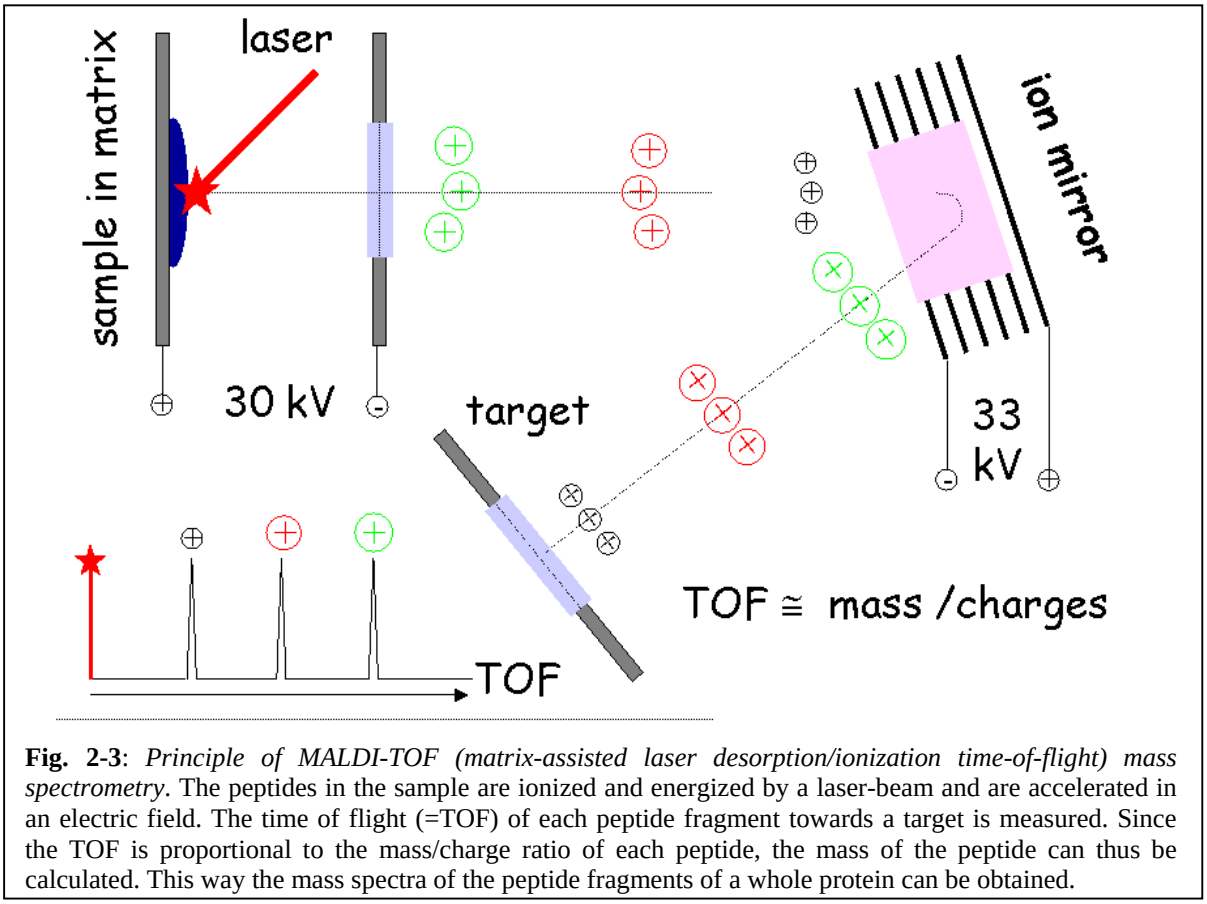

Fig. 2-3: *Principle of MALDI-TOF (matrix-assisted laser desorption/ionization time-of-flight) mass spectrometry*. The peptides in the sample are ionized and energized by a laser-beam and are accelerated in an electric field. The time of flight (=TOF) of each peptide fragment towards a target is measured. Since the TOF is proportional to the mass/charge ratio of each peptide, the mass of the peptide can thus be calculated. This way the mass spectra of the peptide fragments of a whole protein can be obtained.

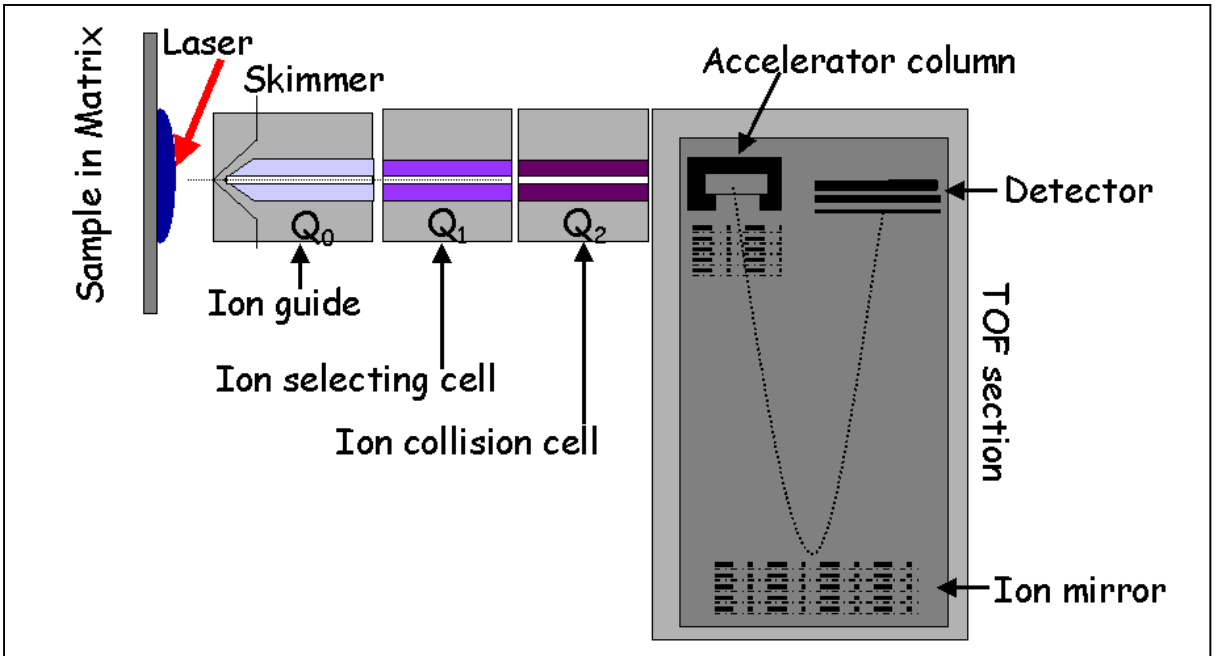

Fig. 2-4: *Principle of MALDI-QTOF (quadrupole time-of-flight) tandem mass spectrometry*. The sample is ionized and energized by a laser-beam and flies into a quadrupole ion guiding cell (Q_0), where the ions are focussed and cooled. Then a peptide of interest (the parent ion) is selected at the quadrupole Q_1-cell and guided into the quadrupole collision cell (Q_2). There the parent ion collides with argon atoms and splits into daughter-ions. The masses of these daughter ions are then measured via TOF mass spectrometry.

2.4.2 Peptide sequencing by MALDI-quadrupole time-of-flight tandem mass spectrometry

The peptide mass data from MALDI-TOF mass spectrometry were used for database searches in order to identify the target protein by peptide mass fingerprinting. Sometimes no positive hit was found or the result did not satisfy the specified stringency criteria, which usually required more than four matched peptides at an accuracy of 0.1 Da. In this case, the peptide sequence of one or two abundant fragments was be determined directly by MALDI-QTOF tandem mass spectrometry. The full amino acid sequence of a peptide provides much more accurate information for further protein identification. It can also be used to confirm the results gained from peptide mass fingerprinting. MALDI-QTOF tandem mass spectrometry uses the MALDI ion source. The quadrupole filters peptides within a selected size range that are later guided into a collision cell to be broken into smaller fragments. The masses of these overlapping fragments are then analyzed by time-of-flight mass spectrometry (Fig. 2-4). Although this method is more complicated to perform, the results are more reliable than peptide mass fingerprinting because the sequence information of one or two peptides usually identifies the protein with high accuracy. Before the analysis with MALDI-QTOF mass spectrometry samples have to be purified by nano-scale reversed chromatography. This procedure removes salts and small chemical compounds of the buffer and thus reduces the chemical noise of the spectra and improves the sensitivity (Annan *et al*., 1996; Gobom *et al*., 2001).

2.4.3 Database search based on peptide mass fingerprint spectra

The obtained spectra of peptide masses are analyzed further by searching though different databases to find the corresponding protein. Each protein in the databases can be "digested in silico" by trypsin and thus provides a theoretical spectrum of its peptide masses. Comparing the experimental with the bioinformatic data, several candidate proteins with high probability scores can be identified. This task can be performed with the help of several search engines on the internet: MASCOT, ProFound, MS-Fit, PeptIdent, PeptideSearch, and PepSea (see "The list of internet sites").

Before the search, several parameters have to be set. These include the taxonomy of the specimen, the used protease and the number of accepted missed cleavages, the peptide mass states (usually the monoisotopic mass), the mass deviation tolerance, and possible modifications. Peptide modifications are important since they influence the peptide masses and might be introduced artificially in the preparation process (e.g. oxidation of methionine-residues). The oxidation of an amino acid (e.g. methonine) in a polypeptide increases its mass by 18 Da. The number of 18 Da deviations should therefore correspond to the number of methionine residues in a certain peptide. On the other hand, this "artifact" may serve as a second independent verification of the identity of a peptide. The search engine gives out a list of best matching proteins.

In general not all peptide masses in the spectra can be matched to the theoretical digestion of a protein. However, the larger the sequence to be covered by the fragments, the more statistically probable the result will be. Deviations between the theoretical peptide mass fingerprint and the experimental one might be due to the following reasons:

- Although several detergents like SDS have already denatured the proteins, any still existing secondary structures would hamper the enzyme to recognize a certain cleavage site. This results in the increase of the number of missed cleavages.

- Any kind of modification would cause a deviation of peptide mass. More than 300 different modification artifacts may be introduced during the whole procedure from protein extraction to identification. The modification of cysteine by acrylamide and the oxidation of methionine are the most frequent modifications. Because of the high reactivity of the sulfhydryl group of cysteine, it would usually combine with the unpolymerized acrylamide during the 2D-electrophoresis. The oxidation of methionine results from its easily reducible sulfhydryl side chain.
- The masses of the peptides are best calculated by using the monoisotopic peak of an internal calibration marker such as the auto-digestion product of bovine trypsin (residues 50-69, $M+H^+$ = 2163.06 Da) and the matrix trimer ion ($3M+H^+$ = 568.14 Da). The readouts of the mass values are sensitively affected by the shape of the peak that depends on the mass/charge ratio (m/z) and the strength of the reflecting electric field. This electric field has a role to focus the molecules of the same mass in order to generate a slim peak. For larger peptides, however, the peak shape of the mass spectrum usually becomes broadened by unsatisfactory focussing. This might lead to false mass calculations. The use of sodium-containing buffers can also lead to broadened peak shapes since the molecule-ion of $(M+Na)^+$ instead of $(M+H)^+$ can be detected wrongly. This would cause an increase of the m/z value.
- If two protein spots lie very close to or overlap each other in the 2D-electrophoresis gel, the overlay of two mass-spectra might disturb the correct identification of the single protein.

Sometimes several less stringent criteria, such as more than one allowed missed cleavage, several kinds of possible modifications, larger mass deviation tolerances have to be granted in order to match the experimental peptide mass spectra to their theoretical ones. If this is not possible, it is advisable to sequence an abundant peptide in the spectrum by MALDI-QTOF tandem mass spectrometry.

The following databases are used for confirmation of the protein matches: PeptideMass, BLAST2SEQUENCE, Swiss-Prot-TrEMBL, and NCBI (see “The list of internet sites”).

3 MATERIALS AND METHODS

3.1 Preparation of lymphoblastoid cell pellets

3.1.1 Chemicals and reagents

Chemicals	**Company**	**Ordering number**
RPMI 1640 (1*with L-glutamine)	Biorad	F1215
fetal calf serum	Gibco/BRL	10270-106
streptomycin	Grünenthal	757753B
penicillin	Grünenthal	E744114
cyclosporine A, Sandimmun^{R}	Sandoz	PZN-2702663
Liquemin^{R} 25 000 U/ml	Hoffmann-La Roche	PZN-3441331
Ficoll^{R} separating solution (density 1.077 g/ml)	Seromed	L6115
dimethylsulfoxide (DMSO)	Merck	9678.0100
colcemid	Gibco/BRL	15210-016

3.1.2 Solutions

culture medium	RPMI 1640	500 ml
	fetal calf serum	50 ml
	streptomycin	50 mg
	penicillin	50,000 U
transformation medium	filtered EBV-containing B95-8 supernatant	50 ml
	RPMI 1640	40 ml
	fetal calf serum	10 ml
	streptomycin	50 mg
	penicillin	50,000 U
	cyclosporin A (Sandimmun^{R})	100 µg
hypotonic solution	KCl	0.075 M
freezing medium	culture medium	9 ml
	DMSO	1 ml
cold fixative	methanol	3 vol
	acetic acid	1 vol

3.1.3 Special equipment

Equipment	**Company**
tissue culture flasks (50 ml)	Nunc
sterile filters Millex HA	Millipore
centrifuge with 3360/BS4402/A rotor	Heraeus sepatech

3.1.4 Procedure

3.1.4.1 Preparation of transformation medium

The protocol has been established by Neitzel (1986). Fig. 3-1 depicts the procedure. The Epstein-Barr-Virus (EBV) for transformation is obtained from the lymphoblastoid marmoset

(monkey) cell line B95-8 that is latently infected with EBV and can release virus particles into the culture medium. About 5 x 10^5 B95-8 cells/ml were suspended in culture medium and the EBV-containing supernatant medium was collected after 5 days of cultivation. Then the supernatant was centrifuged at 400 g for 10 min to remove marmoset cells completely. After additionally being filtered twice through a 0.45 µm membrane filter, the supernatant was diluted 1:1 with fresh RPMI 1640, supplemented with 20% heat-inactivated fetal calf serum, 2 mM L-glutamine, antibiotics and cyclosporin A, to obtain the virus pools, i.e. the transformation medium.

3.1.4.2 Preparation of mononuclear leukocytes from whole blood

The heparinated blood sample (500 IE Liquemin/ml blood) of a normal control patient was diluted 1:1 with RPMI 1640 and was overlaid on 5 ml Ficoll. The volume ratio of blood-

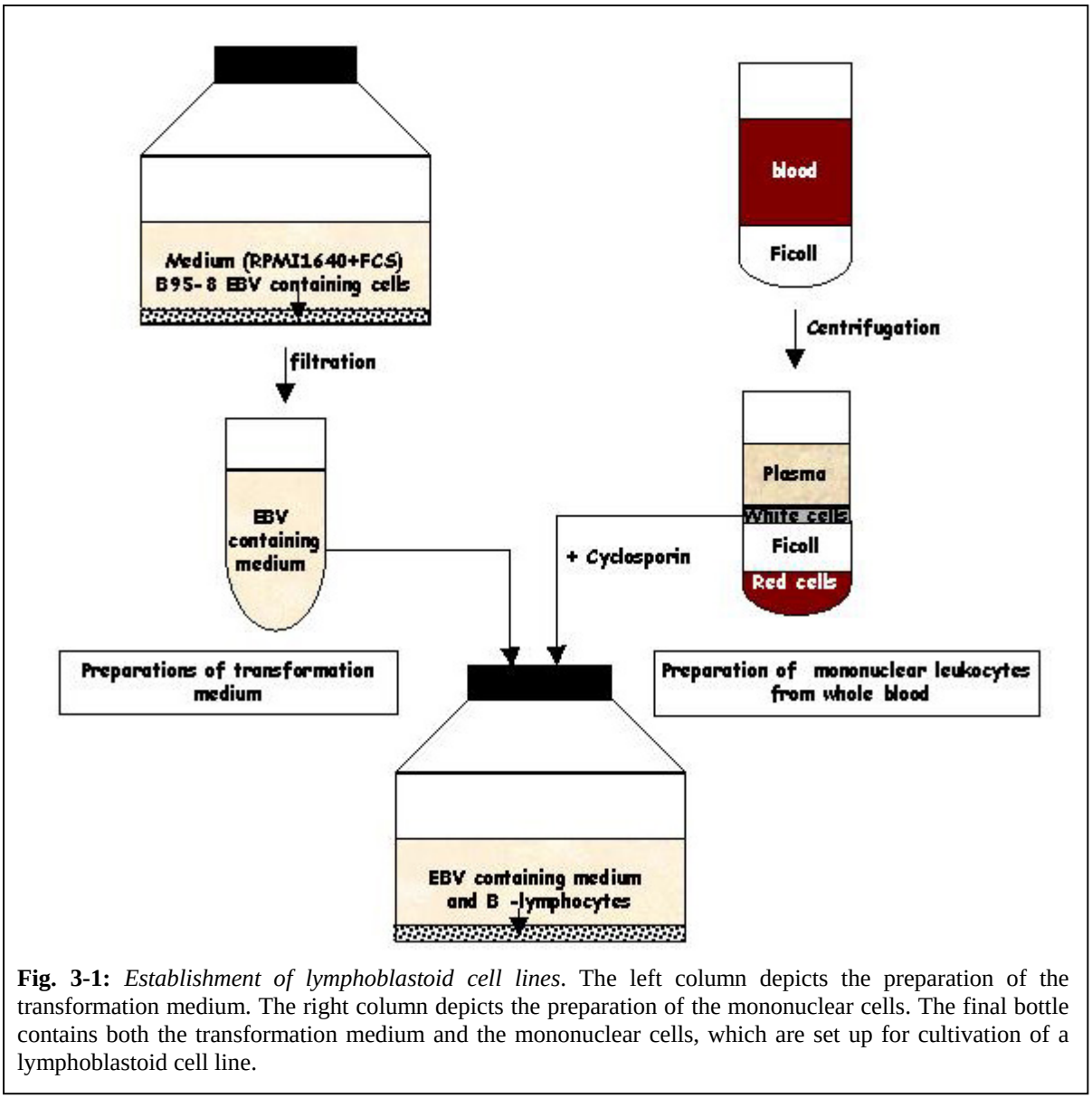

Fig. 3-1: *Establishment of lymphoblastoid cell lines*. The left column depicts the preparation of the transformation medium. The right column depicts the preparation of the mononuclear cells. The final bottle contains both the transformation medium and the mononuclear cells, which are set up for cultivation of a lymphoblastoid cell line.

RPMI mixture to Ficoll is 3-4:1. The step-gradient was centrifuged without brake at 400 g for 40 min in a swinging bucket centrifuge. The ensuing ring of mononuclear cells at the interface

between plasma and Ficoll was aspirated and washed/centrifuged (400 g, 10 min) three times with 10 ml RPMI.

3.1.4.3 Establishment of the permanent cell culture

The mononuclear leukocytes, including T- and B-lymphocytes were suspended in transformation medium. The pH of the cell culture was adjusted to 6.8 by overlaying it with CO_2 and then the cells were incubated at 37°C in a 5% CO_2 atmosphere. The medium was changed once a week by replacing half of the supernatant with a fresh medium containing 1 µg/ml cyclosporin A. Cyclosporin A specifically inhibits the RNA polymerase of T lymphocytes thus removing the interfering T-lymphocytes.

3.1.4.4 Preparation of the lymphoblastoid cell pellet

The lymphoblastoid cell pellet was prepared after the cell line had been cultured for 3-4 weeks. The total cell number was counted with a Neubauer's chamber under a phase contrast microscope at 100 x magnification. The cultured cells were re-suspended by pipetting up and down and were transferred into centrifugation tubes. A pellet was obtained by centrifugation at 1050 g for 8 min.

3.2 Preparation of mitochondria

3.2.1 Chemicals and reagents

Chemicals	**Company**	**Ordering number**
sucrose	Merck	7653.1000
EDTA	Merck	8418.0250
3-morpholinopropanesulfonic acid (MOPS)	Fluka	69948
bovine serum albumin (BSA)	Fluka	05488
triethanolamine	Fluka	90278
digitonin	Fluka	37006
Percoll	Fluka	77237
Metrizamide	Fluka	69753

3.2.2 Solutions

medium A	sucrose	100 mM
	EDTA	1 mM
	MOPS (pH 7.4)	20 mM
	BSA	1 g/l
medium B (homogenization buffer)	medium A	
	triethanolamine	10 mM
	Percoll	5%
	digitonin	0.1 mg/ml

3.2.3 Special equipment

Equipment	**Company**
motor driven tightly fitting Potter-Elvehjem homogenizer RZR 2051 (glass tube with Teflon pestle, diameter 6,8 mm)	Heidolph

lumbar puncture syringe-needles (length: 7 cm, volume: 1 ml)	Braun Melsungen AG
ultracentrifuge with T1270 rotor (Sorvall ultra Pro 80)	DuPont de Nemours GmbH

3.2.4 Procedure

The present protocol has been adapted and modified from Madden *et al.* (1987), Bourgeron *et al.* (1992) and Strack *et al.* (2001). Fig. 3-2 shows the procedure and the result of mitochondrial isolation.

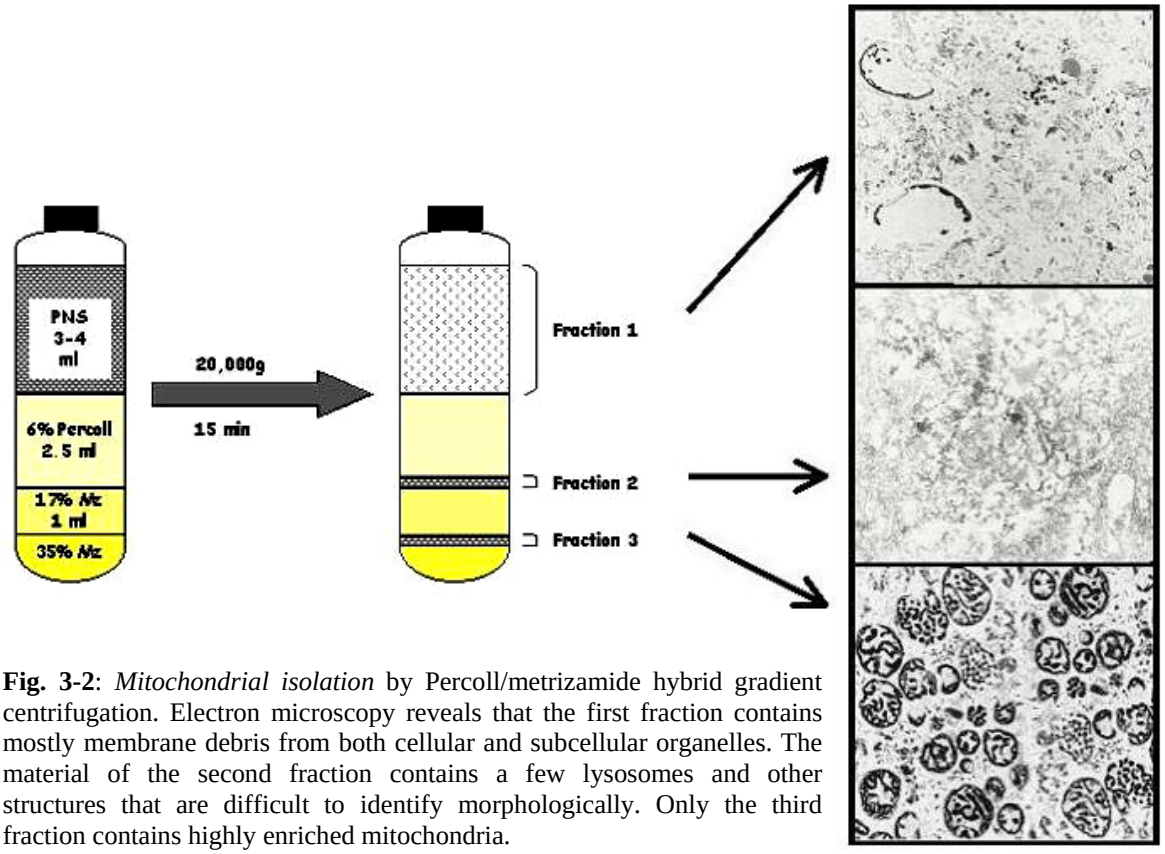

Fig. 3-2: *Mitochondrial isolation* by Percoll/metrizamide hybrid gradient centrifugation. Electron microscopy reveals that the first fraction contains mostly membrane debris from both cellular and subcellular organelles. The material of the second fraction contains a few lysosomes and other structures that are difficult to identify morphologically. Only the third fraction contains highly enriched mitochondria.

3.2.4.1 Preparation of the post-nuclear supernatant

All procedures were carried out at 4°C to minimize protease activity. At first the cell pellet was washed and centrifuged (1050 g, 8 min) two times with medium A. Then it was resuspended with medium B and incubated for 5 minutes. Medium B contains digitonin that is incorporated into the cell membrane and thus makes the subsequent break-up of cells easier. The cells were disrupted with 5 up- and down-strokes of a Potter-Elevhjem-homogenizer at 500 rpm. The homogenate was centrifuged at 1300 g for 5 min, and the supernatant was collected. The pellet was resuspended again in medium B and disrupted once more with the homogenizer. This step was repeated twice and the supernatants from each centrifugation-step were pooled as the “post-nuclear supernatant”.

3.2.4.2 Preparation of a hybrid Percoll/Metrizamide discontinuous gradient

A hybrid gradient was prepared from 35% Metrizamide (density 1.1304 g/ml), 17% Metrizamide (density 1.1029 g/ml), and 6% Percoll (density 1,0331 g/ml). All solutions were pre-

pared with 0.25 M sucrose and the concentrations were expressed as w/v. Gradients were poured into cellulose-nitrate ultracentrifugation-tubes. 1 ml of 35% Metrizamide was overlaid with 1 ml of 17% Metrizamide followed by 2.5 ml of 6% Percoll. The tubes were then gently filled with post-nuclear supernatant (about 3.7 ml) up to 4 mm below the upper rim. The solutions were overlaid on top of one another with a long lumbar puncture syringe-needle. Centrifugation was performed at 20,000 g without brake for 15 min at 4°C in an ultracentrifuge.

3.2.4.3 Preparation of the mitochondrial pellet

After centrifugation several distinct bands can be detected in the discontinuous hybrid Percoll/Metrizamide gradient. The band at the interface between 17% and 35% Metrizamide is highly enriched in mitochondria [Madden *et al.*, 1987; Strack *et al.*, 2001]. This band was aspirated with a Pasteur-pipette, diluted 1:4 with 0.25 M sucrose and centrifuged at 10,000 g for 10 min to wash away the remaining Metrizamide and to obtain a concentrated mitochondrial pellet at the floor of the centrifugation tube. An additional washing step could be added if necessary.

3.3 Sample preparation of mitochondrial proteins

3.3.1 Chemicals and reagents

Chemicals	**Company**	**Ordering number**
NaH_2PO_4*$2H_2O$	Merck	6580
Na_2HPO_4	Merck	3090
KCl	Merck	4933
$MgSO_4$*$7H_2O$	Sigma	M-1880
urea	Biorad	161-0730
pepstatin A	Sigma	P-4265
phenylmethylsulfonylfluoride	Biorad	161-0202
protease inhibitor mini (Complete^R)	Roche	1.836.153
glycerin	Merck	4093
3-[(3-cholamidopropyl)-dimethylammonio] -propan-sulfonate (CHAPS)	Merck	1.11662.0001
1,4-dithioerythritol (DTT)	Biorad	161-0610
Servalyte^R pH 2-4	Serva	42902

3.3.2 Solutions

P_2-CHAPS buffer	KCl	0.2 M
	glycerin	20%
	phosphate buffer (0.2 M NaH_2PO_4 and 0.2 M Na_2HPO_4, pH 7.2)	0.1 M
P_2-CHAPS/$MgSO_4$	P_2-CHAPS buffer	
	$MgSO_4$*$7H_2O$	1 mM
	CHAPS	0.14 M

protease inhibitor (H1) (solved in ethanol)	pepstatin A	1.4 µM
	phenylmethylsulfonylfluoride	1.0 mM
protease inhibitor 4 (H4)	P2-CHAPS-Buffer	0.4 ml
	protease inhibitor mini (Complete^{R})	1 tablet
DTT solution	DTT	21.6%

3.3.3 Special equipment

Equipment	**Company**
sonicator (Transsonic 310)	Faust
polished glass beads (diameter 2.5 mm)	Carl Roth GmbH + Co Karlsruhe

3.3.4 Procedure

The protocol was performed according to Klose *et al.* (1999a). The mitochondrial pellet was weighed to calculate the required volume of each solution, including P_2-CHAPS/$MgSO_4$, protease inhibitor 1 (H1), protease inhibitor 4 (H4), and the required number of glass beads. The required volume of P_2-CHAPS/$MgSO_4$ was 1.25 times the weight of the mitochondrial pellet.

H1 protease inhibitor was calculated to be 0.02 fold and H4 protease inhibitor to be 0.08 fold of the combined masses of the mitochondrial pellet and P_2-CHAPS/$MgSO_4$. The number of the required glass-beads equaled to 0.034 x of the sum of the weight of mitochondrial pellet plus the volumes of all other solution components. The solutions were added directly onto the pellet. After adding the glass-beads to the homogenate, it was sonicated in an ice-cold water bath for 10 seconds followed by 40-45 seconds stirring and one minute keeping on ice. This sonication-round was repeated six times to guarantee that most of the mitochondrial proteins were solubilized. After 15 min stirring in a cold room, the required volume of benzonase was added to remove the mtDNA. The volume of the required benzonase equaled 0.025 x the weight of the homogenate after sonication. The homogenate was stirred for another 15 min at 4°C before the protein-concentration was measured by the BCA protein-assay. This assay required about 1-5 µl homogenate. The rest of the homogenate was mixed with urea, DTT and ampholine pH 2.0-4.0 to yield final concentrations of 9 M urea, 70 mM DTT, and 2% ampholine 2.0-4.0. The homogenate was stored at –80°C before the 2D-electrophoresis was started.

3.4 Bicinchoninic acid (BCA) protein assay

3.4.1 Chemicals and reagents

Chemical	**Company**	**Ordering number**
BCA protein assay reagent (includes reagent A, reagent B, and albumin standard)	Pierce	23225BN

3.4.2 Special equipment

Equipment	**Company**
spectrophotometer (MRX)	Dynal Biotech & Nordic
microwell-plate	NUNC ^{TM} Brand Products

3.4.3 Procedure

3.4.3.1 Preparation of diluted BSA serial standards

The BSA standards were prepared by diluting a 2.0 mg/ml BSA stock standard serially with the same diluent as my sample. A list of standard dilutions with a working range from 20 µg/ml to 2000 µg/ml is shown bellow:

Volume of BSA	**Volume of diluent**	**Final BSA concentration**
300 µl of Albumin Standard	0 µl	2000 µg /ml
(A) 375 µl of albumin standard	125 µl	1500 µg /ml (A)
(B) 325 µl of albumin standard	325 µl	1000 µg /ml (B)
(C) 175 µl of (A)	175 µl	750 µg /ml (C)
(D) 325 µl of (B)	325 µl	500 µg /ml (D)
(E) 325 µl of (D)	325 µl	250 µg /ml (E)
(F) 325 µl of (E)	325 µl	125 µg /ml (F)
(G) 100 µl of (F)	400 µl	25 µg /ml (G)

3.4.3.2 Protein quantification assay

The BCA working reagent was prepared by mixing 50 parts of BCA protein assay reagent A (contains BCA) with one part of reagent B (contains $CuSO_4$). Then 20 µl of each standard, the sample or diluent (as empty control) were pipetted into wells of a microwell-plate. 400 µl working reagent were added into each well sequentially. The plate was then covered and incubated at 37°C for 30 minutes in a water bath. After incubation, the plate was cooled to room temperature before final measurement. The protein concentration was measured colorimetrically at λ=570 nm with a spectrophotometer. The program "Revelation Version 2.0" provided by the manufacturer was used for data processing.

3.5 Two-dimensional protein electrophoresis

3.5.1 Chemicals and reagents

Chemicals	**Company**	**Ordering number**
acrylamide	Biorad	161-0100
piperazine diacrylamide	Biorad	161-0202
TEMED	Biorad	161-0800
persulfate	Biorad	161-0700
urea (for gel solution)	Biorad	161-0730
urea (for electrode solutions)	Merck	8484
glycerin	Merck	4093
ethylenediamine	Merck	800947
85% phosphoric acid	Merck	573
Sephadex G-200^R	Pharmacia	17-0081-01
Tris-base	Sigma	T-1503
Tris-HCl	Sigma	T-3253
sodium dodecyl sulfate (SDS)	Merck	1.06498
glycine	Serva	23390
Pharmalyte^R pH 3.5-10	Pharmacia	80-1125-87
Pharmalyte^R pH 6.5-9.0	Pharmacia	17-454-01

Pharmalyte^{R} pH 4.0-6.5	Pharmacia	17-452-01
Pharmalyte^{R} pH 5.0-8.0	Pharmacia	17-453-01
Sevalyte^{R} pH 2.0-11	Serva	42-900
Amberlite^{R} IRN-150	Serva	1-0341
ethanol	Herbeta	21847
methanol	Baker	8045
acetic acid	Merck	8.00947

3.5.2 Solutions

ampholine-mix	Pharmalyte pH 3.5-10	12.5% (v/v)
	Sevalyte pH 2.0-11	12.5% (v/v)
	Pharmalyte pH 6.5-9.0	12.5% (v/v)
	Pharmalyte pH 4.0-6.5	37.5% (v/v)
	Pharmalyte pH 5.0-8.0	25% (v/v)
1D-separation gel	acrylamide	3.5% (w/v)
	piperazine diacrylamide	0.3% (w/v)
	urea	9 M
	TEMED	0.06% (v/v)
	glycerin	5% (w/v)
	ampholine-mix	4% (v/v)
	persulfate	0.02% (w/v)
1D-anode solution	urea	3 M
	phosphoric acid	0.742 M
1D-cathode solution	urea	9 M
	glycerin	5% (w/v)
	ethylenediamine	0.749 M
Sephadex mixture	Sephadex G-200	12.5% (w/v)
	glycerin	12.5% (w/v)
	DTT	1.08% (w/v)
	ampholine-mix	2% (v/v)
	urea	9 M
1D-incubation solution	Tris-base	125 mM
	glycerin	40% (w/v)
	DTT	65 mM
	SDS	3% (w/v)
2D-gel solution	acrylamide	15% (w/v)
	bisacrylamide	0.2% (w/v)
	Tris-base/Tris-HCl	0.375 M
	TEMED	0.03% (v/v)
	SDS	0.1% (w/v)
	persulfate	0.08% (w/v)
2D-electrode solution (both upper and lower)	Tris-base	0.025 M
	glycine	0.192 M
	SDS	0.1 M
2D-fixation solution (silver stain)	ethanol	50% (v/v)
	acetic acid	10% (v/v)
2D-fixation solution (Coomassie stain)	methanol	50% (v/v)
	phosphoric acid	2% (v/v)

3.5.3 Special equipment

Equipment	Company
apparatus for IEF and 40 cm glass tubes of two different diameters (0.9 mm and 1.5 mm) Fig. 3-3A	self built
apparatus for SDS-PAGE (Desaphor VA 300) Fig. 3-3B	DESAGA
circular cooling machine F25	Julabo
PowerPac 3000 electrophoresis power supply	Biorad
1D-gel tube stand with special gel-solution groove	self built
polymerization stand Desaphor VA (2D polymerization stand)	DESAGA
1D-precision glass tubes 40 cm x 0.9 mm or 1.5 mm	Schott
pH-meter 766 with a micro electrode (type Inlab 422)	pH-meter: Knick electrode: Roth

Fig.3-3A: equipment for isoelectric focussing.

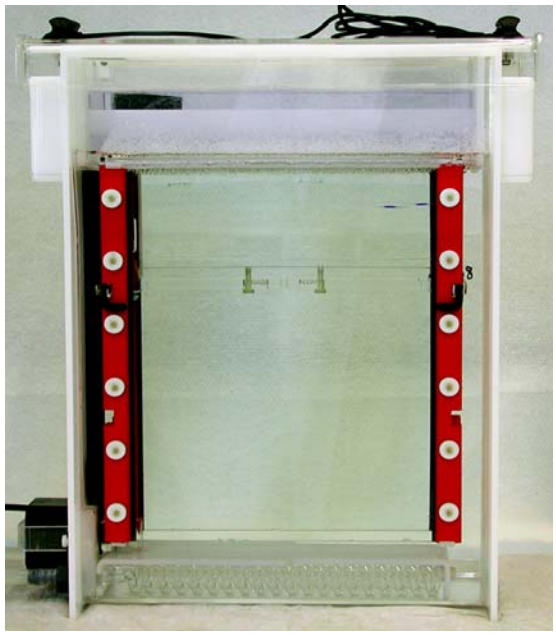

Fig. 3-3B: equipment for SDS-PAGE.

3.5.4 Procedure

3.5.4.1 First dimension-isoelectric focussing (IEF)

The isoelectric focussing is performed according to a protocol by Klose (1999b). In the first dimension two alternative gel containers were used. These are high precision capillary glass tubes with an internal diameter of 0.9 mm (thin) or 1.5 mm (thick) and a length of 400 mm. Gel solution was filled into the tubes by using accurately fitting nylon strings as plungers. After filling, the tubes were kept at room temperature to polymerize for 3-4 days before use. Before the protein samples were loaded onto the anodic end of the IEF-gel, a Sephadex mixture – acting as a sieve – was loaded to a height of 2 mm. Gels were electrophoresed serially at 100 V for 1 hour, followed by 300 V for 1 hour, 1000 V for 23 hour, 1500 V for 30 min and finally at 2000 V for 10 min. After the IEF-run was finished, the gels were expelled directly into the 1D-incubation solution by a nylon string. They were incubated for 10 min at room temperature under continuous shaking and then placed completely relaxed onto the gel

grooves and stored at –70°C until the second dimension separation of the 2D-electrophoresis was performed.

3.5.4.2 Sodium dodecyl-sulfate polyacrylamide gel electrophoresis

In the second dimension, 0.75 mm (thin) or 1.5 mm (thick) thick plastic spacers were used to fix the distance between the two glass plates of the electrophoretic cell. The first dimension (IEF) gel was gently transferred from the groove onto the surface of the SDS-PAGE gel with the help of a special wire-hook. Care was taken, not to stretch the gel. The IEF gel had to be in tight contact with the SDS-PAGE gel. The inclusion of air or solution between the gels had to be avoided. 1 % agarose solution was overlaid up to the edges of the glass cells to restrict the movement of the IEF gel. Gels were electrophoresed for the first 15 min at 65 mA (thin gel) or 130 mA (thick gel) and then at 75 mA (thin gel) or 150 mA (thick gel) for ca. 6-7 hours. The temperature of the lower electrode solution was kept at 15°C by a spiral glass tube fixed to a circular cooling pump. Electrophoresis was finished when the bromophenol blue line in the gels reached a line that has been etched 2 cm from the lower edge of the frontal gel plate. After electrophoresis, the gels were transferred into 1 liter/gel 2D-fixation solution. After shaking for 2 hours, the gels were left standing overnight in the same solution at room temperature.

3.5.4.3 Measurement of the pH-gradient of the IEF-gel

The isoelectric focussing of two Ø 1.5 mm tube gels was performed as described above. One of the gels was loaded with 10 µl of mitochondrial protein sample, the other was left empty as a control. After the isoelectric focussing was finished, the gels were expelled and cut into 5 mm sections which were put directly into individual Eppendorf test tubes with 40 µl degassed aqua bidest. The Eppendorf tubes were closed in a nitrogen atmosphere. The gel sections were sonicated in an ice-cold water bath for 15 min in order to release the ampholytes from the gel into the water. The pH-measurement was carried out with a microelectrode. The pH of each gel-section was measured for 2 min until stable readings were obtained.

3.6 Gel staining and drying

3.6.1 Chemicals and reagents

Chemicals	**Company**	**Ordering number**
sodium acetate	ICN	195496
sodium thiosulfate	ICN	191447
glutardialdehyde	Merck	8.20603
ethanol	Herbeta	21847
sodium carbonate	Merck	1.06392.0500
silver nitrate	ICN	195495
formaldehyde	ICN	194047
EDTA	Merck	1.08418.0250
thimerosal	ICN	103044
ammonium sulfate	Sigma	A-9141
Serva Blue G-250 ^{R}	Serva	35050

3.6.2 Solutions

S-incubation solution	sodium acetate	0.5 M
	sodium thiosulfate	0.2% (w/v)
	glutardialdehyde	0.5% (v/v)
	ethanol	30% (v/v)
S-stain solution	silver nitrate	0.1% (w/v)
	formaldehyde	0,01% (v/v)
S-wash solution	sodium carbonate	2.5% (w/v)
S-developer solution	sodium carbonate	2.5% (w/v)
	formaldehyde	0.01% (v/v)
S-stop solution	EDTA	0.05 M
	thimerosal	0.02% (w/v)
C-incubation solution	methanol	34% (v/v)
	phosphoric acid	2% (v/v)
	ammonium sulfate	17% (w/v)
C-stain solution	methanol	34% (v/v)
	phosphoric acid	2% (v/v)
	ammonium sulfate	17% (w/v)
	Serva Blue G-250	0.066% (w/v)
C-wash solution	methanol	25% (v/v)

3.6.3 Special equipment and material

Equipment	**Company**
shaker (3016)	Gesellschaft für Labor mbH
plastic troughs (bottom 30*40 cm)	Brukle-Labo-Plast
drying/vacuum incubator (type UL-60)	Memmert
water-saving vacuum pump (type TOM JET 1/A4)	Genser Wissenschaftliche Apparate
water-jet vacuum pump	Th. Geyer
cellophane	Gehring & Neidweiser GmbH & Co

3.6.4 Procedure

3.6.4.1 Silver staining

The silver staining was performed according to a protocol by Klose (1999b). Silver staining is a very sensitive method with a detection limit between 1-10 ng. It is based on the high reducibility of silver ions. The silver ions form complexes with proteins much stronger than with the polyacrylamide gel. Complexed silver ions can be reduced much faster than free silver ions. During the whole procedure of silver staining, the gels were shaken continuously. After each step, the solutions were removed by suction of a water-jet pump. The gels were at first incubated in S-incubation solution for 2 hours. During this period, the sodium thiosulfate and glutardialdehyde in the solution act as complexing agents and link the proteins by forming covalent bonds. After that, two rinsing steps with distilled water were performed for 20 min. This had to be done to minimize background staining by washing away the unbound glutaraldehyde. The silver staining lasted for 30 min. In this step formaldehyde was used as reducing agent. After that, the gels were washed in S-wash solution for 1 min and developed by S-developer solution for several minutes and then finally stopped by S-stop solution.

3.6.4.2 Colloidal Coomassie staining

The colloidal Coomassie staining was performed according to a protocol by Klose (1999b). Coomassie staining is a method that visualizes proteins due to the unspecific binding of the dye to their amino acid residues. The detection limit is around 1 μg. Compared to the standard Coomassie staining method, the colloidal Coomassie staining is more specific and sensitive, since the colloidal Coomassie dye is much finer than the standard Coomassie dye. The colloidal Coomassie dye penetrates better through the polyacrylamide gel and thus binds to the proteins more easily. The whole procedure of colloidal Coomassie staining was carried out under continuous shaking. After overnight fixation in C-solution, the gels were at first washed three times with distilled water for 30 min. Then they were incubated in C-incubation solution for 1 hour followed by 5 days staining with Coomassie brilliant blue G-250. The destaining step with C-wash solution lasted 1-2 hours by using a piece of sponge which acts as adsorbent for the washed out dye. The whole procedure was stopped when the protein spots stood out clearly from the background. One should not destain the gels for too long since the color of the protein spots also faded with time.

3.6.4.3 Gel drying and preserving

After staining the results had to be stored and the gels had to be preserved. Still wet, the gels were scanned on a transilluminating scanner and stored as TIFF-files with a resolution of 150-300 dpi. Later the gels were dried to preserve them for the records. They were "sandwiched" between two sheets of wet cellophane and thick filter papers and were put on a drying panel. Excess water as well as air bubbles between the layers of filter paper, cellophane, and the gel were expelled with a ruler. The gels were then dried in a heated vacuum incubator for approximately 2-3 hours at 80°C. The dried gels were labeled with the sample name and the date and stored in large envelopes tagged with all the information of the 2D-electrophoresis runs.

3.7 Sample preparation for MALDI-TOF protein mass fingerprinting

3.7.1 Chemicals and reagents

Chemicals	**Company**	**Ordering number**
trypsin	Roche	1047841
ammonium bicarbonate (NH_4HCO_3)	Sigma	A-6141
acetonitrile	Baker	9017-54
formic acid	Sigma	F-0507
α-cyano-4-hydroxy cinnamic acid	Sigma	C2020
trifluoroacetic acid (TFA)	Merck	8178.0050

3.7.2 Solutions

destaining solution	100 mM NH_4HCO_3	60% (v/v)
	acetonitrile	40% (v/v)
trypsin solution	trypsin	10 ng/μl
	NH_4HCO_3	50 mM
formic acid solution	formic acid	5% (v/v)

matrix	α-cyano-4-hydroxy cinnamic acid	15 mg/ml
	0.1% (v/v) TFA	30% (v/v)
	acetonitrile	70 % (v/v)

3.7.3 Special equipment

Equipment	**Company**
skin-biopsy punch (various diameters)	Stiefel
vacuum centrifuge (Speedvac) (PLCT 60-E)	Heraeus
incubator (PersonalHyb)	Stratagene
shaker (AVM)	E^{TS} Jean Robin

3.7.4 Procedure

3.7.4.1 In-gel digestion

Protein spots were excised from the gel with a skin-biopsy punch and placed into the destaining solution. After shaking overnight at room temperature, they were dehydrated by addition of 100 µl acetonitrile. The liquid phase was removed, and the gel pieces were completely dried in a vacuum centrifuge. The gel pieces were then re-hydrated in the trypsin solution at 4°C for 45 min to let the trypsin permeate into the gel pieces without self-digestion. The digestion was allowed to proceed overnight at 37°C by keeping the gel pieces wet. Peptides were extracted by letting the gel-piece swell three times with 5% formic acid and shrink four times with acetonitrile. The whole liquid phase was collected and finally dried down in a vacuum centrifuge.

3.7.4.2 Sample preparation for MALDI analysis

The peptide-samples were solved in 10 µl 0.1% TFA. 1 µl of the sample was spotted onto the MALDI target plate and mixed with 1 µl of 2% TFA and 1 µl matrix. After the sample spots had air-dried completely, they were rinsed twice with 5-10 µl 0.1% TFA, and the remaining liquid was evaporated with pressurised air.

3.8 Peptide mass fingerprinting by MALDI-TOF mass spectrometry

3.8.1 Special equipment

MALDI-TOF mass spectrometer (Reflex II from Bruker-Daltonik, Bremen)

3.8.2 Procedure

Mass spectra of the peptide mixture were obtained using the Bruker Reflex II mass spectrometer operated in the reflector mode. The instrument is fuctions in the “delayed extraction” mode that ensures a mass resolution up to at least 6000 Da over the entire mass range and a mass accuracy of better than 0.1 Da with internal calibration. A total of 100-140 single-shot spectra were accumulated from each sample. They were calibrated using the monoisotopic peak from a known auto-digestion product of bovine trypsin (residues 50-69, $M+H^+$ = 2163.06 Da) and the matrix trimer ion ($3M+H^+$ = 568.14 Da) as internal standards. The XMASS 5.0 software packages provided by the manufacturer were used for data processing.

3.9 Computer aided analysis of protein mass fingerprints

The identification of proteins by their peptide mass fingerprints was mainly performed with the Mascot Software (Matrix Science Ltd.) and additionally with ProFound or PeptideSearch as search engines. The parameters were choosen as shown in Fig. 3-4.

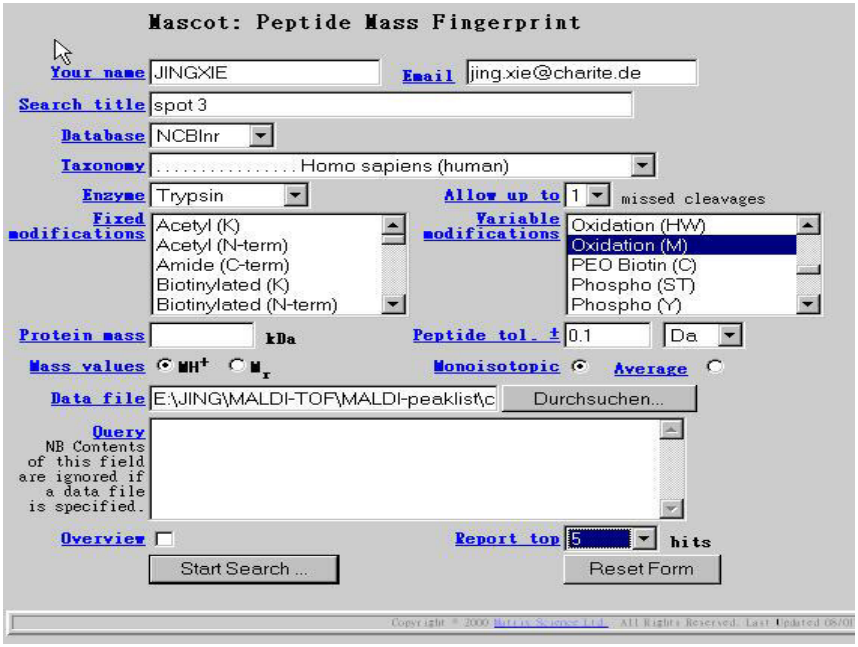

Fig. 3-4A: *the first step of database search for proteins*. Example of the parameters used for the database search with the Mascot search engine. The parameters such as taxonomy, allowed missed cleavages, variable modifications, and peptide mass tolerance were restricted as shown. Only the monoisotopic peptide masses were considered in this search.

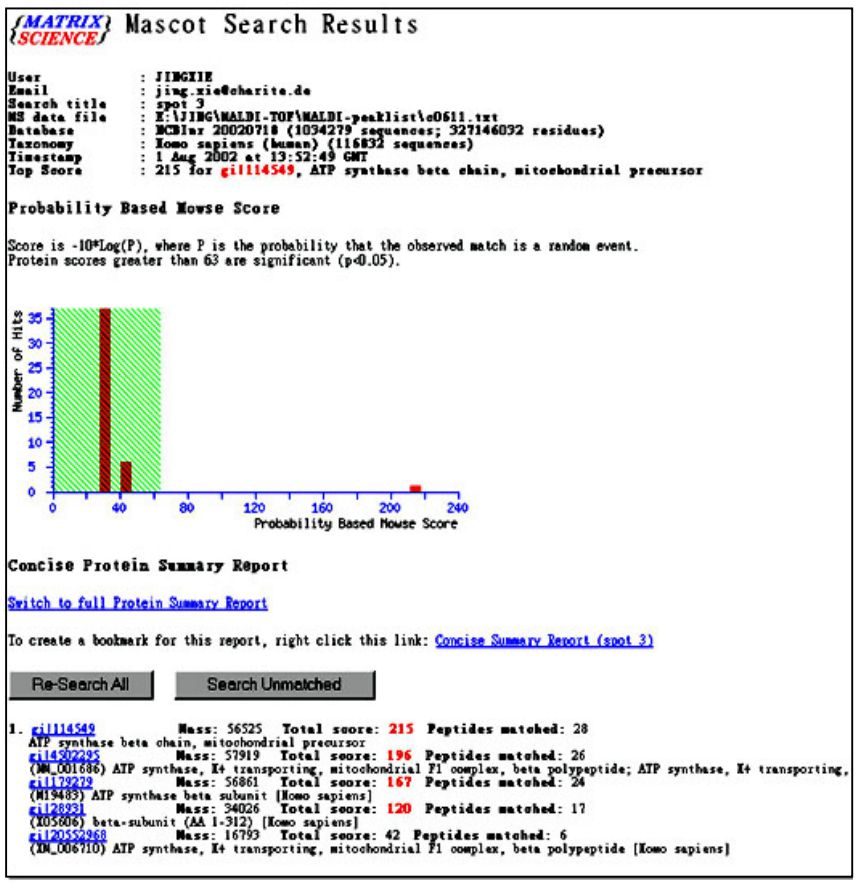

Fig. 3-4B: *the second step of database search for proteins*. The first protein is usually the best fit. The full name of the candidate protein together with its gi-number, the theoretical molecular weight, the probability based Mowse-score and the number of matched peptides are all listed. Normally, there are several peptides or proteins listed in one suggestion. They generally are various fragments of the same protein.

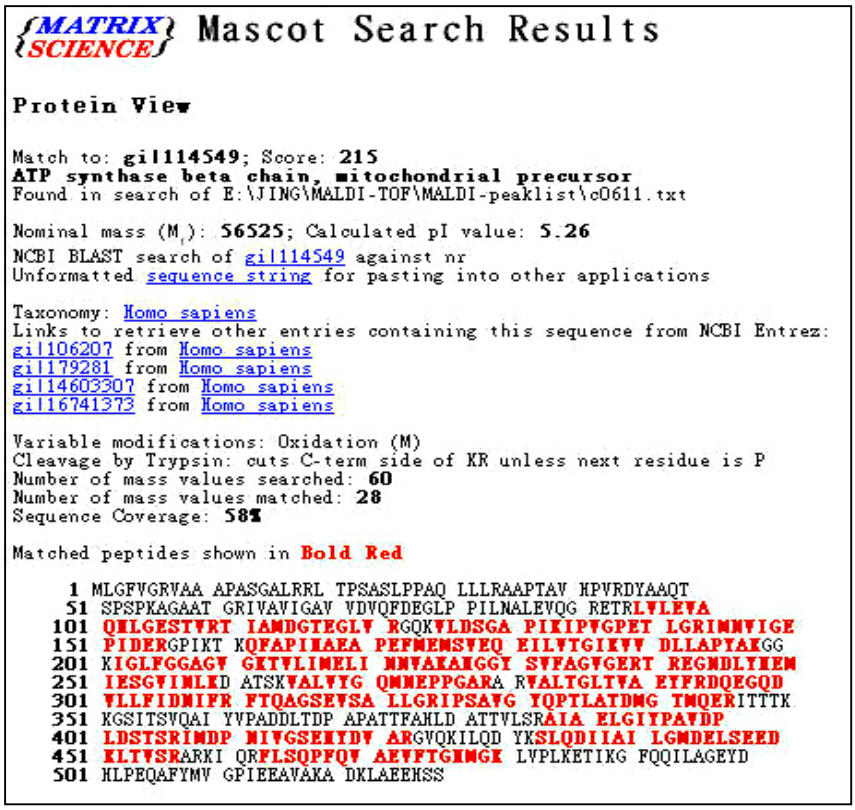

{MATRIX SCIENCE} Mascot Search Results

Protein View

Match to: **gi|114549**; Score: **215**
ATP synthase beta chain, mitochondrial precursor
Found in search of E:\JING\MALDI-TOF\MALDI-peaklist\c0611.txt

Nominal mass (M_r): **56525**; Calculated pI value: **5.26**
NCBI BLAST search of gi|114549 against nr
Unformatted sequence string for pasting into other applications

Taxonomy: Homo sapiens
Links to retrieve other entries containing this sequence from NCBI Entrez:
gi|106207 from Homo sapiens
gi|179281 from Homo sapiens
gi|14603307 from Homo sapiens
gi|16741373 from Homo sapiens

Variable modifications: Oxidation (M)
Cleavage by Trypsin: cuts C-term side of KR unless next residue is P
Number of mass values searched: **60**
Number of mass values matched: **28**
Sequence Coverage: **58%**

Matched peptides shown in **Bold Red**

```
    1 MLGFVGRVAA APASGALRRL TPSASLPPAQ LLLRAAPTAV HPVRDYAAQT
   51 SPSPKAGAAT GRIVAVIGAV VDVQFDEGLP PILNALEVQG RETRLVLEVA
  101 QHLGESTVRT IAMDGTEGLV RGQKVLDSGA PIKIPVGPET LGRIMNVIGE
  151 PIDERGPIKT KQFAPIHAEA PEFMEMSVEQ EILVTGIKVV DLLAPYAKGG
  201 KIGLFGGAGV GKTVLIMELI NNVAKAHGGY SVFAGVGERT REGNDLYHEM
  251 IESGVINLKD ATSKVALVYG QMNEPPGARA RVALTGLTVA EYFRDQEGQD
  301 VLLFIDNIFR FTQAGSEVSA LLGRIPSAVG YQPTLATDMG TMQERITTTK
  351 KGSITSVQAI YVPADDLTDP APATTFAHLD ATTVLSRAIA ELGIYPAVDP
  401 LDSTSRIMDP NIVGSEHYDV ARGVQKILQD YKSLQDIIAI LGMDELSEED
  451 KLTVSRARKI QRFLSQPFQV AEVFTGHMGK LVPLKETIKG FQQILAGEYD
  501 HLPEQAFYMV GPIEEAVAKA DKLAEEHSS
```

Fig. 3-4C: *The third step of the database search.* The detailed view of a certain protein, e.g. the ATP synthase beta-chain, includes information on the protein and on the sequence of the protein covered by the peptide mass fingerprint (highlighted in red). The full information of the protein can be accessed from the NCBI database, by clicking on the accession number (gi number) of the protein.

After a protein had been found, the fingerprint data were compared with the theoretical digestion product of the protein. If no clear relation of the molecular weights between the "experimental" and the "theoretical" fragments could be found, I tried to use several less stringent criteria to improve the matching rates. This was expecially the case for large peptide fragments with molecular weights above 2,000 Da. The less stringent criteria comprised the allowance of up to four missed cleavages, the modification of cysteine by acrylamide and a larger tolerance of mass deviation of ± 0.5 Da.

3.10 Peptide sequencing by MALDI-QTOF mass spectrometry

3.10.1 Chemicals and reagents

Chemicals	**Company**	**Ordering number**
acetonitrile(HPLC-grade)	Baker	9017-54
2,5-dihydroxybenzoic acid	Sigma	G-5254
isopropanol	Merck	1.09634.1000
POROS 10 R2 reversed-phase chromatography medium [R]	PerSeptive Biosystems	1-1118-02

3.10.2 Solutions

matrix	2,5-dihydroxybenzoic acid	5 mg/ml
	acetonitrile	3 vol
	0.1% (v/v) TFA	7 vol
POROS 10 R2; reversed-phase chromatography medium solution	POROS 10 R2 reversed-phase chromato-graphy medium saturated with isopropanol	

3.10.3 Special equipment

Equipment	**Company**
GELoader pipette tip	Eppendorf
plastic syringe (1.25 ml)	Eppendorf
API QSTAR Pulsar I mass spectrometer equipped with a MALDI ion source	Applied Biosystems/MDS Sciex

3.10.4 Procedure

3.10.4.1 Sample purification by nano-scale reversed-phase chromatography

Sample purification was performed according to a protocol by Gobom (2001). A long, narrow pipette tip packed with 0.3 ml POROS 10 R2 reversed-phase medium served as a chromatography column. All the sample liquid was driven through the column by a disposable plastic syringe. Prior to use, the column was washed with 15 µl of acetonitrile-0.1 % TFA (8:2 v/v) followed by an equilibration step with 10 µl of 0.1% (v/v) TFA. The peptide sample was acidified with 2 µl 2% (v/v) TFA to obtain a final concentration of about 0.2-0.5 % (v/v). Then the sample was loaded onto the column and was slowly pumped over the reversed-phase medium. A washing step was performed with 10 µl 0.1% TFA, and the column was emptied completely by pressing air through it for a few seconds. Finally, 3 µl matrix as an eluent were loaded on the column and the eluate was loaded directly onto the target of the MALDI-QTOF mass spectrometer.

3.10.4.2 Protein ladder sequencing of peptide fragments

These experiments were performed within the selection cell (Q_1) and the collision cell (Q_2). All ions were transmitted resulting in the measurement of the entire mass range. The ion of interest was selected at first in cell Q_1, then this precursor ion was split in the collision cell Q_2 using argon as a collision gas. The ensuing fragments were analyzed in the TOF section of the instrument. The instrument was calibrated externally with peptides of known masses. The data processing was done with the “ANALYST” software packages provided by the manufacturer.

4 RESULTS

The aim of this study was to establish a reference 2D-electrophoresis map of human mitochondrial proteins. Since this basic work should find its application in future diagnostic tests for patients with mitochondriopathies, I chose a material that can easily be obtained from patients. Immortalized cultured lymphoblastoid cells are easy to handle, can grow in non-adherent cell-cultures and were therefore the material of choice. The combined methods of 2D-electrophoresis and mass spectrometry were used to separate and to identify the proteins. All procedures and their respective results are summarized in Fig. 4-1. The whole project started with the establishment of an immortalized lymphoblastoid cell line. The electron microscopic photographs from the cells show that each lymphoblastoid cell contains about 15-20 mitochondria (Fig. 4-2). The mitochondria were isolated and enriched by homogenization followed by density gradient centrifugation. All three ensuing fractions were examined by electron microscopy (Fig. 3-2). Only the third fraction, which contained the mitochondria, was used in subsequent experiments. The mitochondrial proteins were separated by 2D-electrophoresis and stained with Coomassie brilliant blue. The protein identification was performed with MALDI-TOF mass spectrometry and subsequent database searching. The identified proteins were marked on the 2D-electrophoresis map to get the final reference map.

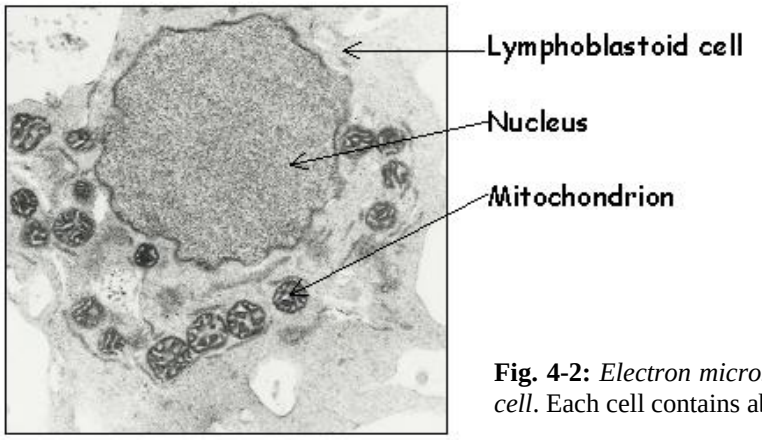

Fig. 4-2: *Electron microscopic picture of a lymphoblastoid cell*. Each cell contains about 15-20 mitochondria.

4.1 Mitochondrial isolation

In order to study the mitochondrial proteome specifically, I chose as raw material the mitochondrial fraction instead of whole lymphocyte preparations. In Fig. 4-3 the 2D-electrophoresis gels of the lymphocyte proteome (A) and the mitochondrial proteome (B) are compared to each other. On the mitochondrial gel there are much less spots than on the whole lymphocytes' gel. Some spots, which are fairly weak or even barely visible on the lymphocytes' gel, show up intensely on the mitochondrial gel (highlighted with red arrows in the mitochondrial gel). For isolation of mitochondria from lymphoblastoid cells the first aim was to gain enough mitochondria from as little material as possible. The second aim was to modify the current protocols of mitochondrial isolation to increase the purity of the mitochondrial fractions. In my experiments a total of 10^8 cells was sufficient to obtain enough purified mitochondria from one patient to be able to perform two large gel 2D-electrophoresis runs, i.e. about 10^8 cells yielded 12-20 mg mitochondria. At the mitochondrial isolation procedure (see chapter 3.2.4), after ultracentrifugation I detected three distinct fractions in the hybrid discontinuous gradient. Floating material could be found between the surface of the gradient and the

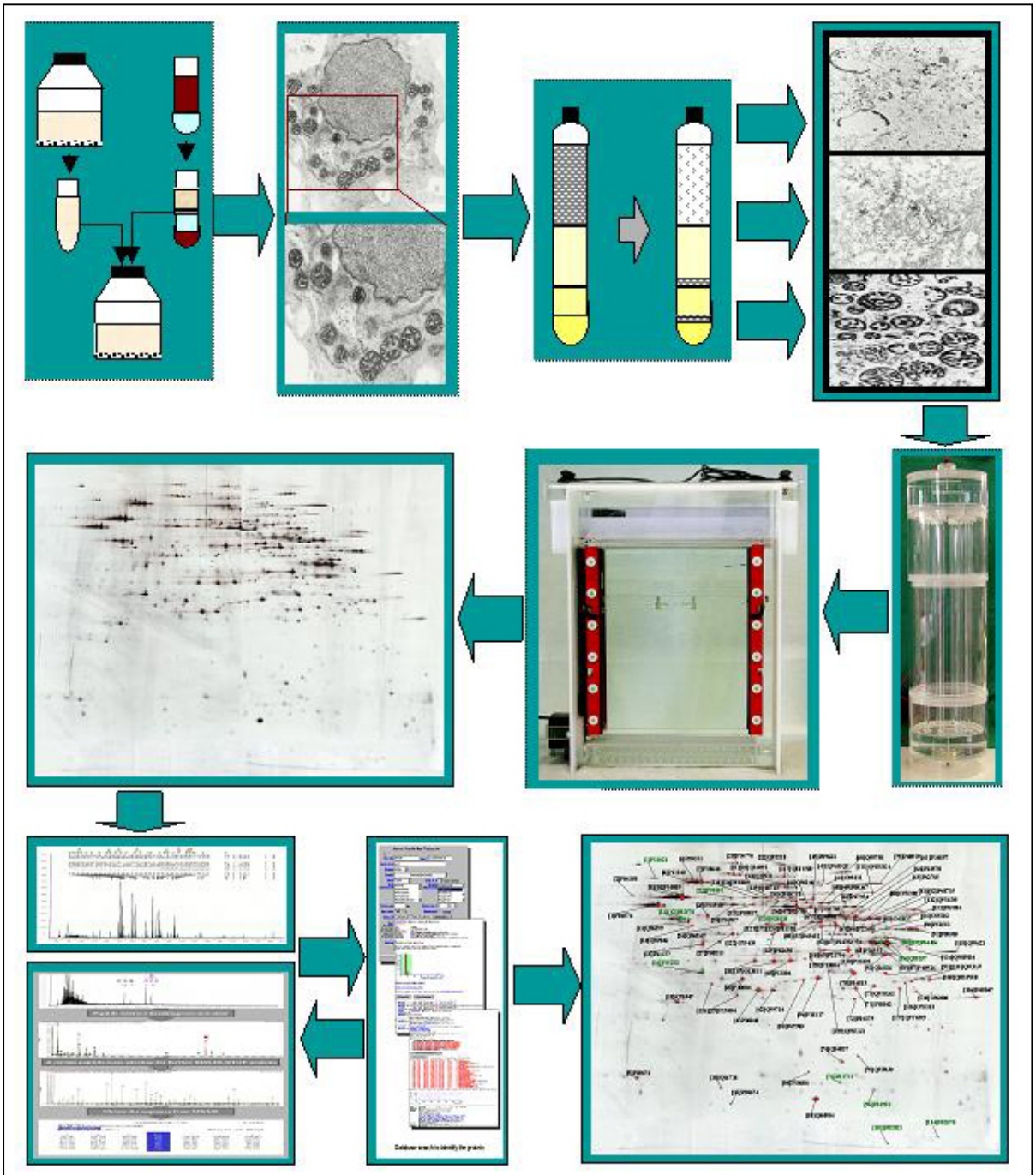

Fig. 4-1: *This summary* describes the procedures and the results of this study step by step. The work started from the establishment of a lymphoblastoid cell line. The electron microscopic photographs showed that each lymphocyte contains about 15-20 mitochondria. The mitochondria were isolated after homogenisation of the lymphocytes followed by density gradient centrifugation. The three fractions were examined by electron microscopy. Only the third fraction was enriched of mitochondria. This fraction was used in subsequent experiments. The mitochondrial proteins were separated by 2D-electrophoresis and stained with Coomassie brilliant blue. The various protein-spots were cut out and were digested with trypsin. A peptide mass fingerprint or a peptide ladder were then generated with MALDI-TOF or MALDI-QTOF respectively. After database searching, the identified proteins were marked on the 2D-electrophoresis gel in order to obtain the final reference map.

interface between sample and 6% Percoll; a second ring was seen at the interface between 6% Percoll and 17% Metrizamide; and a third fraction lay at the interface between 17 % and 35 %

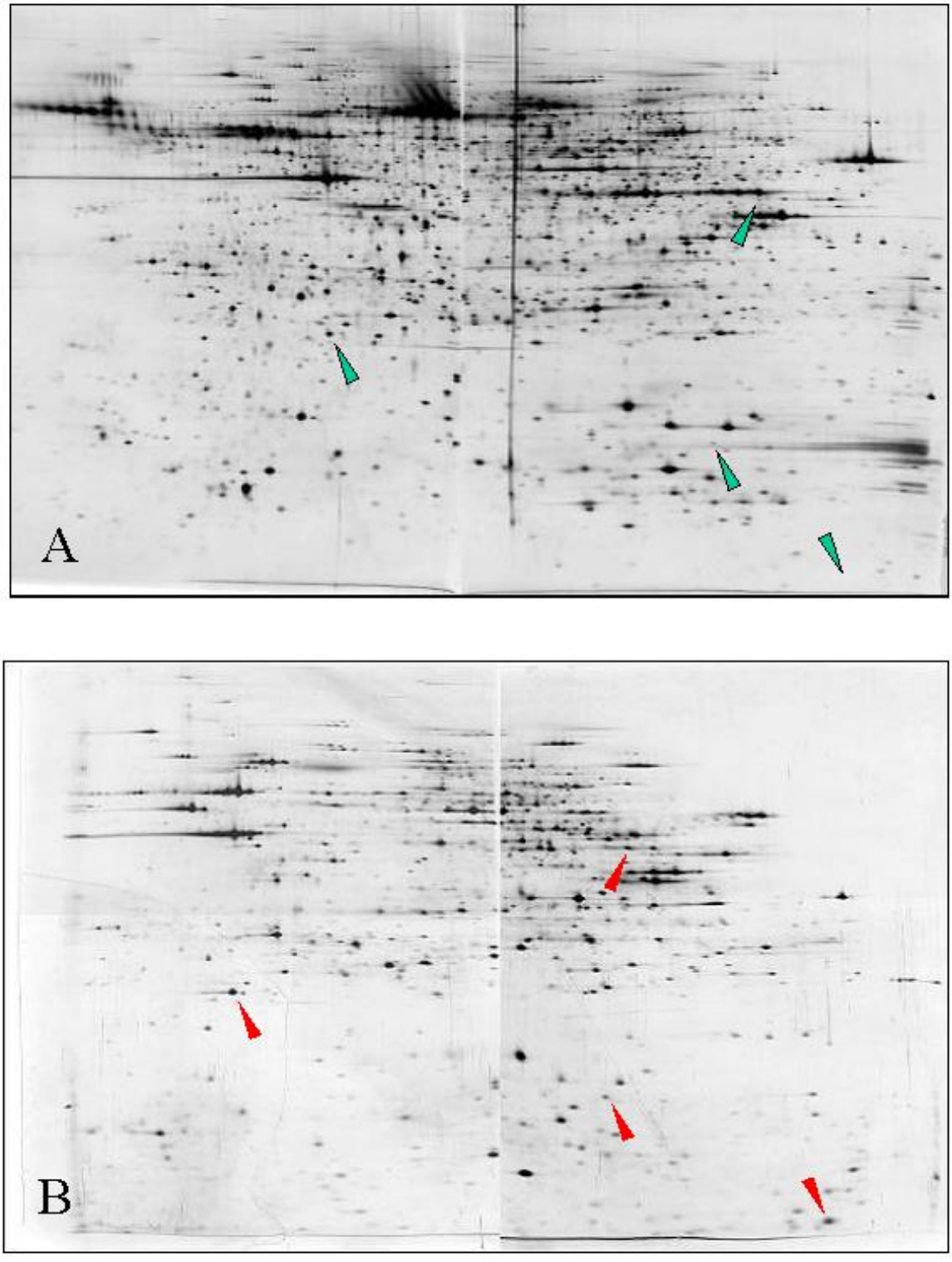

Fig. 4-3: *Comparison of the 2D-electrophoresis maps of lymphoblastoid cells and of isolated mitochondria*. Sub-cellular fractionation can intensify low abundant proteins and let them become visible. (A) depicts the map of lymphoblastoid cells, (B) depicts the map of the mitochondrial subfaction. The red arrows point to some intensified protein spots on the mitochondrial map. The green arrows point to the corresponding spots in the lymphoblastoid map.

Metrizamide. I investigated the pellet of each of the three fractions by electron microscopy (Fig. 3-2). The material of the first fraction contained mainly membranes from both cell and

subcellular organelles. In the second fraction I found a few lysosomes and some other material which was difficult to identify. Only the third fraction was highly enriched in mitochondria. I only used the pellet from the third fraction. The high purity of the mitochondrial fraction was confirmed by the subsequent experiments. Protein analysis by MALDI-TOF mass spectrometry identified only few non-mitochondrial proteins.

4.2 Preparation of protein samples

The protein samples of the mitochondria were prepared according to a protocol by Klose (1999a) (see chapter 3.3). The sample was treated with high concentrations of urea and with a detergent (CHAPS) to solubilize the membrane proteins. The protein concentration of the final sample was measured by using the BCA protein assay method (see chapter 3.4). Fig. 4-4 gives an example of the result of the protein concentration measurement. The concentration of the protein samples of each experiment was around 8-10 mg/ml.

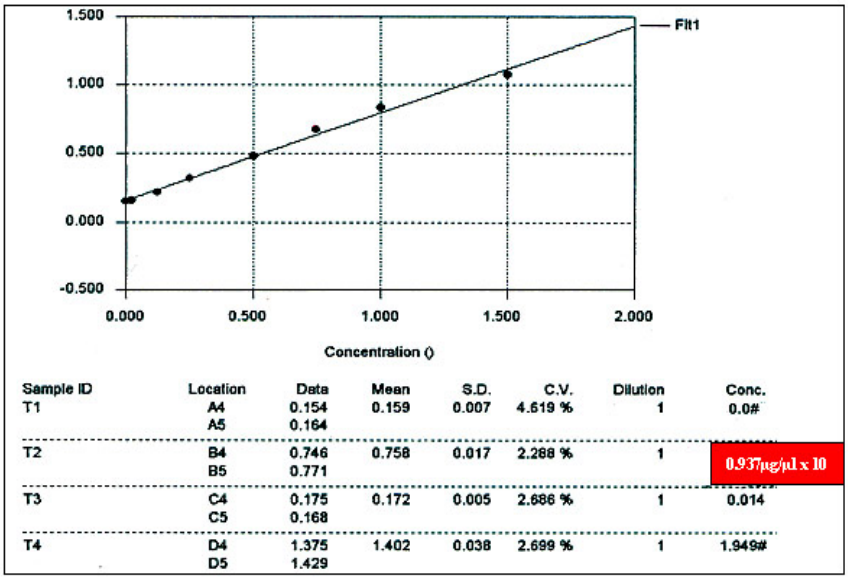

Sample ID	Location	Data	Mean	S.D.	C.V.	Dilution	Conc.
T1	A4	0.154	0.159	0.007	4.619 %	1	0.0#
	A5	0.164					
T2	B4	0.746	0.758	0.017	2.288 %	1	0.937µg/µl x 10
	B5	0.771					
T3	C4	0.175	0.172	0.005	2.686 %	1	0.014
	C5	0.168					
T4	D4	1.375	1.402	0.038	2.699 %	1	1.949#
	D5	1.429					

Fig. 4-4: *Analysis of the protein concentration* with the BCA protein assay. The result has to be multiplied by ten (highlighted with red), since the sample had been diluted 10 times before the measurement.

4.3 2D-electrophoresis of mitochondrial proteins

4.3.1 The pH-gradient of the IEF-gel

The pH-gradient of the IEF-gel was measured as described above (Section 3.5.4.3). The results are shown in Fig. 4-5A. The measured spots tend to lie on a straight regression line (y [pH]= -0.1088x [length of the gel] + 8.8965, starting from the basic end, with a dispersion of R^2=0.939 ($p<0.0001$)). The gradient is linear between the pH-values of 5-9. The effect of the protein sample on the pH-gradient was also investigated (Fig. 4-5B). Despite the fact that the pH-gradient of the protein containing gel fluctuated more than that of the empty gel, the linear regression lines were nearly similar (y = -0.098x + 8.85, R^2=0.922 ($p<0.0001$)). The regression lines, the best fit and the variance were caluclated with the statistic software package “StatView version 4.5.”

4.3.2 Two-dimensional electrophoresis

A total of about 500 µg protein sample was loaded on the anodic end of the isoelectric focussing gel for a thick (1.5 mm) Coomassie stained large gel. In contrast, only one tenth of the protein sample was required for a thin (0.9 mm) silver stained gel. A broad pH-range am-

pholine mixture of pH 2-11 was used for isoelectric focussing in order to get a “panorama view” of the mitochondrial proteins. The isoelectric point of the most acidic spot detectable was at pH 5.00 and that of the most basic one at pH 9.75.

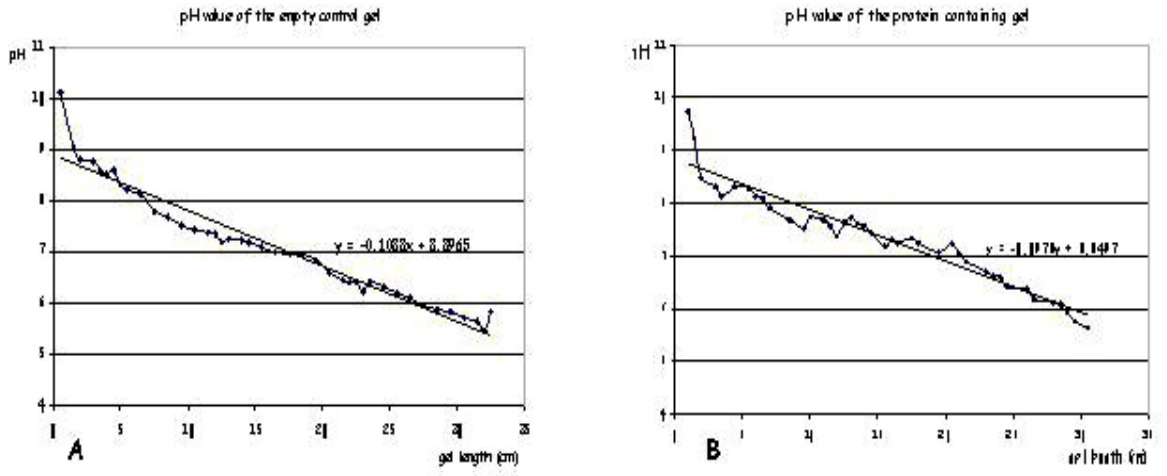

Fig. 4-5A-B: *pH-gradient of 40 cm IEF gels*. The pH-measurement was performed as described in section 3.5.4.3. The results of the empty control gel are depicted in (A). The measured spots tend to lie on a regression line (y = -0.1088x+8.8965, R^2= 0.939 (p<0.0001)). The gradient is linear between the pH-values of 5-9. The effect of the protein sample on the pH-gradient is shown in (B). Although the pH-gradient of the protein containing gel fluctuated more than that of the empty gel, the linear regression lines are similar (y= -0.098x+8.85, R^2= 0.922 (p<0.0001)).

The second dimension gel (SDS-PAGE) was run with a molecular weight standard. The molecular weight range of the standard marker lay between 17.5 and 76 kDa. The reproducibility of the 2D-electrophoresis runs was demonstrated by analyzing an identical sample on four different gels. Most spots were reproduced on each gel except in the case if the extreme ends of the first dimension gels were accidentally lost in the process of expulsion from the glass tube. In Fig. 4-6 a comparison of the same region of the four different gels is shown.

4.3.3 Gel staining

The difference between silver stain and Coomassie stain is that the silver stain is more sensitive but the Coomassie stain has less influence on the proteins. The silver stained gel may show more spots, but for the purpose of protein identification, the Coomassie stain is more favorite since it does not modify the proteins covalently. The silver stain requires only one tenth the amount of protein sample compared to the Coomassie stain. Fig. 4-7 shows the comparison of two gels stained by these two methods. A total of 420 spots could be separated and detected on a silver stained gel from only 50 µg protein sample. In comparison, less than 10 spots were detected on the same gel stained with Coomassie. However, the subsequent protein analysis by MALDI-TOF mass spectrometry showed the drawback of the silver stain. For protein identification a total of 184 spots were excised from two gels stained with colloidal Coomassie brilliant blue. I could identify 115 spots by peptide mass fingerprinting via MALDI-TOF mass spectrometry. The rest of the Coomassie gel was then destained and subsequently restained with silver. The spots now appeared to be much darker than in the preceding Coomassie stain. Additional 300 spots that had not been excised before from the Coomassie-gels were cut out. After reduction of the silver with iodine salt and DTT and subsequent trypsin digestion these spots were also subjected to MALDI-TOF mass spectrometry. In contrast to the spots from the Coomassie gels I could not identify a single spot from the silver stained gel.

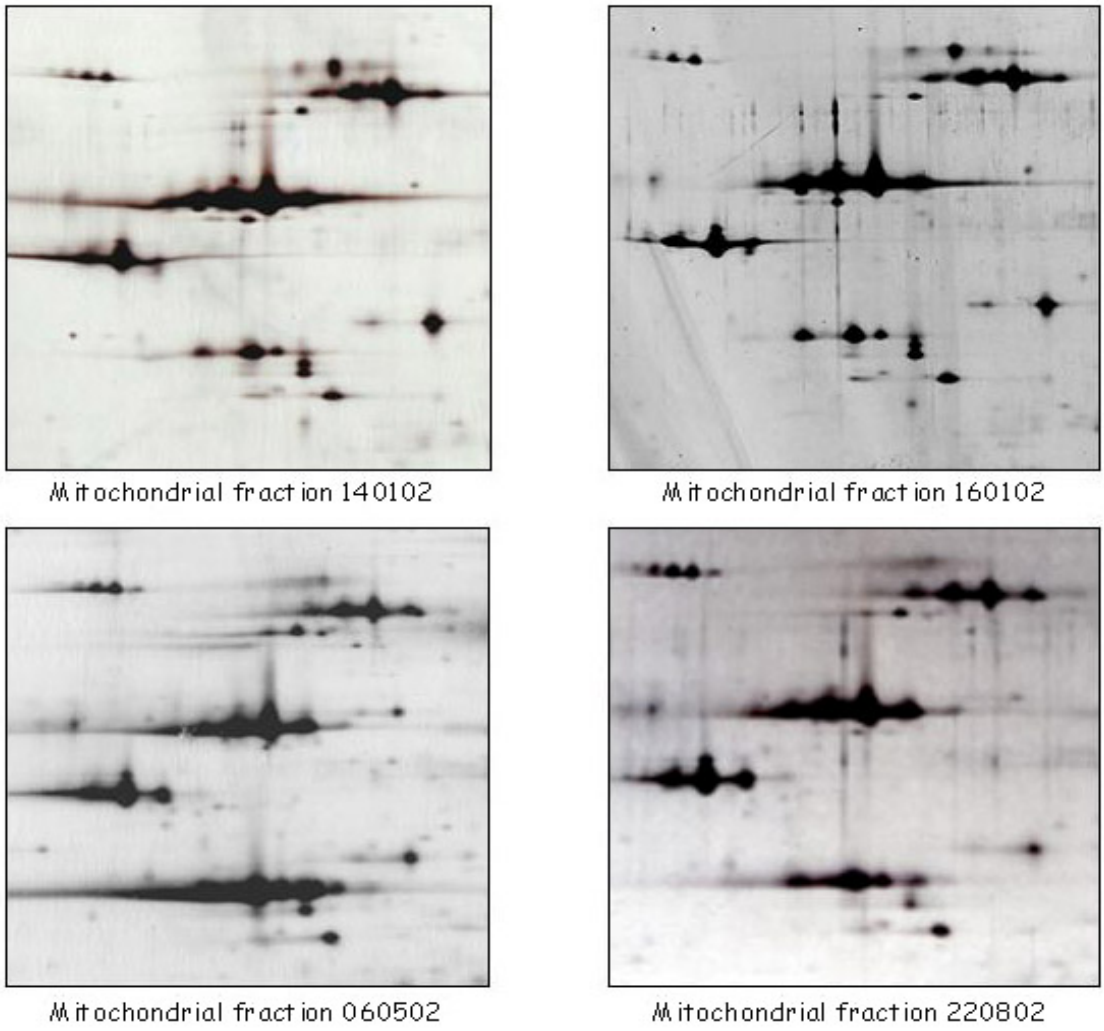

Fig.4-6: These four corresponding gel-sections demonstrate *the reproducibility of 2D-electrophoresis*. All four gels were stained with silver.

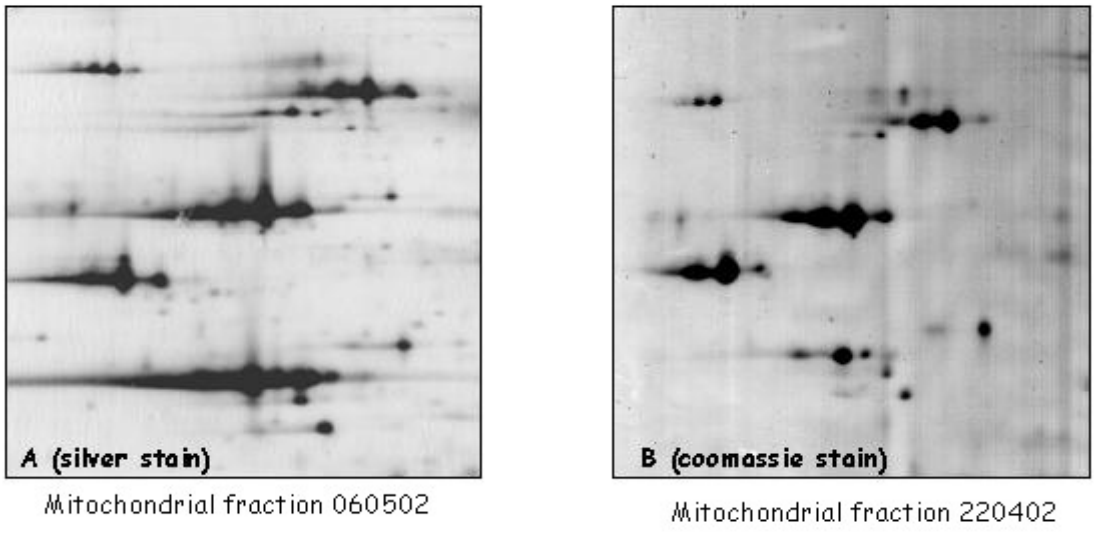

Fig. 4-7: These two gel-sections demonstrate the difference in sensitivity between the silver (A) and the Coomassie G-250-stain (B). Both gels have been run under the same conditions. A total of 525 µg mitochondrial protein were loaded on gel B. In contrast, only 47 µg protein were loaded on gel A. Moreover, it achieved a higher resolution than gel B.

4.3.4 Influence of repeated freezing-thawing cycle on sample quanlity

In order to test the influence of repeated freeze-thaw cycles on sample quality, the same sample was run after the first thawing (gel A) and additionaly after refreezing and rethawing (gel B). Although the amount of sample loaded on gel B was 2 µl more than that of gel A many spots on gel B are much fainter than the corresponding ones on gel A. This experiment demonstrates the loss of proteins during the procedure of repeated freeze-thaw cycles.

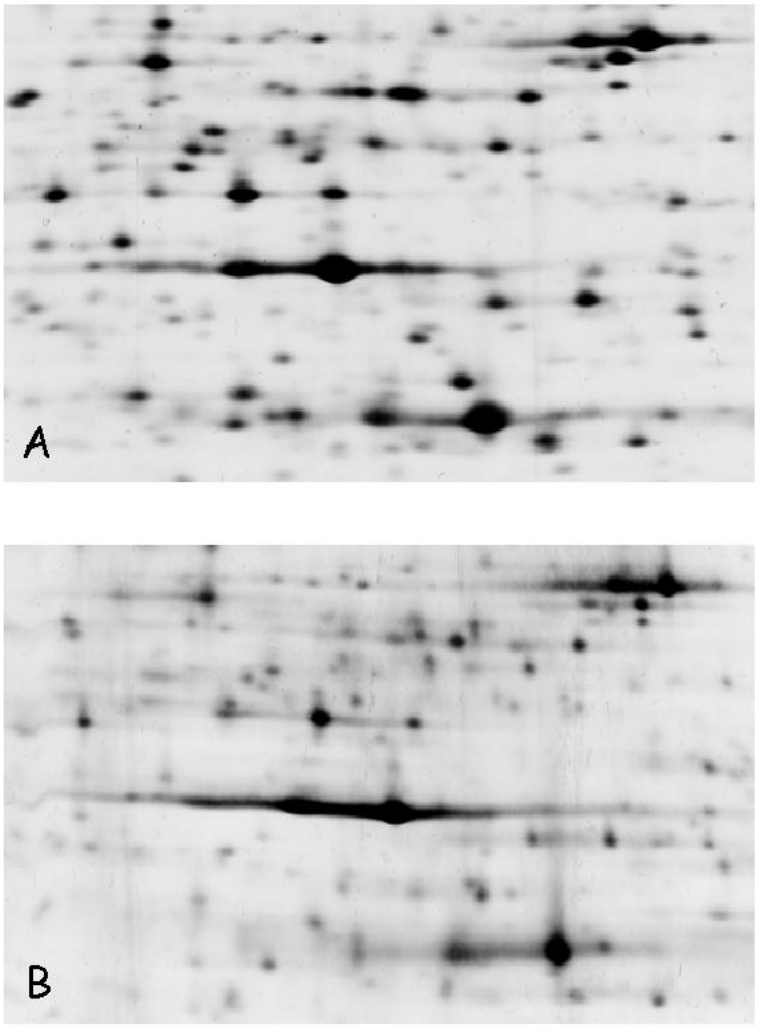

Fig. 4-8: *The effect of repeated freeze-thaw cycles on sample quality*: Comparison of the two gels that have been prepared from frozen stocks. **Gel A** used the sample that was run on the 2D-gel after the first time thawing. **Gel B** used the sample that was run on the 2D-gel after an additional round of freezing and thawing. Although the amount of loaded sample of gel B was 2 µl more than that of gel A, many spots on gel B are much fainter than the corresponding ones on gel A.

4.4 Protein identification

4.4.1 MALDI-TOF and MALDI-QTOF tandem mass spectrometry

The proteins were identified by MALDI-TOF mass spectrometry on the basis of their peptide mass fingerprints, and by MALDI-QTOF tandem mass spectrometry on the basis of their peptide fragment ladders. A total of 184 spots was excised from two large Coomassie-stained 2D-electrophoresis gels. Following in-gel digestion with trypsin, the peptide mixture of each protein was analyzed by MALDI-TOF mass spectrometry (see sections 3.7-3.10).

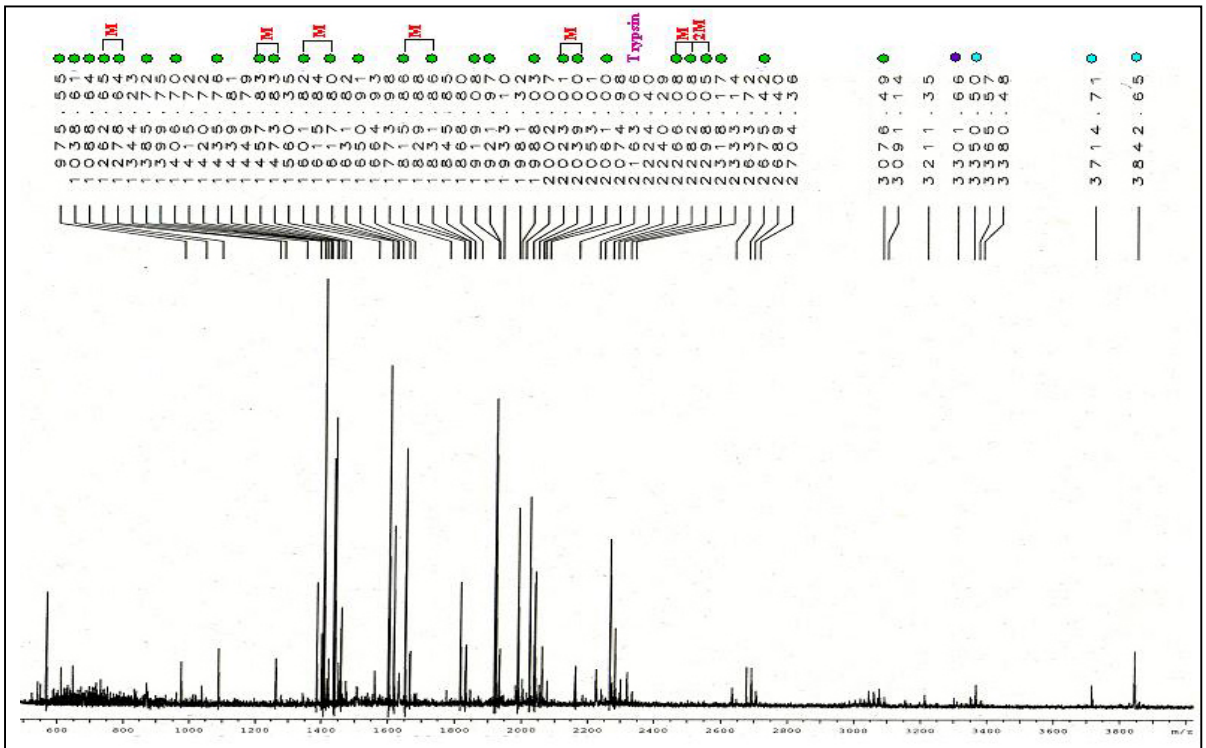

Fig. 4-9: *The mass spectrum of spot 3.* A total of 60 peptides were detected by MALDI-TOF analysis. Using the Mascot search engine, 28 peptides labelled with a green d● ( ) could be matched to the theoretical trypsin digest of the protein (*ATP-synthese beta-chain, mitochondrial precursor*). The parameters for this search were one missed cleavage, possible methionine oxidation and 0.1 Da mass tolerance. All methionine containing peptides and their oxidized derivatives are grouped with the red M (M). The presence of double-peaks separated by 16 Da confirms the presence of methionine residues in the respective peptide fragment. One fragment resulting form trypsin self-digestion is marked with pink color (trypsin). When less stringent criteria were used, some more peptides could be matched. If the mass tolerance is increased to 0.5 Da, additional fragments c●n be matched ( ). If the number of possible missed cleavages is increased to four, an additional large fragme●t can be matched ( ).

Theoretically, all the measured peptide masses should match the corresponding “in silico” digested fragments of a certain protein in the database. However, in the experimental setting the highest percentage of matched peptide masses in my study was 76%. The average percentage of matched peptide masses was 44% and that of the covered sequence was 33%. In order to confirm these primary results, verification of each spot was carried out “by hand”. Fig. 4-9 shows an example using the mass spectrum information of spot 3. Each measured peptide mass was compared to the “in silico” digested ones. The matched peptides were highlighted and marked with a green dot. The methionine containing peptides and their corresponding oxidized derivatives (oxidation of every methionine leads to a mass increase of 16 Da), which strongly confirmed the identity of the peptide, were marked as a group. The peptide masses of the self-digested trypsin fragments were marked as well. Sometimes, in order to match more peptides, less stringent criteria were used. These peptides (e.g. with one or two missed cleavages) were also highlighted. If the mass spectrum was not good enough to secure a protein identity, the amino acid sequence of a single fragment was determined by MALDI-QTOF tandem mass spectrometry. The sequence information could then be used as sequence tag to find the protein in the database.

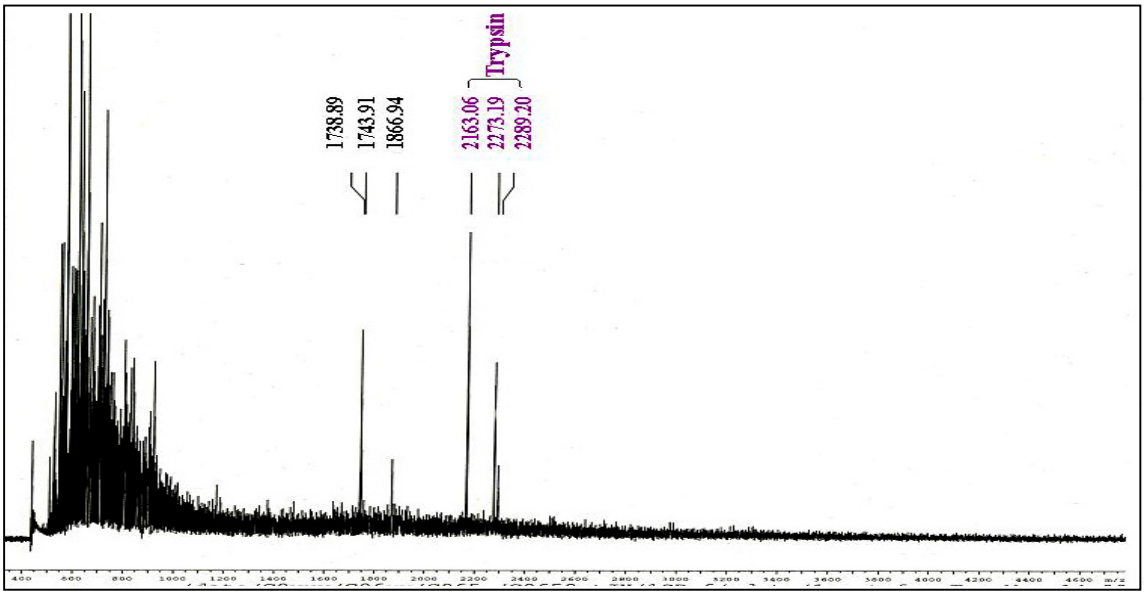

Fig. 4-10A: The mass spectrum of spot 30 measured with MALDI-TOF mass spectrometry. Only 6 peptides were detected including 3 peptides of the self-digested trypsin.

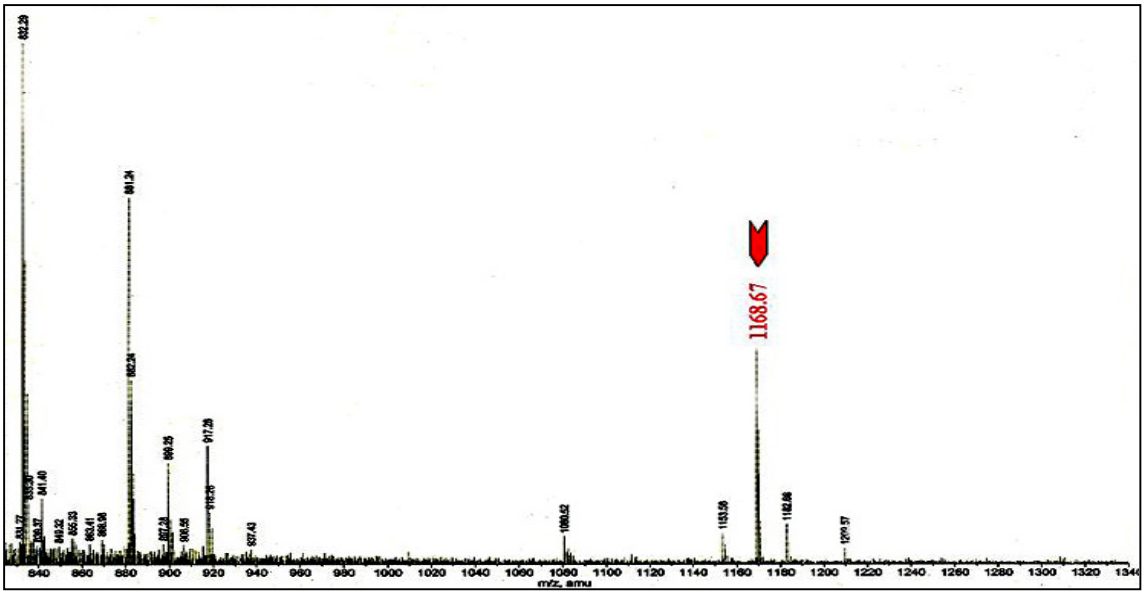

Fig. 4-10B: The mass spectrum of spot 30 after desalting with nano-scale reversed-phase chromatography. A total of 22 peptides was now detected by MALDI-TOF mass spectrometry. One isolated peptide was selected out for further MALDI-QTOF measurement (highlighted with a red arrow). Peptide ladder sequencing had to be performed because this spectrum was still not good enough to identify the protein.

In Fig. 4-10A-D an example of this "manual" process is shown using the mass spectrum information of spot 30. The mass spectrum of spot 30 was not satisfactory when analyzed by MALDI-TOF mass spectrometry. Only six peptides were detected including three peptides generated by trypsin self-digestion. Sometimes salts from the buffer interfere with the MALDI-TOF mass spectrum. Therefore the peptides were first desalted by reversed-phase chromatography (see section 2.4.2). After desalting, a total of 22 peptides of spot 30 could then be detected with MALDI-TOF mass spectrometry. However, since the spectrum

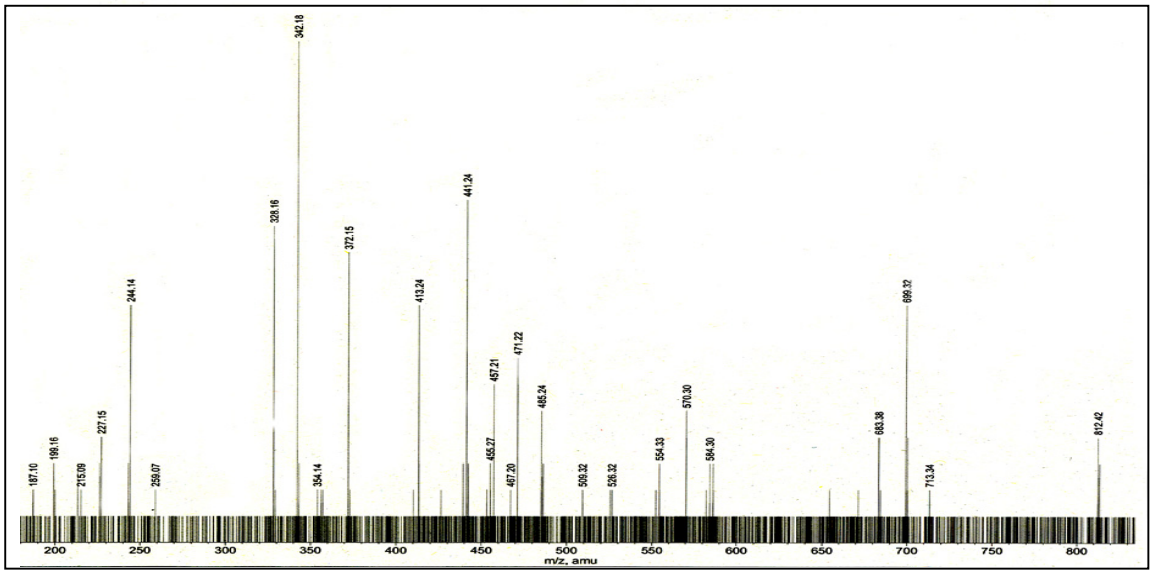

Fig. 4-10C: The mass spectrum of the 1168.67 Da peptide of spot 30 using MALDI-QTOF tandem mass spectrometry. These fragments are used to generate the protein sequence tag by GPMAW32-software on the internet (see following figure).

GPMAW32 Ver. 3.06 [5/14/02]

Sequence:

MS-MS fragmentation on peptide:

ILDVLEEIPK

Mass: 1167.675 Da [Mo.] **[Mass file: AA_MASS]**

A	B	C“	Res:	X	Y“	Z
86.097	114.092	165.124	Ile	-	-	-
199.181	227.176	278.208	Leu	1081.578	1055.599	1036.556
314.208	342.203	393.235	Asp	968.494	942.515	923.472
413.276	441.271	492.304	Val	853.467	827.488	808.445
526.360	554.355	605.388	Leu	754.398	728.419	709.377
655.403	683.398	734.430	Glu	641.314	615.335	596.293
784.446	812.441	863.473	Glu	512.272	486.293	467.250
897.530	925.525	976.557	Ile	383.229	357.250	338.208
994.582	1022.577	1073.610	Pro	270.145	244.166	225.124
1122.677	1150.672	1201.705	Lys	173.092	147.113	128.071

Fig. 4-10D: The sequence result of the isolated 1168.67 Da peptide of spot 30. The peptide fragment ladders were obtained by the MALDI-QTOF mass spectrometry. This sequence tag was later used for database searching in order to identify the protein.

of 22 peptide fragments was still not good enough to identify the protein, MALDI-QTOF analysis had to be carried out on one isolated peptide. The sequence result of the isolated polypeptide of spot 30 led to the identification of the *13 kDa subunit of complex-I*. I identified a total of 115 protein spots that corresponded to 95 different proteins. Most of them were identified by MALDI-TOF mass spectrometry, only five spots needed to be analyzed with MALDI-QTOF tandem mass spectrometry. In Fig. 4-11 the strategy of protein identification is illustrated.

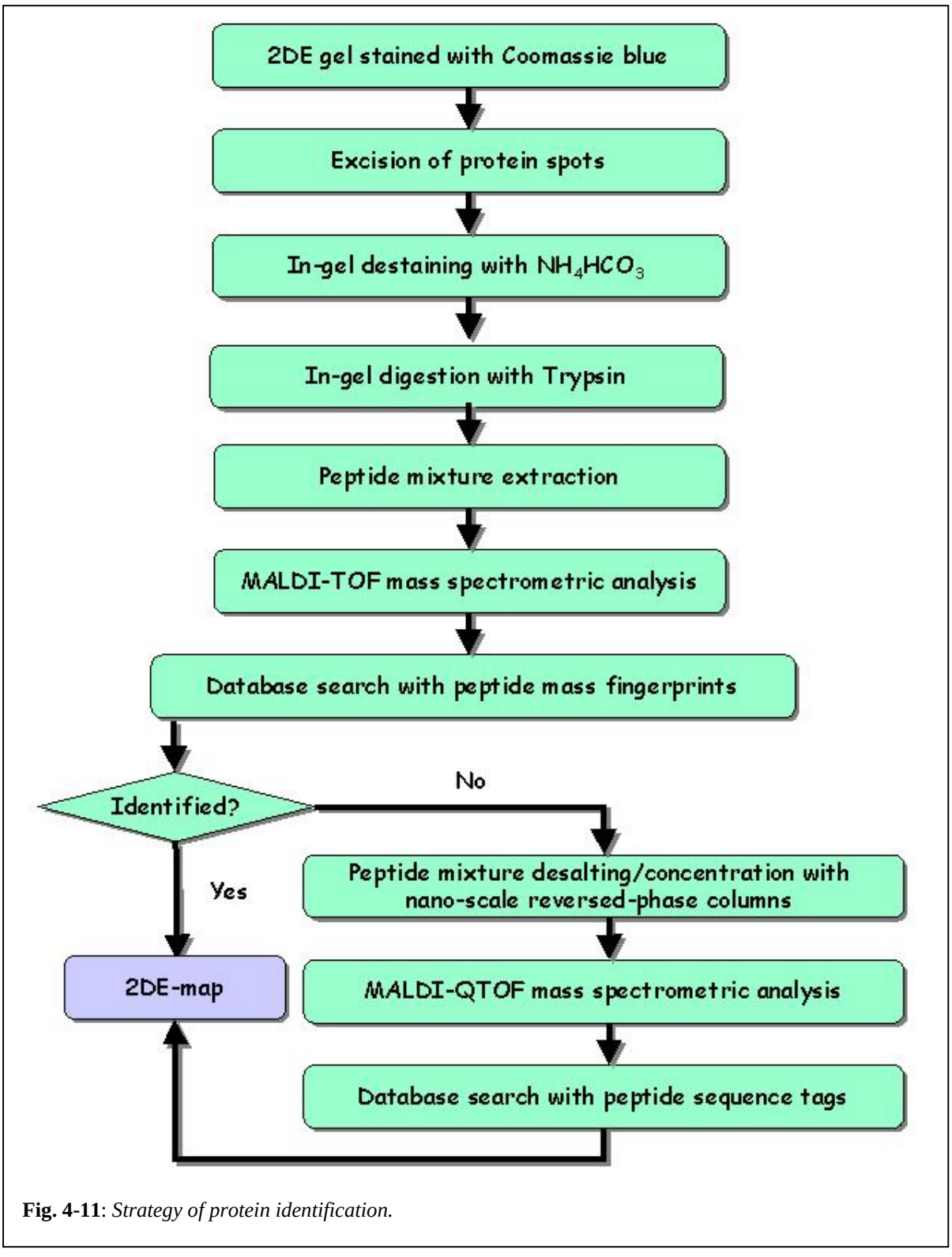

Fig. 4-11: *Strategy of protein identification.*

4.4.2 Database search for protein identification

I used several search engines on the internet including Mascot, ProFound, and MS-Fit. These programs match the peptide masses from a protein spot with the "in silico" digested peptide masses of all known human proteins in the National Centre for Biotechnology Information non-redundant (NCBInr) protein database. At least five or more matching peptides were re-

quired for a secure identity assignment. With the Mascot search engine, most samples could be identified satisfactorily with a significant probability score ($p<0.05$). However, several spectra had to be handled with other search engines like ProFound and MS-Fit. A total of eight spots could be identified additionally that way. As mentioned above there were still five spots that could only be identified by their peptide sequence information gained from MALDI-QTOF tandem mass spectrometry. Finally I identifie 115 spots, which are listed in Tab. 7-1. The theoretical and the experimental molecular weights (*MW*) and isoelectric points (*pI*) of the identified proteins, their corresponding SWISS-PROT accession numbers are also listed, along with the data from the mass spectrometric analysis; i.e. the numbers of matching peptides, the sequence coverage (in percent) and the probability of assignment of a random identity.

4.5 Mitochondrial proteome reference map

4.5.1 Mitochondrial proteome reference map

Fig. 4-12 shows a representative mitochondrial proteome map from human lymphoblastoid cells. All of the identified spots are highlighted in red with the corresponding spot number near them. The *pI* and *MW* are shown as well. The detailed information of the proteins is listed in Tab. 7-1 and also labelled directly in the 12 sectors of the reference map (see supplementary meterial: Fig. 4-12#1 to 4-12#12). A total of 184 spots from two Coomassie stained gels (corresponding to 141 different spots) resulted in the identification of 115 spots (corresponding to 95 different proteins). Out of the 400 visible protein spots on the silver gel I thus could identify 20%. Among the 95 identifed proteins, 77% (n=74) were annotated according to NCBI and SWISS-PROT databases, as mitochondrial proteins. Although our mitochondrial fraction was highly purified, it still contained some proteins from other subcellular organelles. In our sample, 15 spots corresponding to 11 different gene-products belong to subcellular components other than the mitochondria. The location of them is indicated below. There are ten proteins remaining whose functions and/or localization are unknown. For four of them (spots 46, 73, 129, 131) were only found as ESTs in the databases. All of the identified spots are grouped in Tab. 4-1 according to their location and function. The 25 spots that did not give a result on MALDI-TOF mass spectrometry were very weak spots that contained too little protein to produce a satisfactory spectrum.

4.5.2 Locations of the identified proteins

Based on the annotation in the NCBI and SWISS-PROT databases, a total of 74 identified proteins out of 90 spots were annotated as “mitochondria-associated” proteins. 27 of these proteins are located in the mitochondrial matrix, 16 in the mitochondrial inner membrane, 2 in the mitochondrial outer membrane, and 2 in the mitochondrial inter-membrane space. The remaining 27 proteins are surely mitochondrial proteins, however, their exact subcellular location is not clear. A total of eleven proteins out of 15 spots are located elsewhere. Seven of them are located in the cytoplasm, three at the endoplasmic reticulum, and one is known as B-cell-associated protein. The subcellular location of ten proteins is unknown. These data are listed in detail in Fig. 4-13 and in Tab. 4-2.

4.5.3 Functions of the identified mitochondrial proteins

According to the annotation in SWISS-PROT and to the classification system of MITOP, I sorted the identified mitochondrial proteins. The sorting is based on the protein function and is summarized in Tab. 4-1. Most of these proteins (59 proteins) are part of central metabolic

pathways, including the citric acid cycle, the pyruvate dehydrogenase complex, the respiratory chain, the β-oxidation, protein assembly or catabolism (urea cycle). Another group of proteins are transport proteins (seven proteins). Proteins that have a role in cell protection or apoptosis or heme- biosynthesis or cell maintenance, are grouped in "other functions" (eight proteins). The function of only one protein, the *ES1 protein homologue mitochondrial percursor*, is not yet characterized. However, this protein is assumed to play an important role, since a homologous protein has been identified in the zebra fish (*Danio rerio*) and in *Escherichia coli*. One of the most important functions of the mitochondrion is the oxidative phosphorylation at the respiratory chain. 16 of the identified proteins are part of its five protein complexes. Seven proteins belong to complex I, three proteins belong to complex III, two to complex IV, and four proteins are subunits of complex V. I detected no protein subunit of complex II.

4.5.4 Identified membrane proteins

In order to identify putative transmembrane proteins, I analyzed all of the identified proteins with a transmembrane prediction software (SOSUI), which predicts the transmembrane helices by calculating the hydrophobicity, the amino acid charges and the sequence length of a candidate peptide. Although about one third of the identified proteins are membrane-associated proteins located either at the inner membrane (27 proteins) or at the outer membrane (two proteins) of the mitochondrion, only four of them are really transmembrane proteins with one or two transmembrane helices. These are spot 13 (GTP-specific succinyl-CoA synthetase beta-subunit), spot 75 (NADH-ubiquinone oxidoreductase (complex I) B16.6 kDa subunit), spot 90 (isocitrate dehydrogenase, gamma-subunit), and spot 134 (sideroflexin 1). The location of these spots is highlighted in Fig. 4-14.

4.5.5 Multiple spot proteins

A total of 17 proteins on the reference map could be detected in more than one spot (Fig. 4-15). The majority of the multiple spot proteins are most probably isoforms, such as spots 9 and 10 (HSP 60 kDa), spots 11 and 12 (actin-beta), spots 34 and 118 (succinyl CoA: 3-oxoacid CoA transferase), spots 36 and 47 (ATP synthase, H+ transporting F1), spots 37, 123 and 124 (medium-chain acyl CoA isomerase), spots 38 and 39 (similar to delta 3,5-delta 2,4-deinoyl-CoA isomerase), spots 40 and 128 (electron-transfer-flavoprotein, alpha subunit), spots 48 and 49 (glutamate dehydrogenase 1), spots 50 and 51 (Tu translation elongation factor), spots 52 and 67 (acetoacetyl-CoA thiolase), spots 53 and 69 (voltage-dependent anion channel 1), spots 63 and 66 (complex III subunit II), spots 81 and 82 (isocitrate dehydrogenase), spots 85 and 87 (malate dehydrogenase 2), and spots 88 and 89 (glyceraldehyde-3-phosphate dehydrogenase). Spots 5 and 31 (complex IV, subunit Va) correspond to same gene product but have markedly different *pI* and *MW*. Similar to that, spot 114, which was identified by sequence information, corresponds to the same gene product as spots 11 and 12 (actin-beta). Spot 26 was at first identified as an unkown protein for (MGC:9832). After sequence alignment of the amino acids with the help of the protein-BLAST program (see list of internet sites), it was finally verified to be a short isoform of actin-beta.

4.5.6 Comparison of theoretical and the experimental *pI* and *MW*

The theoretical *pI* and *MW* of proteins shown in my protein list were calculated with the "Compute *pI*/*MW*" tool of the SWISS-PROT database. This tool calculates the *pI* of a protein

by calculating the mean of the pK values of its amino acids as described by Bjellqvist *et al.* (1993). The *MW* of a protein was calculated as the sum of the average isotopic masses of

function	spot #	number of spots	*number of proteins*
mitochondrial		**90**	***74***
respiratory chain		**19**	***16***
complex I	[6] [29] [30] **[75]** [126] [137] [138]	7	*7*
complex II	no		
complex III	[25] [55] [63]/[66]	4	*3*
complex IV	[5]/[31] [56]	3	*2*
complex V	[3] [18] [36]/[47] [106]	5	*4*
fat metabolism		**19**	***13***
ß-oxidation	[28] [37]/[123]/[124] [38]/[39] [40]/[128] [52]/[67] [54] [65] [79] [92] [133]	15	*10*
other proteins for fat metabolism	[34]/[118] [45] [64]	4	*3*
nucleotide metabolism		**5**	***5***
	[61] [74] [93] [135] [130]	5	*5*
protein metabolism		**14**	***12***
	[20] [35] [43] [48]/[49] [50]/[51] [84] [91] [119] [122] [125] [127] [140]	14	*12*
carbohydrate metabolism			
	[13] [15] [24] [27] [32] [60] [62] [80] [81]/[82] [83] [85]/[87] **[90]**	**14**	***12***
transport proteins		**10**	***7***
HSP	[7] [9]/[10] [33] [58]	5	*4*
VDAC	[53]/[69]	2	*1*
TOM	[67/2]	1	*1*
TIM	[21]/[22]	2	*1*
other functions		**9**	***9***
cell protection	[41] [72] [121]	3	*3*
heme biosynthesis	[68]	1	*1*
apoptosis	[44]	1	*1*
sulfide oxidation	[132]	1	*1*
iron transport	**[134]**	1	*1*
maintenance and cell growth	[70]	1	*1*
unknown	[71]	1	*1*
other compartments		**15**	***11***
cytoplasmic	[11]/[12]/[26]/[114] [16] [86] [88]/[89] [96] [101] [120]	11	*7*
endoplasmic reticulum	[1] [23] [42]	3	*3*
B-cell-specific	[103]	1	*1*
location unknown		**10**	***10***
function unknown	[2] [46] [73] [105] [129] [131] [136]	7	*7*
nucleotide metabolism	[117]	1	*1*
HSP	[8] [14]	2	*2*
Total		**115**	***95***
membrane proteins	***[13] [75] [90] [134]***	***4***	***4***

Tab. 4-1: Sorting of the identified proteins according to their subcellular locations and functions. Proteins with transmembrane domains predicted by the SOSUI-algorithm are listed and highlighted separately.

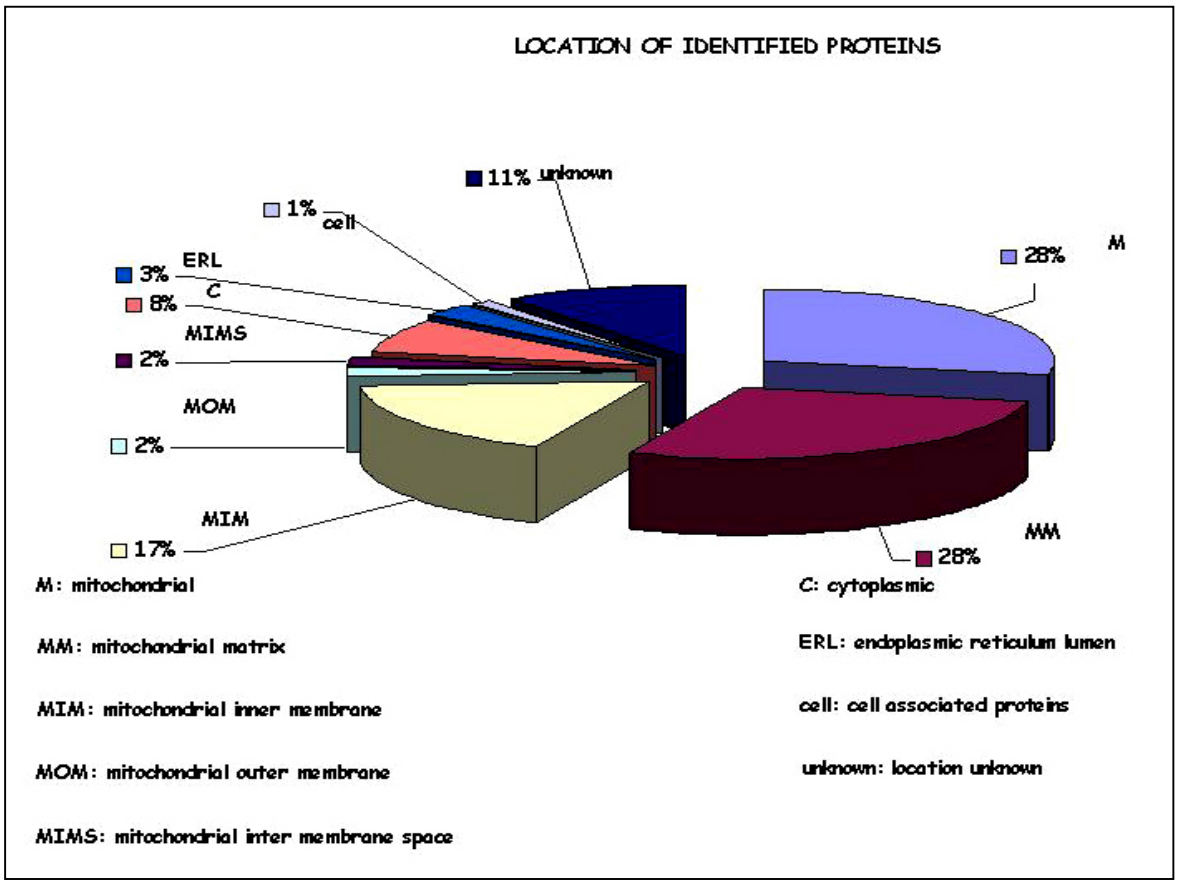

Fig. 4-13: Classification of the identified proteins according to their location. The mitochondrial group (M) includes those proteins that are definitively mitochondrial but for which no further information exists on their exact location.

location	spot number	protein number	percent
mitochondrial total	**90**	**74**	**77%**
M: mitochondria	31	27	28%
MM: mitochondrial matrix	36	27	28%
MIM: mitochondrial inner membrane	18	16	17%
MOM: mitochondrial outer membrane	3	2	2%
MIMS: mitochondrial intermembrane space	2	2	2%
other compartments	**15**	**11**	**12%**
C: cytoplasmic	11	7	8%
ERL: endoplasmic reticulum lumen	3	3	3%
cell: cell associated proteins	1	1	1%
location unknown	**10**	**10**	**11%**
Total	**115**	**95**	**100%**

Tab. 4-2: Classification of the identified proteins according to their location. The mitochondrial group (M) includes those proteins that are definitively mitochondrial but for which no further information exists on their exact location.

amino acids in the protein and the average isotopic mass of one water molecule.

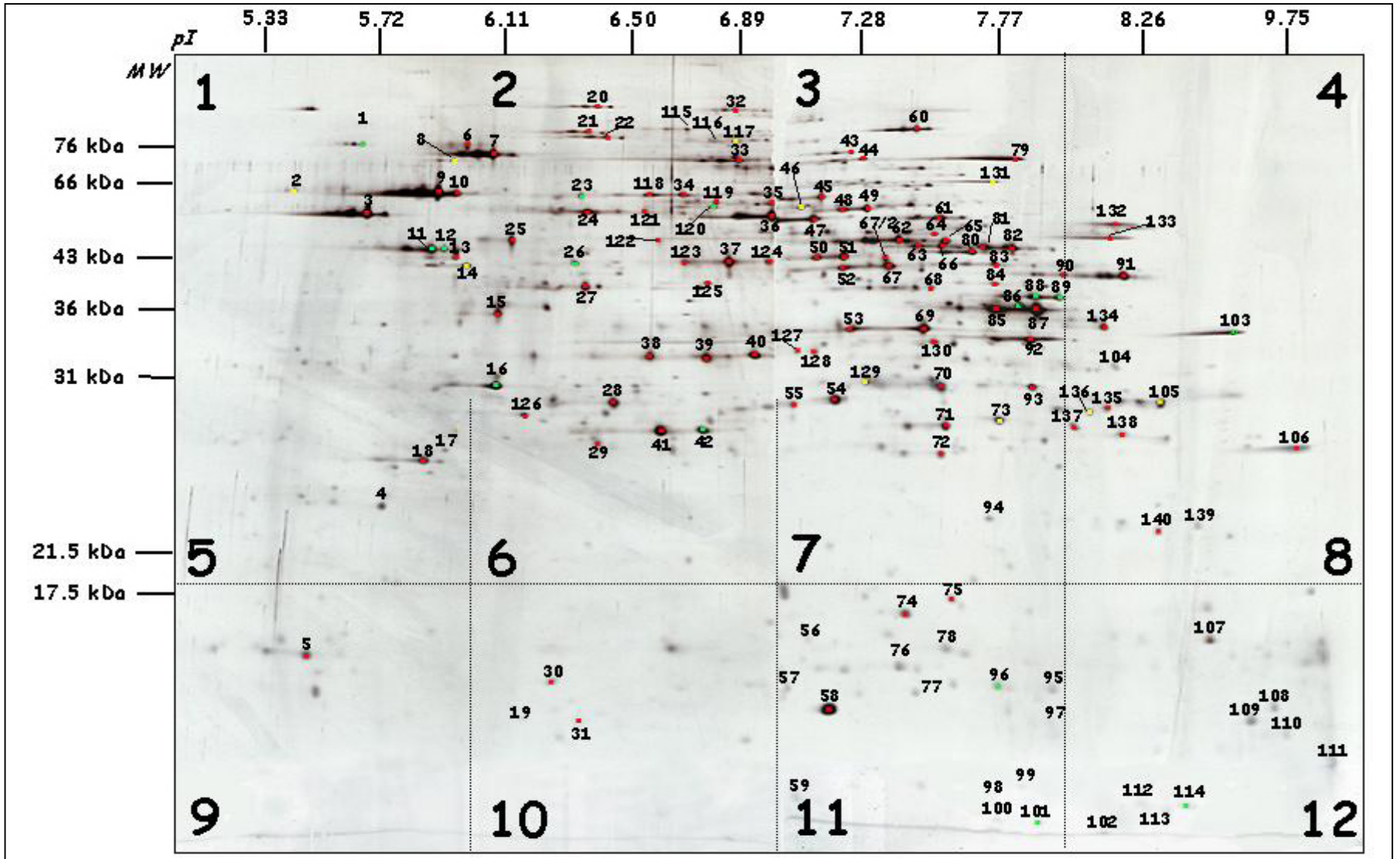

Fig. 4-12: *The reference map of the mitochondrial proteome from human lymphoblastoid cells.* All the measured spots are highlighted (red: mitochondrial proteins; green: other cytoplasmic proteins; yellow: proteins which locations remain unknown). The corresponding spot numbers are shown at the spots. The *MW* and *pI* ranges of the whole gel are shown at the left and above the gel.

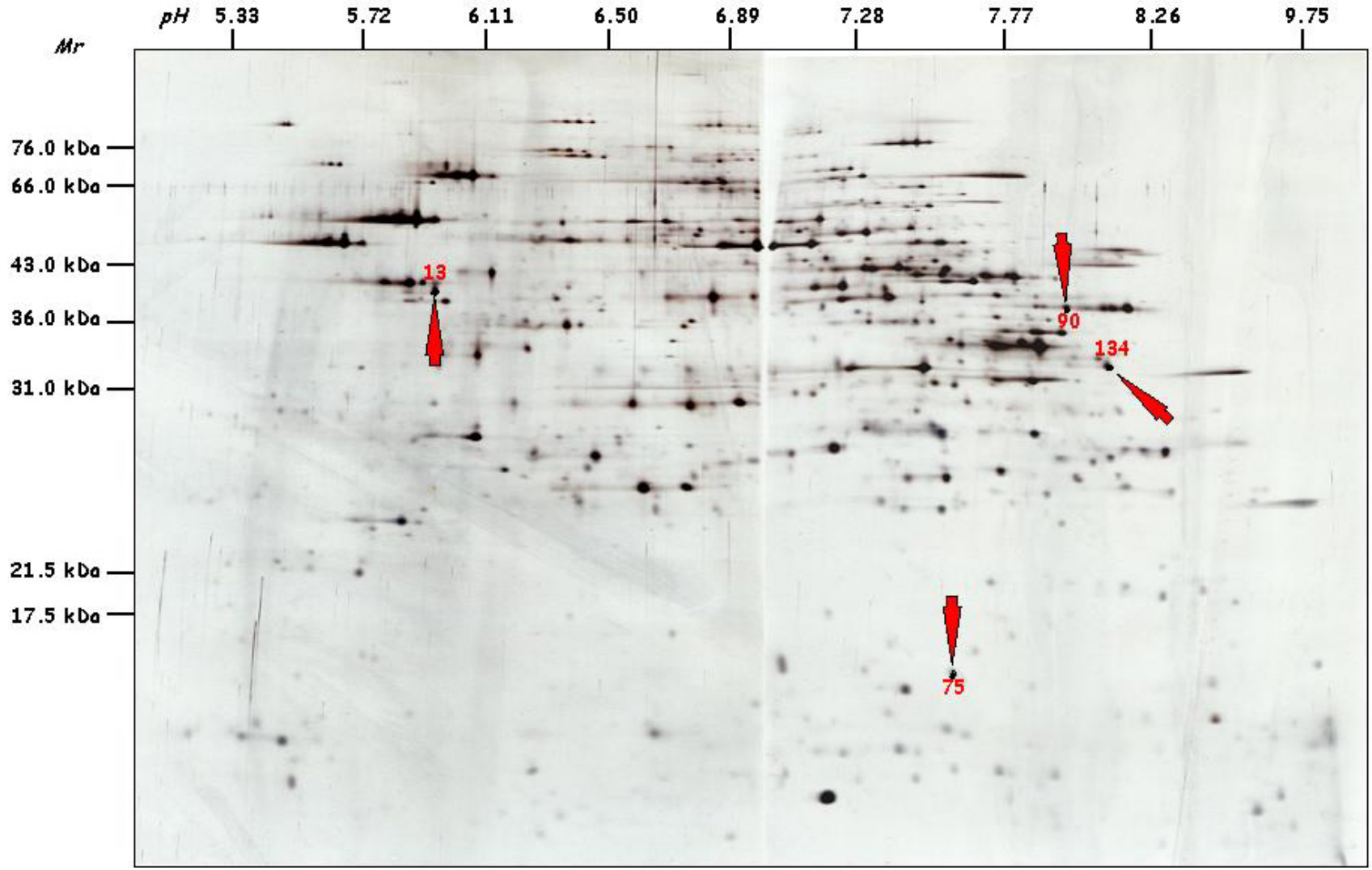

Fig. 4-14: *Identified mitochondrial membrane proteins.* Among the 74 identified mitochondrial proteins, only four carry transmembrane domains. One spot (#75) belongs to complex I of the respiratory chain, other two spots (#13 and #90) function in the citrate acid cycle and the fourth spot (#134) is an iron transport protein.

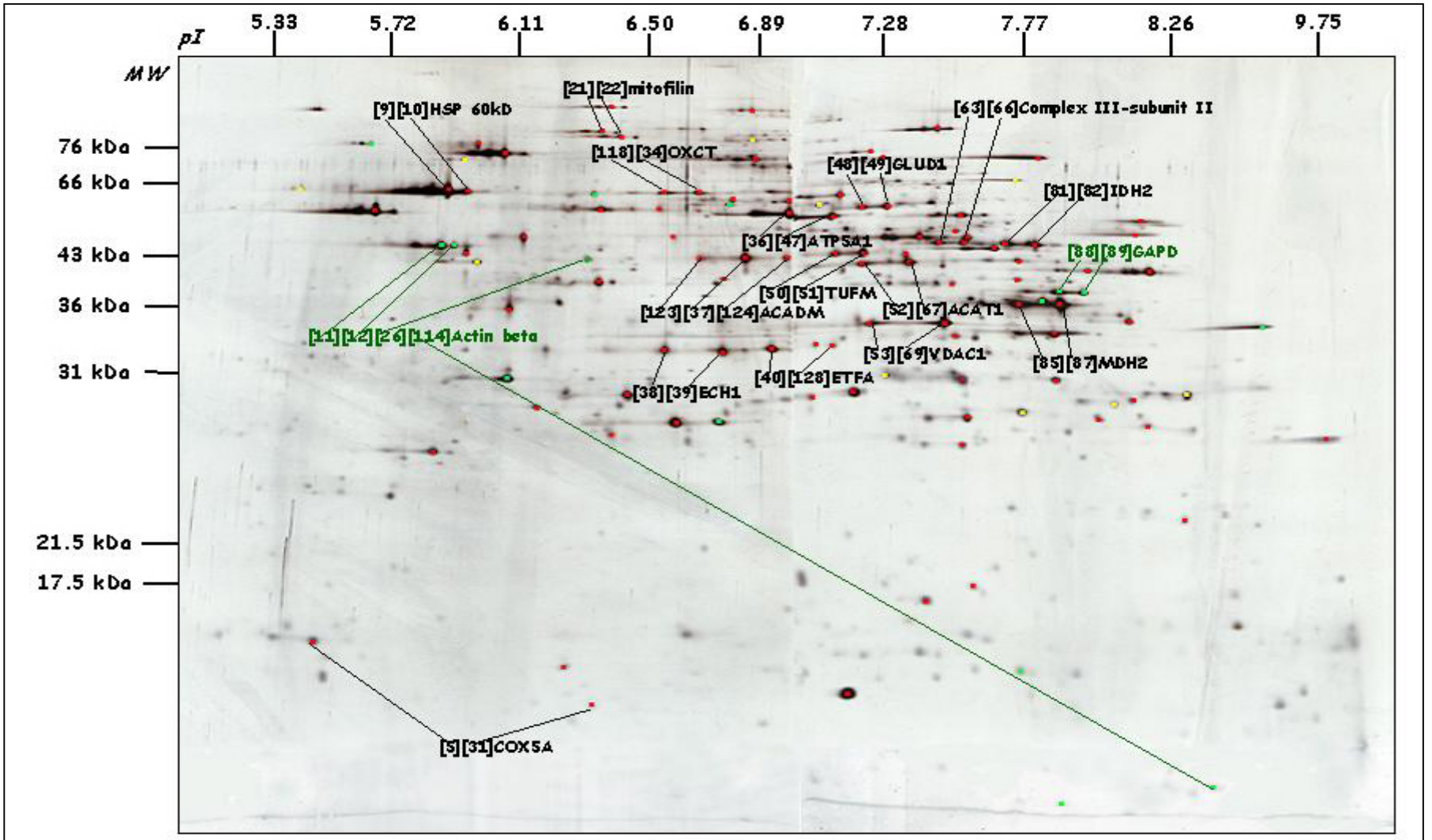

Fig. 4-15: *multiple spots proteins*. A total of 17 proteins on the reference map could be detected in more than one spot. Most of the multiple spot proteins are probably isoforms of the same proteins. However, spots 5 and 31 (complex IV, subunit Va) correspond to the same gene but show a marked difference in *pI* and *MW*. Similar to that, spot 114 that was identified by sequence information, corresponds to the same gene as spots 11 and 12 (actin-beta). Spot 26, which originally corresponded to a unknown protein, was finally identified to be a short isoform of actin-beta.

The experimental *pI* of each protein was calculated by using the regression formula that I had obtained from the measurement of the pH gradient (see section 4.3.1). Similar to that, the experimental *MW* was calculated with the regression formula derived from a series of *MW* standard markers. The correlation between the experimental and the theoretical *pI* and *MW* values was analyzed with the ANOVA statistics software (Fig. 4-16). The correlation between the coupled *pI* or *MW* values was tested by the coupled t-test. The correlation coefficient (R) of the coupled *pI* values is equal to 0.873 ($p<0.0001$) and that of the *MW* values is equal to 0.941 ($p<0.0001$). The absolute differences between theoretical and experimental *pI* values are between 0.01 and 1.81 pH values. (median = 0.69 pH values, interquartile distance = 0.35 pH values). Similar to that, the absolute differences between theoretical and experimental *MW* values are between 0.08 to 43.09 kDa (median = 3.48 kDa, interquartile distance = 3.76 kDa).

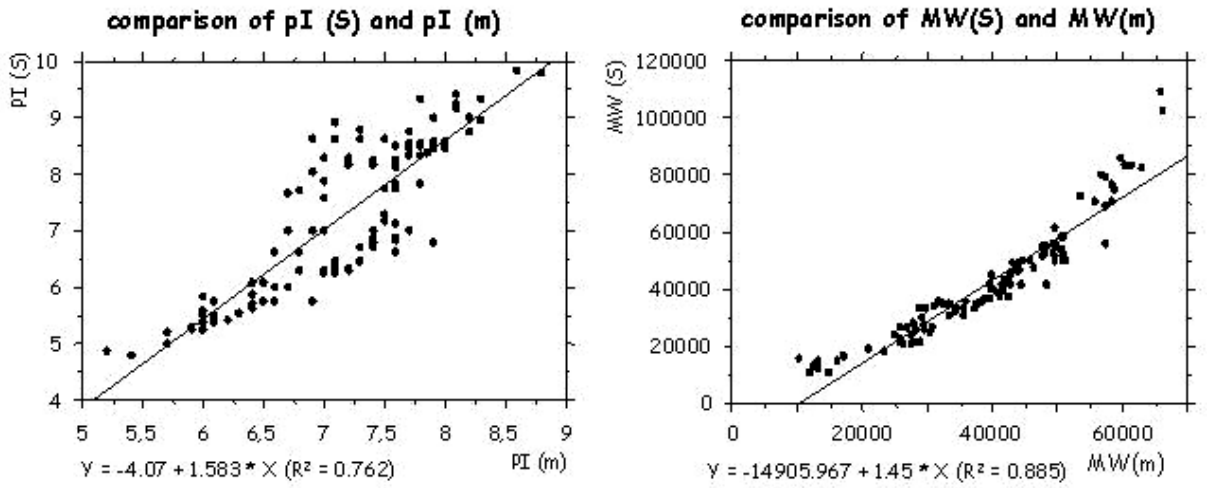

Fig. 4-16: *Comparison of the theoretical and experimental pI and MW of the identified proteins.* The left regression diagram depicts the relation of the *pI* values between the measured values (m) and the theoretical calculations (S). Similar to that, the right regression diagram depicts the relation between the two different *MW* values. The linear regression formulas and the lateral dispersion (R^2) are depicted below the diagrams.

5 DISCUSSION

5.1 Choice of material

The aim of this study was to establish a reference 2D-electrophoresis map of the human mitochondrial proteome that could be used in subsequent studies to identify patients with mitochondrial disease. I chose immortalized lymphoblastoid cells as the material to investigate. Compared to other possible materials like muscle cells and fibroblasts, lymphoblastoid cells can be more easily obtained from patients. Routinely, 5-10 ml heparinized whole blood are sufficient to establish a permanent cell culture. This procedure is more acceptable to parents and children as compared to muscle or skin biopsies. Lymphocytes can be cultured in vitro which allows the yield of enough material for my investigation. Since the cells can grow in suspension, high cell density can be obtained without too much expenditure of work and cost. Lymphoblastoid cells are transformed with Epstein-Barr Virus (EBV) for immortalization. EBV-transformation as compared to SV40-transformation has the advantage of higher chromosomal stability during subsequent passages [Jha *et al*., 1998]. Another advantage of lymphoblastoid cells is that they express a respiratory chain defect – in contrast to fibroblasts – more frequently [Bourgeron *et al*., 1993]. Although the number of mitochondria in lymphocytes (about 15-20/cell) is far lower than that in liver cells (2,200/cell [Rohr *et al*., 1976]), the easier access to lymphoblastoid cells compared to liver cells counterbalances this shortcoming.
In recent years, several studies of the human mitochondrial proteome have been carried out on other materials like placental cells, transmitochondrial cybrids and neuroblastoma cell lines [Rabilloud *et al*., 1998 and 2002; Lopez *et al*., 2002; Fountoulakis *et al*., 2003]. However, for diagnostic purposes these cells are generally not available. In contrast, lymphoblastoid cells can be obtained from any patients at any age without anaesthesia. This also allows the study of mitochondrial proteins in normal control individuals at different age-groups in order to find out age-related changes. Additionally it also allows investigation of the genetic variability in a larger number of control patients at any given age.

5.2 Mitochondrial isolation

Isolation of mitochondria is the first step to investigate mitochondrial function in vitro and to analyze their proteome. Subfractionation of cellular components can intensify the low-abundance proteins and make their detection easier. The effect of enrichment of mitochondrial proteins is illustrated in Fig. 4-3. The number of spots in the mitochondrial gel is distinctly reduced compared to that of the gel from whole lymphocyte proteins. The background noise and the complexity of the sample are thus reduced. This simplifies and focusses the study on the mitochondrial proteome. I have introduced several modifications to standard protocols in my experiment in order to solve some basic problems of mitochondrial isolation. First of all, in order to disrupt the cell membrane more easily, the use of digitonin is necessary. However, this membrane destabilizing agent disrupts membranes indiscriminately, i.e. the membrane of subcellular organelles can be attacked as well. Bronfman *et al.* (1998) found out that subcellular organelles are only affected if the concentration of digitonin is higher than 0.5-1.0 mg/ml. I therefore used only low concentrations of digitonin (0.1 mg/ml). The electron microscopic photographs of the mitochondrial pellet demonstrate that most of the mitochondria have intact inner and outer membranes. The slight swelling of the mitochondria may be due to the lower osmotic pressure of the used buffer. Secondly, I repeated the mechanical homogenizing cycle three times to insure the disruption of all cells. After the third round of homogenization about

97% cells were disrupted. The number of repetitive homogenizing cycles depends not only on the type of biological material but also on the type of pestle and on the rotating speed of the homogenizer. Thirdly, I separated mitochondria from other subcellular organelles by centrifugation on a discontinuous hybrid density gradient. Since the densities of mitochondria and lysosomes are very close to each other (1.11 g/ml of mitochondria versus 1.07 g/ml of lysosomes), the separation of these two fractions is of special importance. For this task standard protocols suggest the use of a continuous Percoll gradient which forms during centrifugation. However, this method did not lead to a satisfactory result. Since the density-gradient was continuous, more than five bands were formed after centrifugation. Three of them were the mitochondrial bands and lay very close to each other. In addition the mitochondrial band was too broad. Therefore, it was difficult to assure the purity of the product, especially when the original material was limited. So I opted for a discontinuous gradient (35% and 17% metrizamide and 6% Percoll, with the densities 1.1304 g/ml, 1.1029 g/ml and 1.0331 g/ml), in order to separate the mitochondria from the lysosomes sharply at two different interfaces. The electron microscopic photographs of the products from each interface confirmed that they contained the expected subcellular fractions. Disadvantage of the discontinuous gradient is the high cost of the metrizamide and the additional work to prepare the gradient.

5.3 Two-dimensional electrophoresis

5.3.1 The choice of carrier ampholytes for isoelectric focussing.

I used carrier ampholytes for isoelectric focussing instead of commercially available immobilized pH-gradients. In Tab. 5-1 the advantages and disadvantages of these two methods are compared. Several advantages for my special task made me to use carrier ampholytes to run IEF-separations. A very good protein resolution can be expected by using long

Carrier ampholytes	**Immobilized pH-gradients**
excellent protein resolution	good protein resolution
the pH-gradient may drift depending on the time of electrophoresis	the pH-gradient is stable
variable gel-lenghts can be prepared	only commercially available gel-lengths can be chosen
easy blending of a ampholytes according to the pH-range of interest	self preparation not possible
special experience needed	easier to handle
good reproducibility (thin tube gels)	excellent reproducibility
batch-to-batch differences present in self-cast gels	IPG-strips only commerically aveilable, therefore no batch-to-batch differences
minor lot-to-lot differences in the commercially available ampholytes	minor lot-to-lot differences in the precast gels
the pH- gradient can be influenced by the concentration of proteins and of salts	the pH-gradient can also be influenced by the concentration of proteins espacially at high concentrations.
the *pI*- resolution is 0.010 pH unit	the *pI*- resolution is 0.016 pH unit

Tab. 5-1: *Comparison of carrier ampholytes and immobilized pH-gradients for first dimension isoelectric focussing.*

gradients of carrier ampholytes [Klose, 1999b; Lopez, 1999]. Secondly, variable pH ranges can be prepared by the blending of different ampholytes. In addition, the preparation of a tube gel is much easier than that of immobilized pH-gradients and does not require complex gradient casting equipment. However, a variable batch-to-batch reproducibility, the effect of protein concentration on the shape of the pH-gradient, and the cathodic drift of the pH-gradient with time are some drawbacks.

Since the aim of my study was to detect as many mitochondrial protein spots as possible, optimum resolution was paramount. I thus chose carrier ampholytes to run my IEF-separations. On the other hand, the disadvantages of carrier ampholytes were minimized since I blended a large volume of gel stock-solution and aliquoted it into small portions so that all experiments were carried out with the same batch of ampholyte mixture. The cathodic drift of the pH-gradient with time was controlled by using a programmable power supply. This added to the standardization of IEF-running conditions. The effect of the protein sample on the pH-gradient was also investigated and is discussed below.

5.3.2 Reproducibility

The reproducibility of 2D-separations can be assessed by three aspects:

A) *The presence/absence of spots*: the reproducibility of protein resolution,
B) *The position of spots*: the reproducibility of protein spot location on the gel and
C) *The quantity of spots*: the reproducibility of protein abundance.

In order to test the reproducibility of my gel-runs, I isolated mitochondrial proteins from the same cell line and run them on four different gels.

A) The gel-runs achieved a satisfactory reproducibility of protein resolution since each spot on one gel was reproduced on the other test-gels.

B) The reproducibility of position was only satisfactory when spots were compared to one another in a small perimeter of 3-5 cm from a certain anchor-point, i.e. the corresponding spots were only congruent when the gels were compared subsection by subsection. These running differences between two large gels might be due to minor inconsistencies of running conditions (temperature, buffer-composition), gel quality or protein-concentration.

C) Most of the protein spots achieved satisfactory quantitative reproducibility. However, the varying reproducibility of certain protein spots might be due to additional interfering factors. Spots 11 and 12, which correspond to the protein actin-beta, are examples. Since the test-samples of four gels were isolated from four different aliquots of the same cell line, the reproducibility of the mitochondrial isolation method was tested indirectly as well. The tight affiliation of actin-beta with the outer membrane of the mitochondria makes its removal difficult. The degree of actin-beta removal most probably depends on the cell fractionation process, which is the most difficult step to keep completely uniform.

Several other factors can also impair the reproducibility. For example if the protein samples are thawed more than once not only the resolution of the protein spots but also their quantity is reduced (Fig. 4-8). This phenomenon is most probably due to the degradation of proteins

during the freezing and thawing process. As expected the effect is most pronounced in low abundance proteins.

5.3.3 The number of the visualized proteins on the gel

In order to resolve as many protein spots as possible I used the large gel 2D-electrophoresis method with a length of 40 cm for isoelectric focussing [Klose, 1999b]. This way I separated 420 protein spots on a silver stained 2D-electrophoresis gel. I do not know how far this number is from the actual mitochondrial protein content. Until now, a total of 525 different proteins have been registered in a special database of mitochondrial proteins (Human Mitochondrial Proteins Database). This database comprises information from "SwissProt", "LocusLink", "Protein Data Bank" (PDB), "GenBank", "Genome Database" (GDB), "Online Mendelian Inheritance in Man" (OMIM), "Human Mitochondrial Genome Database" (mtDB), MITOMAP, and "Neuromuscular Disease Center and Mendelian Inheritance and the Mitochondrion" (MitoDat).
Additionally, the existence of protein-isoforms increases the spot-number considerably. The number of isoforms of a certain protein varies between two to ten [Rabilloud *et al.,* 1998; Jung *et al.,* 2000; Fountoulakis *et al.,* 2003]. Although not all spots of putative isoforms were analyzed in my study, from a representative sample of heat shock 60 kDa proteins (spot 9 and 10) one can assume that the horizontal arrays of spots are isoforms of the same protein. In my sample, the number of isoforms of a protein ranged from two to six.
Loss of proteins is doubtless taking place during the whole process from protein preparation until the staining of the gel. In order to minimize this loss I used a highly standardized sample preparation protocol introduced by Klose (1999a). One key point of this protocol is to solubilize hydrophobic proteins and keep them soluble. This is achieved by using CHAPS and high concentrations of urea to break up non-covalent interactions and by using DTT to break up disulfide-bridges. Another key point is to reduce protein degradation as good as possible. This is achieved by adding a cocktail of protein inhibitors and by performing all preparations in the cold at 4°C.

5.3.4 Staining of the gel

In my experiments the silver stain was much more sensitive than the Coomassie stain. This has already been demonstrated in other studies [Switzer *et al.*, 1979; Rabilloud, 1990; Shevchenko *et al.,* 1996a]. On the other hand, for the purpose of protein identification by MALDI-TOF mass spectrometry the Coomassie stain seemed to be superior. None of my silver stained spots could be identified. However, this disappointing result might not be due to the silver stain itself but due to the fact that I only cut out those silver spots, which could not be identified on the Coomassie stained gel or which had been very weak. Therefore, the reason of the zero identification rate of my silver-stained spots was more likely to be caused by low protein abundance than by a strong influence of silver ions on the proteins. Other authors like Shevchenko (1996a) and Rabilloud (1998) have demonstrated that silver-stained gels can indeed be used for satisfactory mass spectrometric identification of proteins.

5.4 Protein identification

The proteins were identified mainly by MALDI-TOF mass spectrometry on the basis of their peptide mass fingerprints and in some cases by sequencing a peptide tag with MALDI-QTOF tandem mass spectrometry.
According to the annotations in SWISS-PROT and NCBI, 78% of the identified proteins were human mitochondrial proteins. The other 22% identified proteins included 12% non-

mitochondrial proteins (cytoplasmic, endoplasmic reticulum or B-cell-associated) and 10% unknown proteins (most of them were only present as expressed sequence tags (EST)). The majority of my spectra was of good quality which allowed rather easy protein identification. The high accuracy in mass determination of the peptide fragments is made possible by MALDI-TOF mass spectrometry with "delayed extraction". The delayed extraction method allows peptide fragments of the same weight to be better focused. This leads to sharp and accurate spectra which allow the reliable identification of proteins even with limited sequence coverage [Jensen *et al.,* 1996]. Therefore, my results were reliable even with low sequence coverage of around 12-17%. The array of identified proteins contained eleven proteins from other cell compartments. This "contamination" cannot simply be attributed to the purification method of the mitochondria. Such proteins as the B-cell associated protein (spot 103) are very abundant and/or specialized for the lymphoblastoid cells. These proteins are difficult to remove completely and are absent when mitochondria from other tissues were investigated (e.g. placenta [Rabilloud *et al.,* 1998] or neuroblastoma cells [Fountoulakis *et al.,* 2003]). However, I cannot rule out that these eleven proteins might interact with the mitochondria as well, since some other non-mitochondrial proteins are known to have very tight links to the mitochondria. They either bind to the outer membrane of mitochondria or transport material to the mitochondria. An example for these proteins is actin-beta, which is attached to the outer membrane of the mitochondrion and is involved in the movement of mitochondria within the cell.

There are 25 spots in the list, which could not be identified. This might be due to the fact that the spectrum was not good enough or that the spectrum could not be matched with a protein from the databases. Besides the low abundance of certain proteins in the sample, several other reasons could also account for this. If two spots are very close to each other on the gel or overlapping each other, the proteins are mixed during excision of the spot. The spectra from those overlapping spots may confuse the database search. Peptide loss during the tryptic digest or the failure to extract the peptides from the gel pieces for MALDI-TOF mass spectrometry may be another reason for low amplitude mass spectra.

Notably, a large part (72%) of the unidentified spots comprises small proteins whose molecular weights are below 17.5 kDa. Some of these proteins are fragments of larger proteins. Spot 114 is an example for that. This spot is the smallest protein among the identified ones. Its molecular weight is around 5-10 kDa and it could only be identified by protein ladder sequencing to be a small fragment of actin-beta.

5.5 The mitochondrial proteome reference map

I established a reference map of the mitochondrial proteome of human lymphoblastoid cells. This map will be used as a tool for further investigation of mitochondrial proteins of patients with mitochondrial diseases. A total of 95 proteins, 74 of them of sure mitochondrial origin, have been identified on this reference map (Fig. 4-12). The sub-mitochondrial location and the function of each identified mitochondrial protein were looked up in various databases and original publications.

5.5.1 The identified membrane proteins

Similar to previous analyses of the mitochondrial proteome [Jung *et al.,* 2000; Lopez *et al.,* 2000; Fountoulakis *et al.,* 2003], most of my identified proteins are hydrophilic or easy to solubilize proteins. Although 18 proteins of the list were annotated to be membrane-associated proteins, only four of them were clearly transmembrane proteins with at least one transmembrane helix.

Unfortunately none of the mtDNA-encoded proteins could be identified in my study. The mitochondrion is rich in membrane-associated proteins. Most of the 13 mtDNA-encoded proteins are components of multi-protein-complexes and are located at the inner mitochondrial membrane. Analysis of putative transmembrane domains in these 13 proteins with the SOSUI-algorithm revealed that all of them are transmembrane proteins. If the proteome-map is to be used to elucidate mitochondrial diseases, the representation of membrane-proteins is paramount and has to be further worked on.

The difficulty of the detection of membrane proteins seems to be connected to the principle of 2D-electrophoresis. This method has certain limitations to detect four kinds of proteins [Gygi *et al*., 2000; Nordhoff *et al*., 2001]:

A) hydrophobic proteins,
B) proteins of multi-protein-complexes,
C) proteins with a very basic *pI* and
D) very small proteins

The critical point for sufficient membrane-protein separation is the isoelectric focussing in the first dimension:

A) Since membrane proteins are mostly hydrophobic proteins, they need to be solubilized to make them migrate in an electric field. This can be achieved by detergents (e.g. SDS or CHAPS). These detergents, however, affect the isoelectric point of the protein [Rabilloud, 1996]. Therefore, only urea as a protein denaturant can be added to the isoelectric focussing gel to keep the proteins in solution. CHAPS, a zwitterionic detergent, is added to the sample buffer to facilitate the solubility of hydrophobic proteins during sample preparation. However, its effect subsides as soon as the proteins enter the IEF-gel. It seems that the urea in the IEF-gel can hardly counteract the tendency of the hydrophobic proteins to aggregate. Therefore, only a few membrane-proteins maintain their solubility and migrate towards their isoelectric points. The rest of the membrane proteins seem to aggregate and do not even enter the IEF-gel.

B) The proteins that are part of multi-protein-complexes are also denatured and solubilized by the use of CHAPS and urea during sample preparation. When the proteins enter the IEF-gel the effect of CHAPS begins to subside and some of the proteins start to refold and partially reconstitute themselves into multi-protein aggregates that cannot migrate though the pores of the 3.5% polyacrylamide IEF-gel.

C) If the proteins have a very basic *pI* (>10) which is often the case for membrane proteins, they do not focus properly in the IEF-gel. At the basic end of the IEF-gel the pH gradient does not reach its equilibrium [Klose, 1995]. This would cause the loss of the very basic proteins unless they are captured in a higher percentage cap-gel.

D) Small proteins with a molecular weight below 10 kDa are difficult to detect [Klose, 1995]. This is due to the fact that the pores of the 15% second dimension SDS-PAGE-gel are too large to focus the small proteins properly [Carroll *et al.,* 2002]. For proteins of this size a polyacrylamide-percentage of 20-22% would be appropriate. This could be achieved by pouring a 5-20% gradient-gel. This procedure is very laborious and difficult to reproduce exactly. It would make different second dimension separations difficult to compare. Beyond that, the small proteins fail to stain with Coomassie blue.

This is due to their low absolute peptide content despite the fact that they might be present in the same molar range as high molecular weight proteins. Even if they can be detected on Coomassie stained gels they might be difficult to identify via MALDI-TOF mass spectrometry since there are only few peptide fragments available for a peptide fingerprint analysis. In this case one has to resort to the sequence determination of a peptide fragment by MALDI-QTOF tandem mass spectrometry.

The under-representation of transmembrane-proteins on a regular 2D-gel is a severe drawback of the method. Further work has to be done to make these proteins more soluble and accessible for isoelectric focussing. [Rabilloud *et al.,* 1996, 1999; Henningsen *et al.,* 2002; Navarre *et al.,* 2002]

5.5.2 Multiple spots proteins

17 proteins in my list are represented by multiple spots (2-3 in average). Most of them (n = 15) are present in pairs and are probably isoforms of the same protein.

The isoforms could be subdivided into:

- *Naturally occurring isoforms* that are formed by any kind of *in vivo* post-translational modification of proteins, such as phosphorylation, glycosylation or acetylation

- *Isoforms caused by artifacts during sample preparation*, which might be generated by the reaction of unpolymerized acrylamide with SH-groups or by oxidation of methionin residues during sample preparation.

These modifications do not change the molecular weight of a protein so much that a difference in molecular weight might be detected in the second dimension run. However, they might well cause a shift of the isoelectric points either to the acidic or to the basic side.

I also found proteins that were present in multiple spots and differed considerably in molecular weight and/or isoelectric point: COXA (spots 5 and 31), mitofilin (spots 20 and 21), and actin-beta (spots 11,12, 26 and 114). The large differences in molecular weight could be caused by differential splicing of the same precursor-mRNA. Proteolysis during the whole procedure might be another possible reason.

5.5.3 Comparison of my results with other mitochondrial proteomic projects

Two groups have established a human mitochondrial proteome database before. One is Rabilloud *et al.* (1998 and 2002) who investigated mitochondria from human placenta. The other group is Fountoulakis *et al.* (2003) who analyzed mitochondria from a human neuroblastoma cell line IMR-32. The database of Rabilloud *et al.* (2002) contains 68 proteins in total. The other database of Fountoulakis *et al.* (2003) contains 185 different proteins. I re-identified 29 proteins in Rabilloud's database and 65 in Fountoulakis' database (Fig. 5-1). Excitingly, in comparison to these two databases, I identified 26 new proteins. 54% of them are of definitive mitochondrial origin. 35% of them were unidentified proteins only present in EST databases. Interestingly, three of my four transmembrane proteins were identified for the first time.
Similar to my experience, Rabilloud's and Fountoulakis' databases do not include many transmembrane proteins either. Using the SOSUI-algorithm, I controlled all the proteins in Rabilloud's database. Only two proteins in this database carry transmembrane domains. A

similar check was done with the proteins from Fountoulakis' database, which carried a SWISS-PROT accession number. None of these proteins had a transmembrane domain. None of the mtDNA-encoded proteins were identified in both databases either. Since their experiments were carried out with the same methods, the limitation and drawbacks of the 2D-electrophoresis become clear.

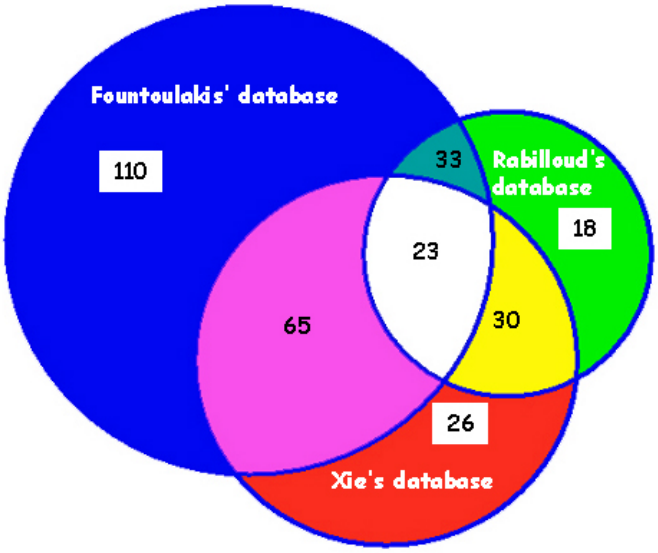

Fig. 5-1: *Comparison of my results to Rabilloud's and Fountoulakis' mitochondrial proteome databases.* Compared to the 95 proteins in my database, the database of Rabilloud contains 68 proteins in total and the other database contains 185 different proteins. The shared proteins between the different databases are depicted in the overlaying

5.5.4 Comparison of the theoretical and the experimental *pI* and *MW*

5.5.4.1 Comparison of the experimental pI and the theoretical pI

The correlation between experimental and theoretical *pI* values in my study is not as thight as described by other authors (Bjellqvist *et al.*, 1993; Perrot *et al.*, 1999). However, the correlation between the experimental and the theoretical *pI* still tends to lie on a linear regression line (Fig. 4-16) with a correlation coefficient of R = 0.873 and a lateral dispersion of R^2 = 0,762. The proteins with a large difference between experimental and theoretical *pI* values were studied separately. They fall into the following catagories:

- Most of the mitochondrial proteins are nuclear encoded. They are synthesized in the cytosol as preproteins with a N-terminal transit sequence of about 20-30 amino acids. After import into the mitochondrion this transit-sequence is cleaved and the proteins fold into its mature conformation. Therefore, most mitochondrial proteins in my 2D-map are assumed to be mature proteins. The site of cleavage has not been determined experimentally for most of the proteins and in the databases it is generally only calculated from primary characteristics of mitochondrial import sequences [Claros *et al.*, 1996]. In some proteins of my database (n = 7) the putative cleavage point was impossible to determine by calculation. The calculation of *pI* of these seven proteins therefore only takes into account the pre-protein sequences. The *pI* is thus wrongly shifted towards the basic side.
- For seven proteins in my database only ESTs were available in the public databases. Since ESTs might be incomplete or encode a pre-protein, the theoretical *MW* and *pI* of the EST derived proteins were unraliable.

- Variation in protein expression patterns might be due to alternative splicing events on mRNA-level or due to post-translational modification. These modifications may be due to glycolysation, partial hydrolysis or phosphrylation and might cause a substantial difference between the experimental *pI* value and the theoretical one. This was verified by the fact that eight of those obviously deviating spots (*pI*-difference >1.00 pH unit) were found to be isoforms of four proteins.
- By direct measurement, the linearity of the pH-gradient in the IEF-gel could only be verified between pH 5-9. The pH-gradient of the IEF-gel is not linear any more close to its basic end. Therefore, the experimental *pI* values of those proteins focussing at the basic end were unreliable. This results in a *pI*-difference larger than 1.00 pH unit for almost all the basic proteins whose theoretical *pI* is larger than pH 9.00.
- Preparation artifacts (e.g. partial hydrolysis by proteases) might cause protein degeneration. The ensuing fragments run differently on the 2D-gel than the intact proteins and might be as well a reason for lager deviations between the theoretical and the experimental *pI*-values.

5.5.4.2 Comparison of the experimental MW and the theoretical MW

The correlation of experimental and theoretical molecular weights is better (correlation coefficient: R = 0.941) than that of the isoelectic points. The values lie on a regression line with a lateral dispersion of R^2=0.885. In my study I used a mass reference marker set which only spanned the range betweeb 17.5 kDa and 76 kDa. Therefore, the *MW* of the proteins could not be determined with certainty when they run below 17.5 kDa or above 76 kDa. It is exactly these proteins which deviated most from the regeression line (Fig. 4-16).

6 CONCLUDING REMARKS

The establishment of a reference mitochondrial proteome map of human lymphoblastoid cells provides a basic and useful tool for researchers working in the field of mitochondrial diseases. This 2D-reference map displays a different subset of proteins as compared to total cell homogenates and gives an overview of the proteins present in the mitochondria.

This reference map makes it possible to look for abnormal expression of mitochondrial proteins in patients with mitochondrial diseases.

However, there are still many unsolvend problems remaining. The major problem is the limited identification rate of membrane proteins. The separation of these proteins is especially important for researchers in the mitochondrial field, since one can assume that the double membrane structure of the mitochondrion carries many transmembrane proteins. Therefore improvements of the 2D-electrophoresis should be especially focussed on the resolution of membrane proteins. The identification of mtDNA-encoded proteins is another difficult task that I chose for my further research.

Another major task for further study is to elucidate the variability (e.g. the polymorphisms) of mitochondrial protein expression patterns in healthy controls. This implies a lot of routine work, however it is doubtless very important. Whether a deviating protein pattern has a meaning for pathophysiology can only be verified based on thorough studies of the variation in the normal population.

SUPPLEMENTARY MATERIAL

On the following pages the 12 subsections of Fig. 4-12 are depicted in greater detail with protein labels. The numbers in brackets refer to the protein number of the list depicted in Tab. 7-1.

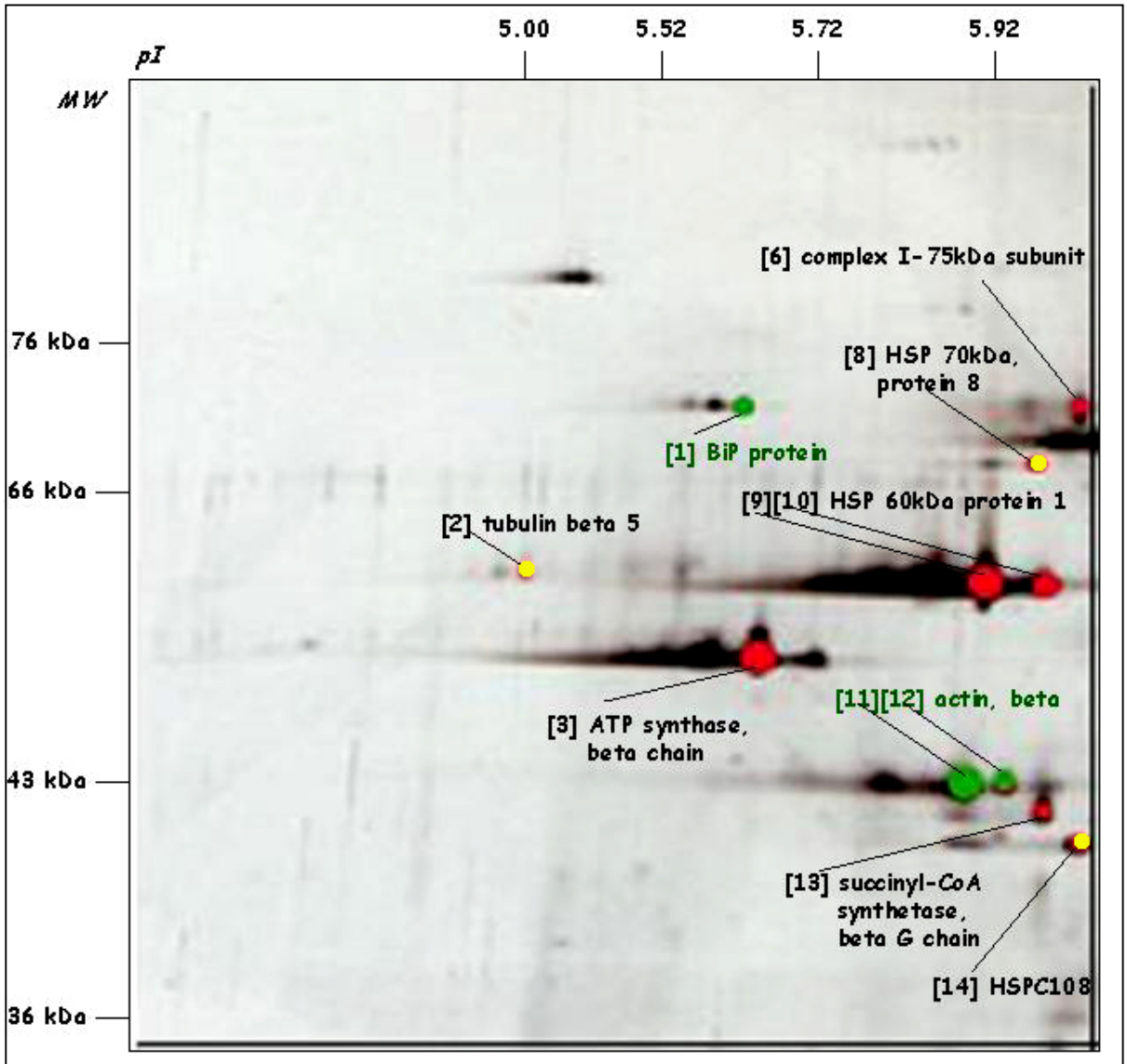

Fig. 4-12#1: Section 1 of mitochondrial the proteome map

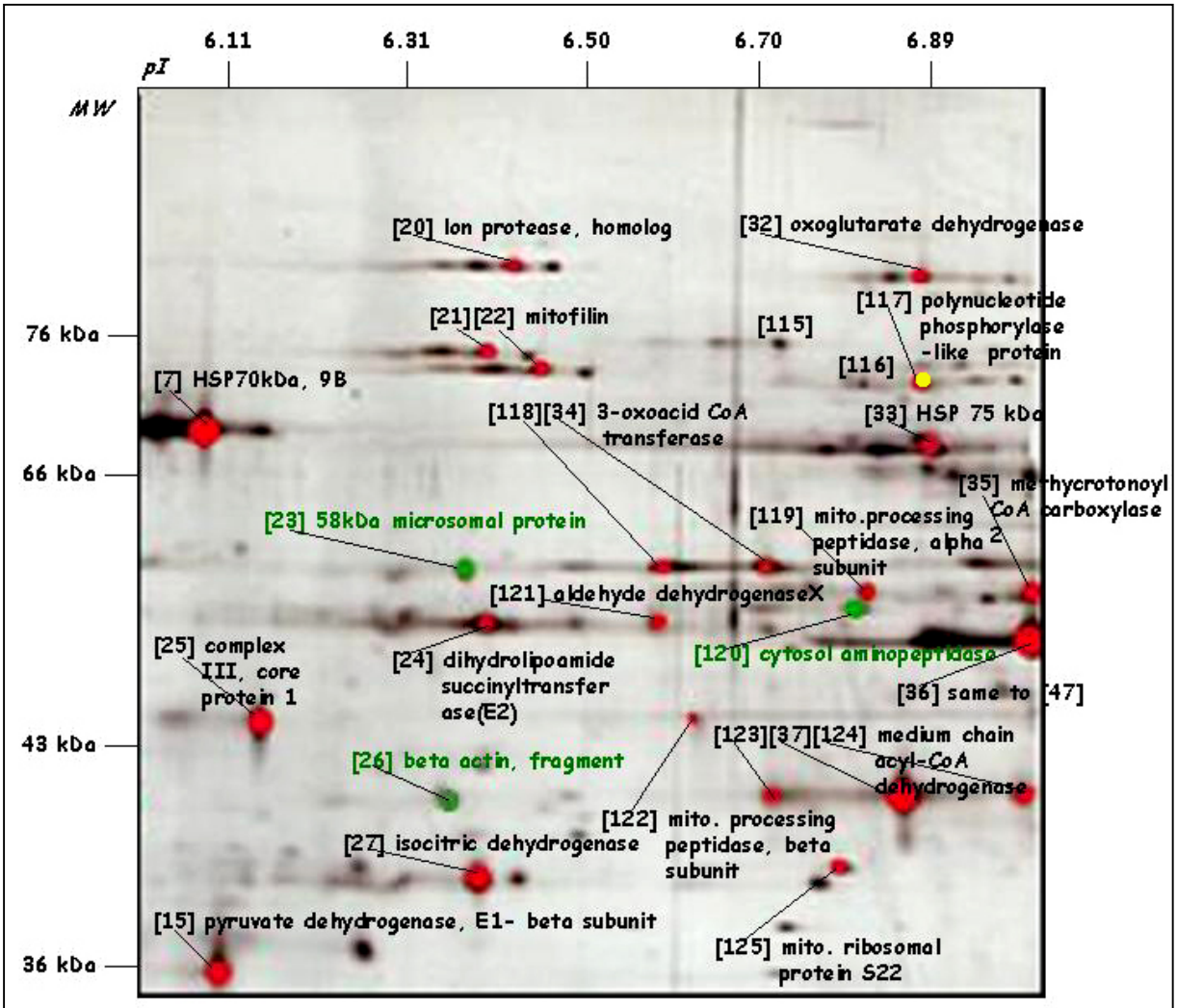

Fig. 4-12#2: Section 2 of the mitochondrial proteome map

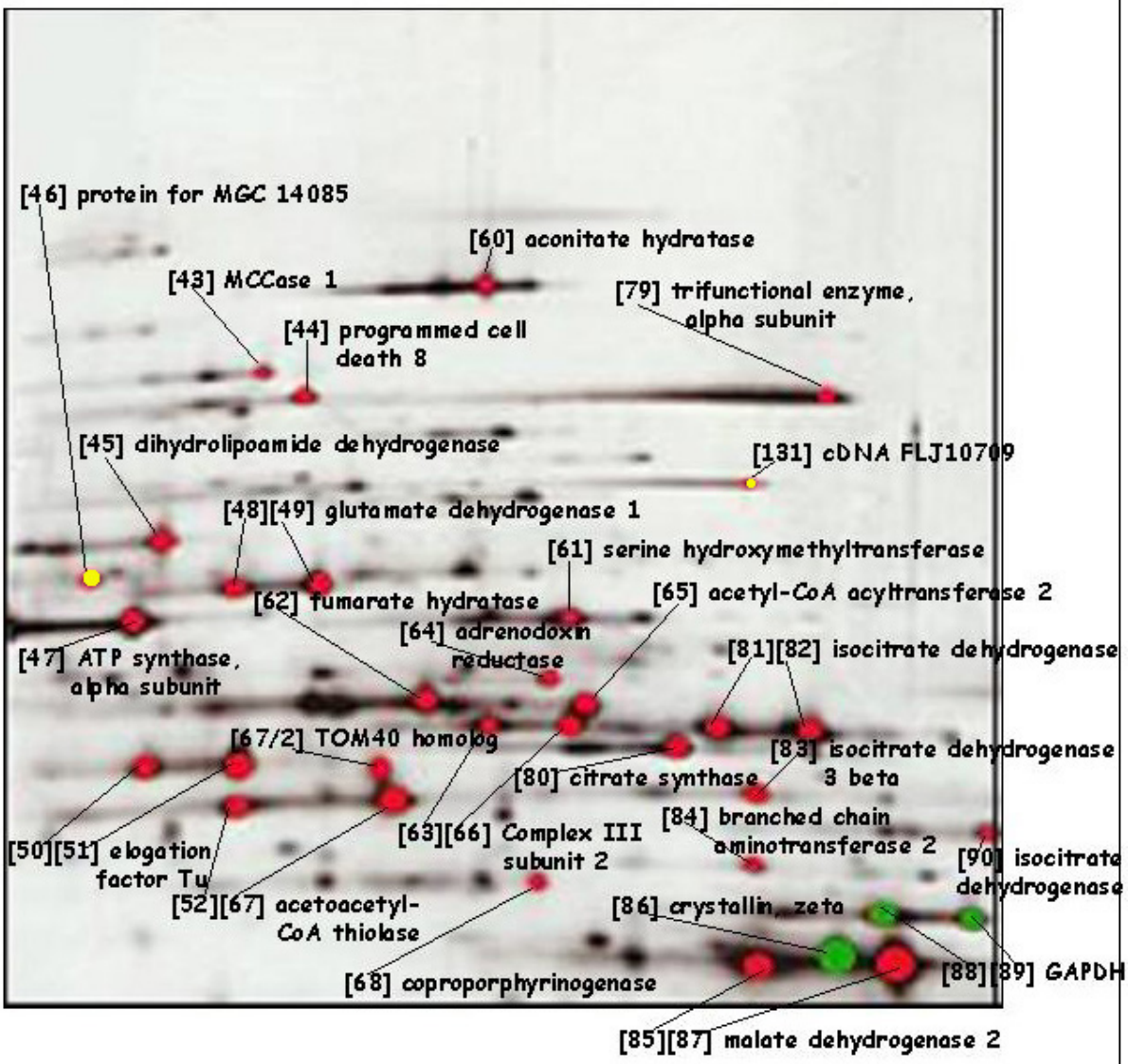

Fig. 4-12#3: Section 3 of the mitochondrial proteome map

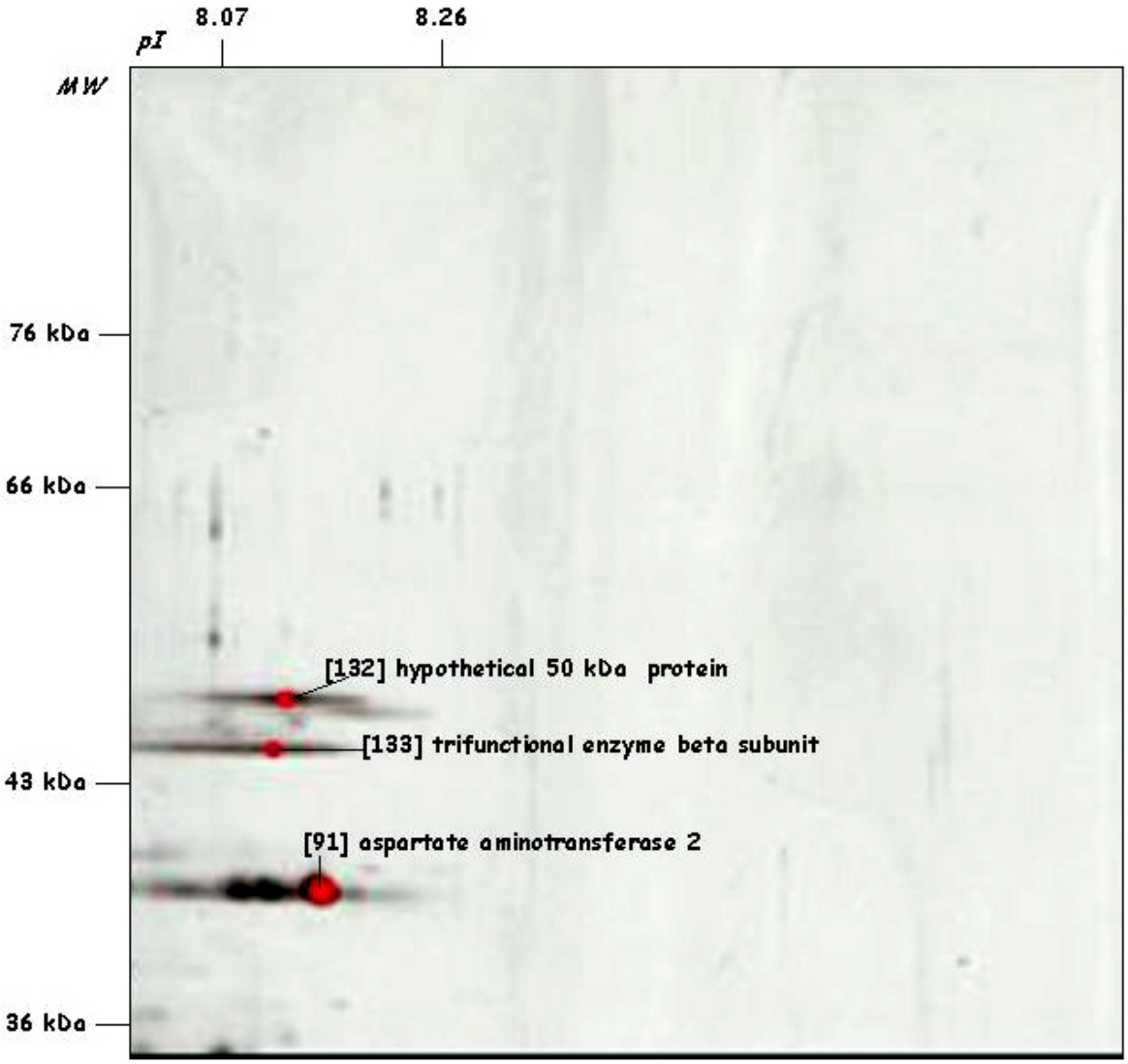

Fig. 4-12#4: Section 4 of the mitochondrial proteome map

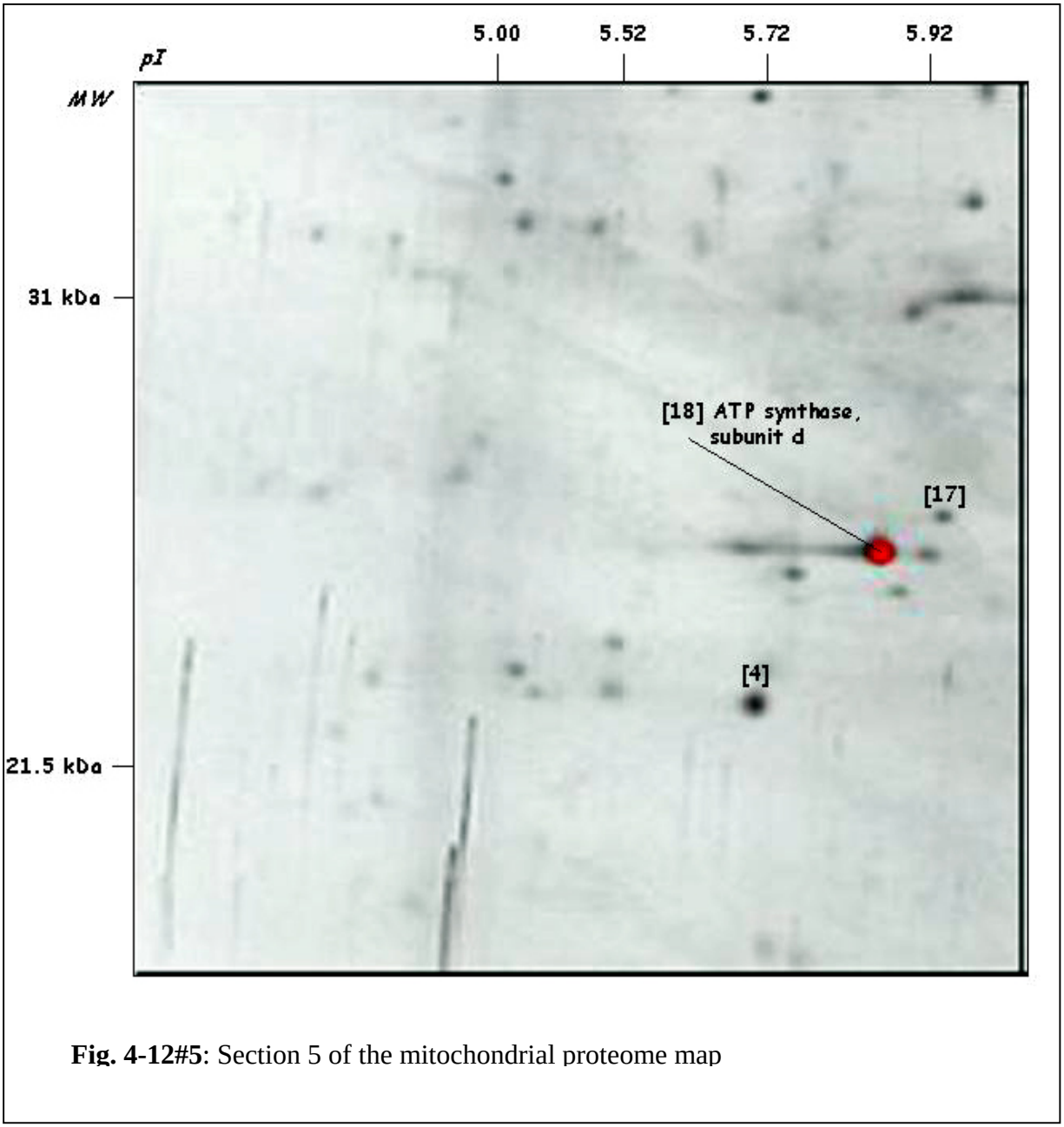

Fig. 4-12#5: Section 5 of the mitochondrial proteome map

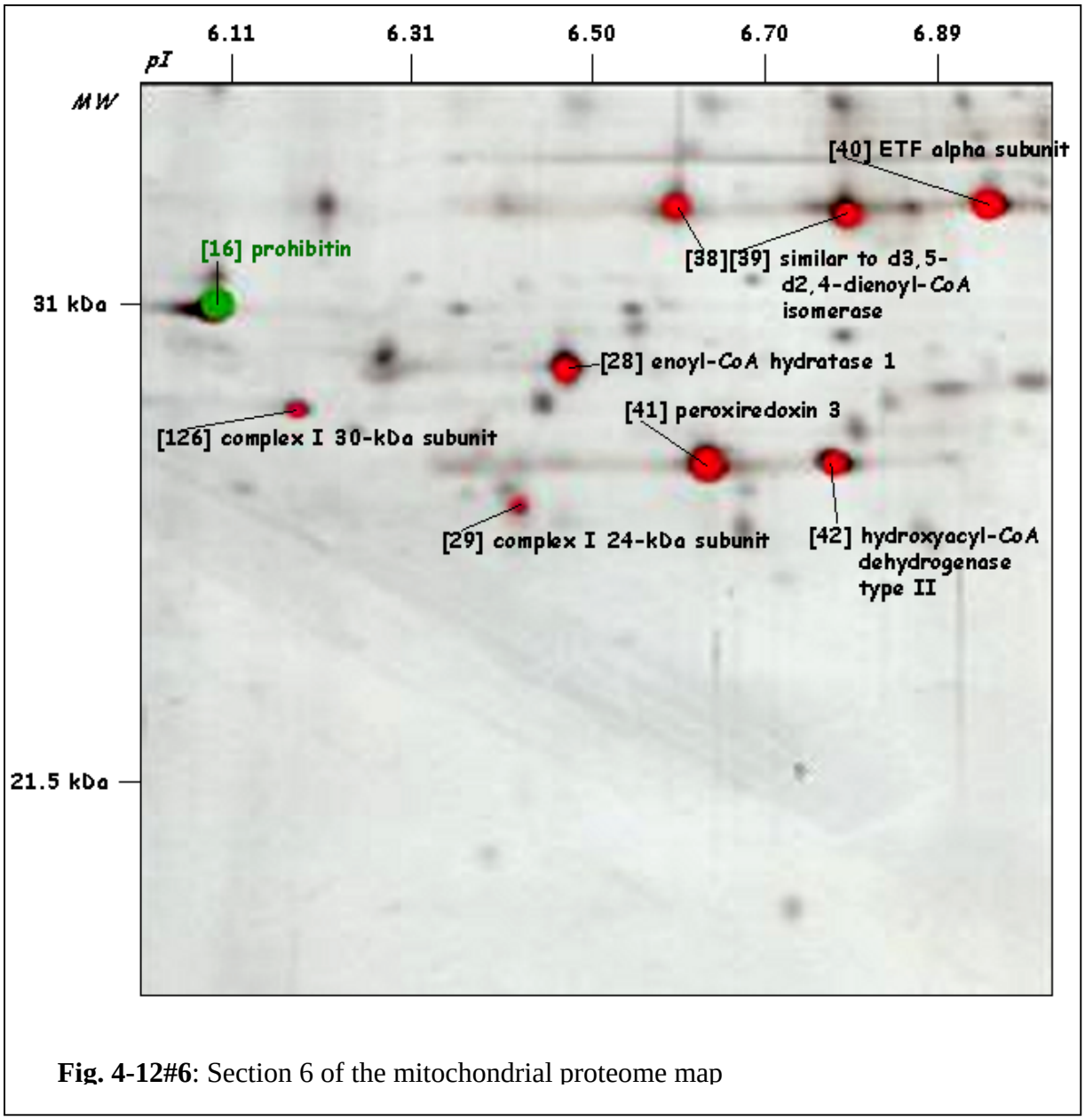

Fig. 4-12#6: Section 6 of the mitochondrial proteome map

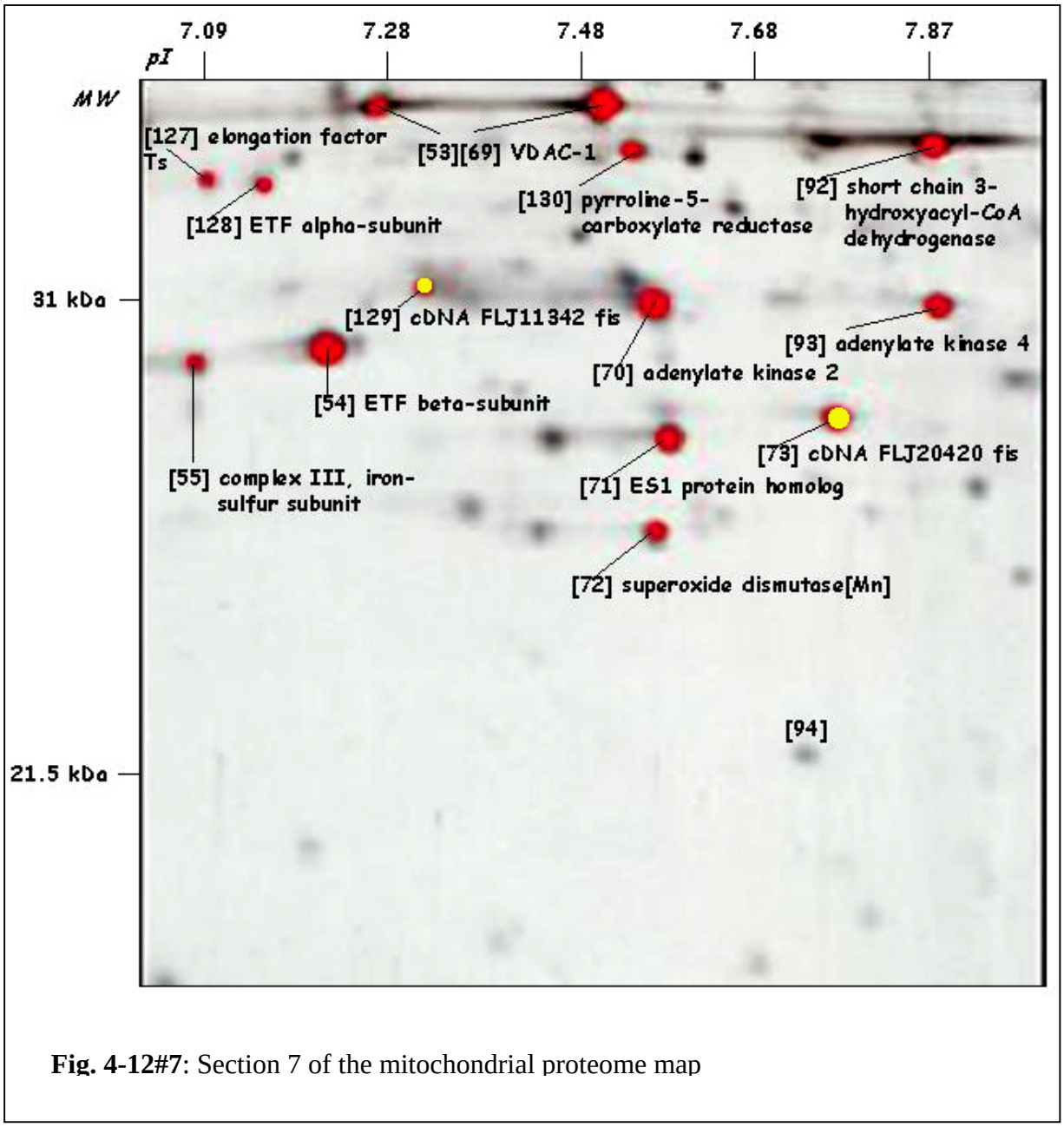

Fig. 4-12#7: Section 7 of the mitochondrial proteome map

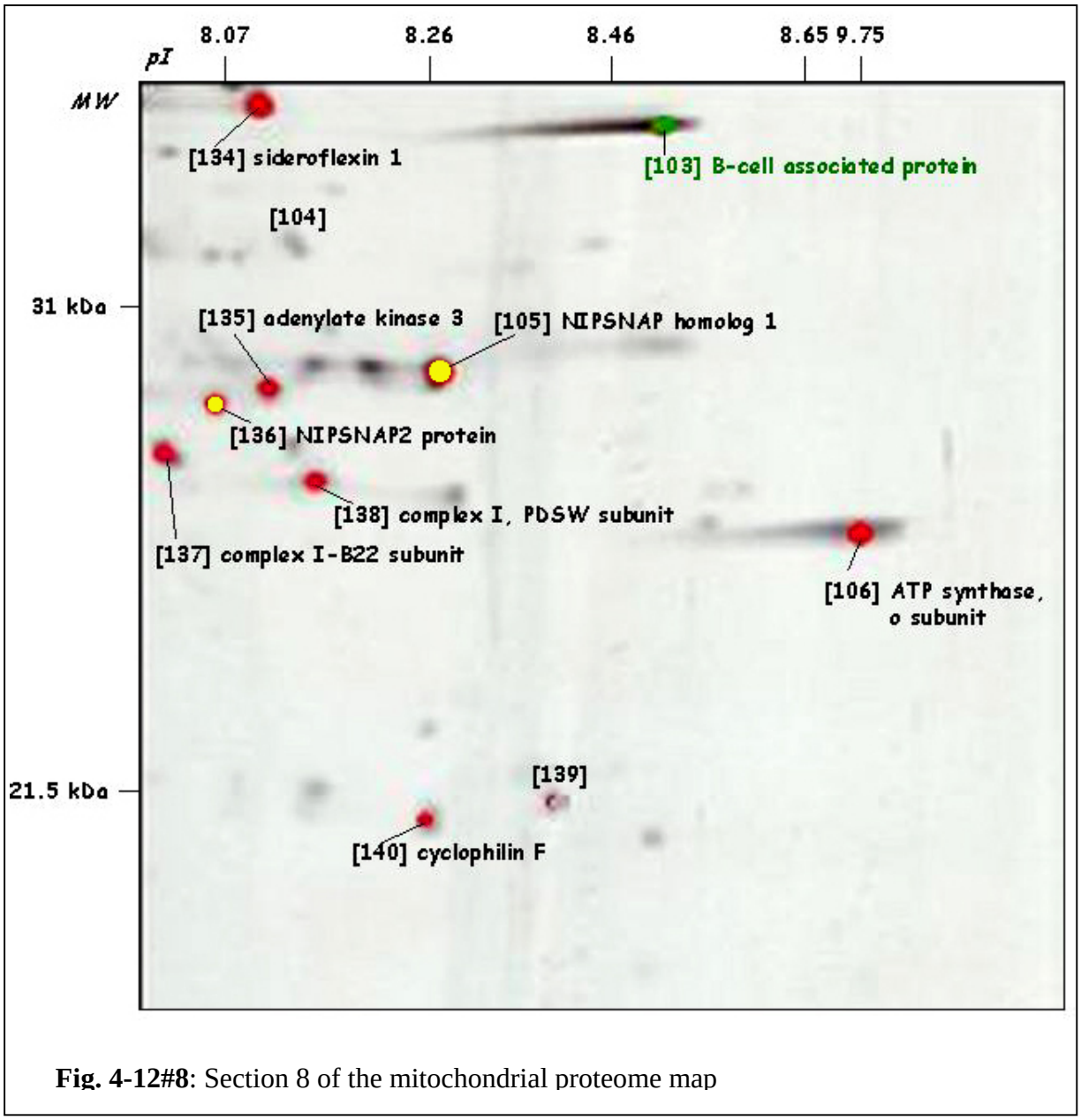

Fig. 4-12#8: Section 8 of the mitochondrial proteome map

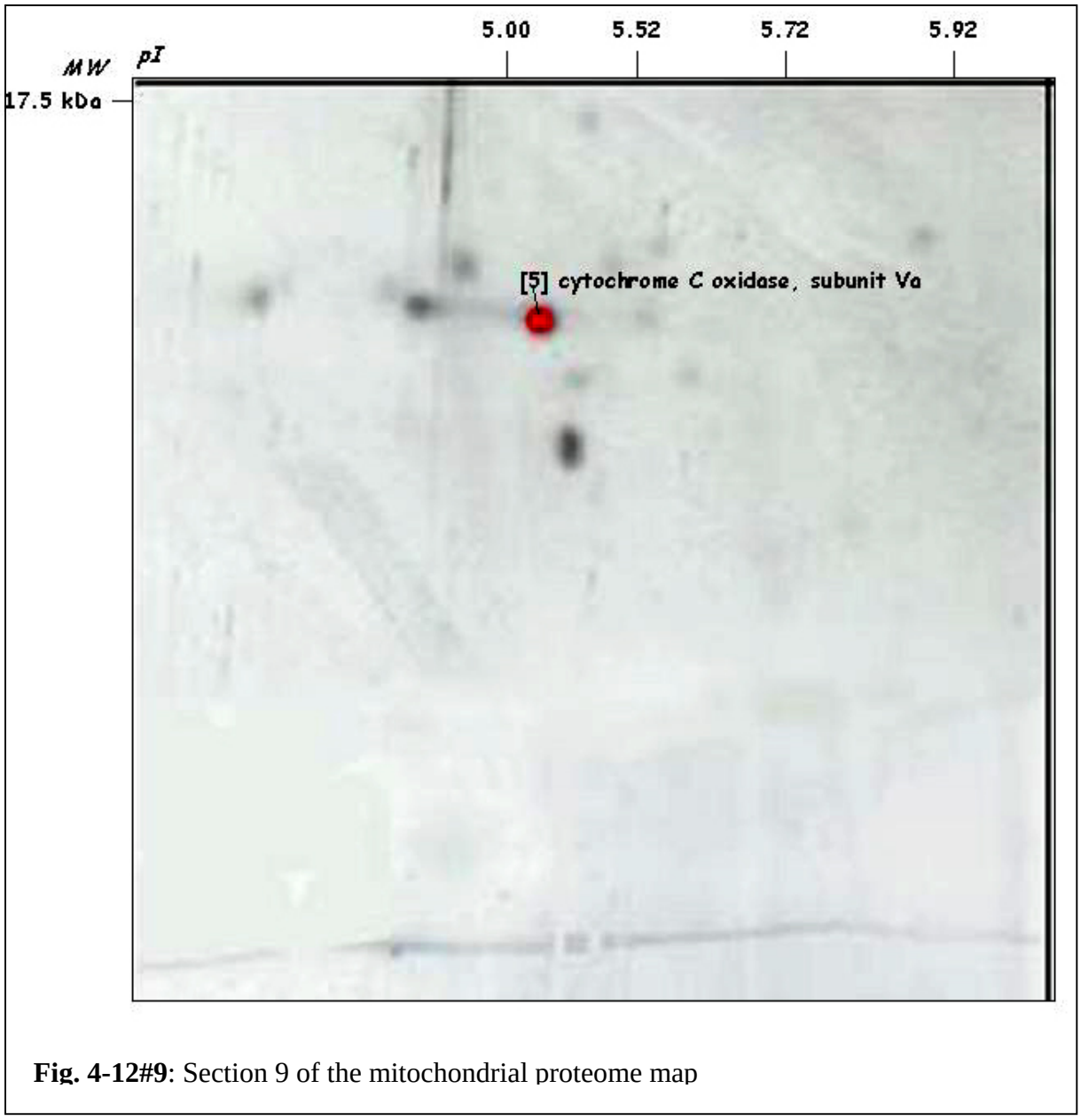

Fig. 4-12#9: Section 9 of the mitochondrial proteome map

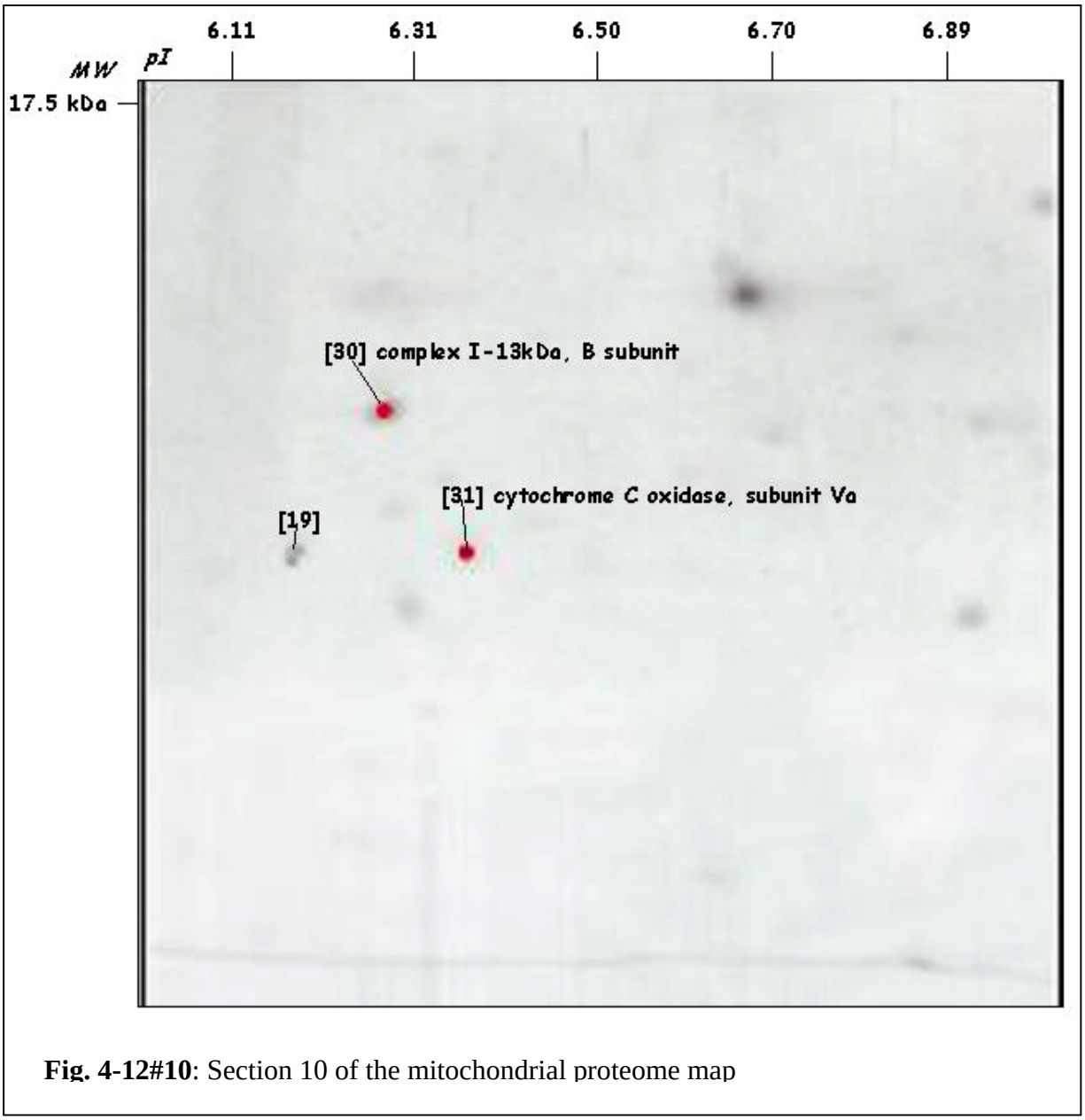

Fig. 4-12#10: Section 10 of the mitochondrial proteome map

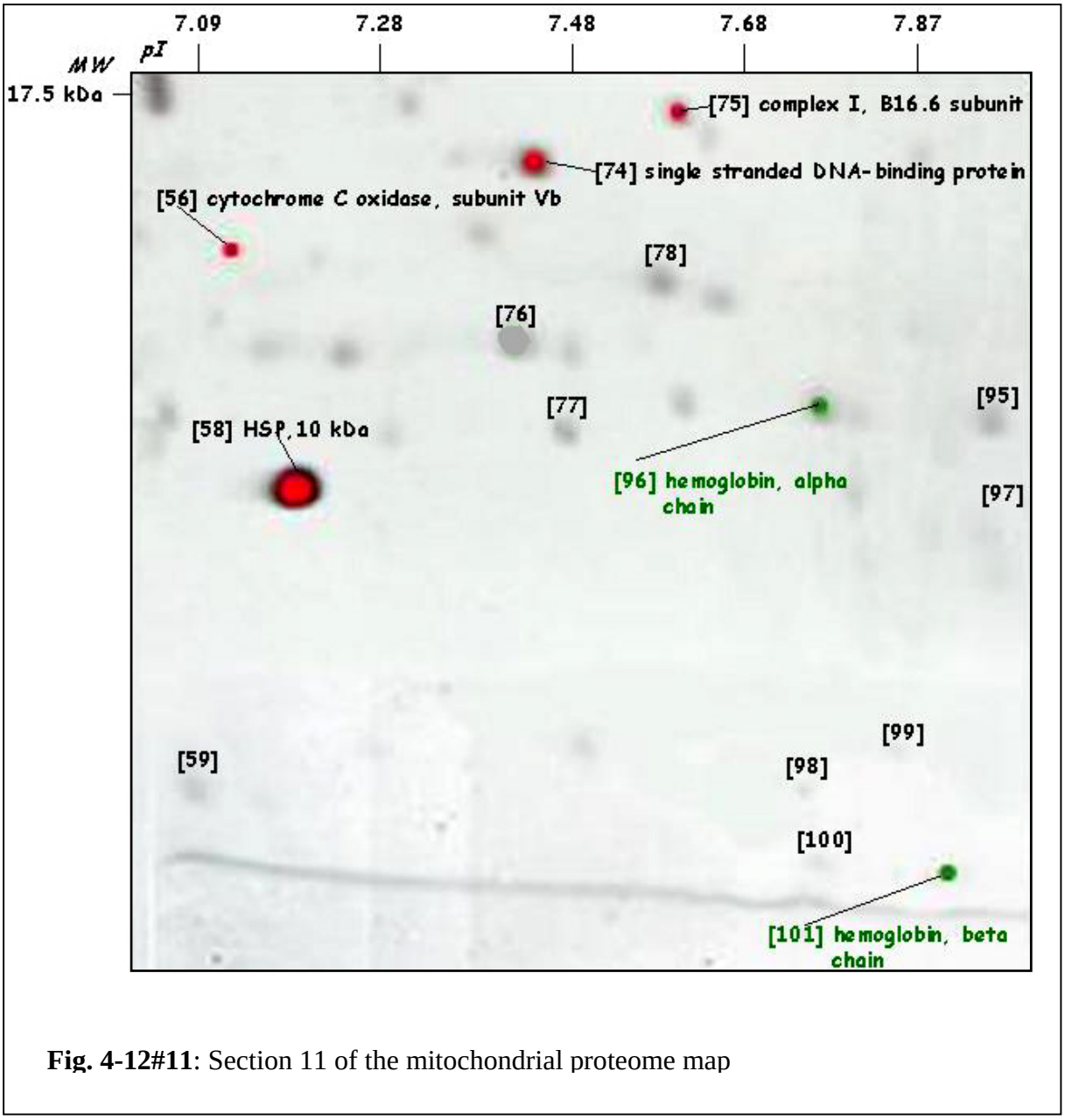

Fig. 4-12#11: Section 11 of the mitochondrial proteome map

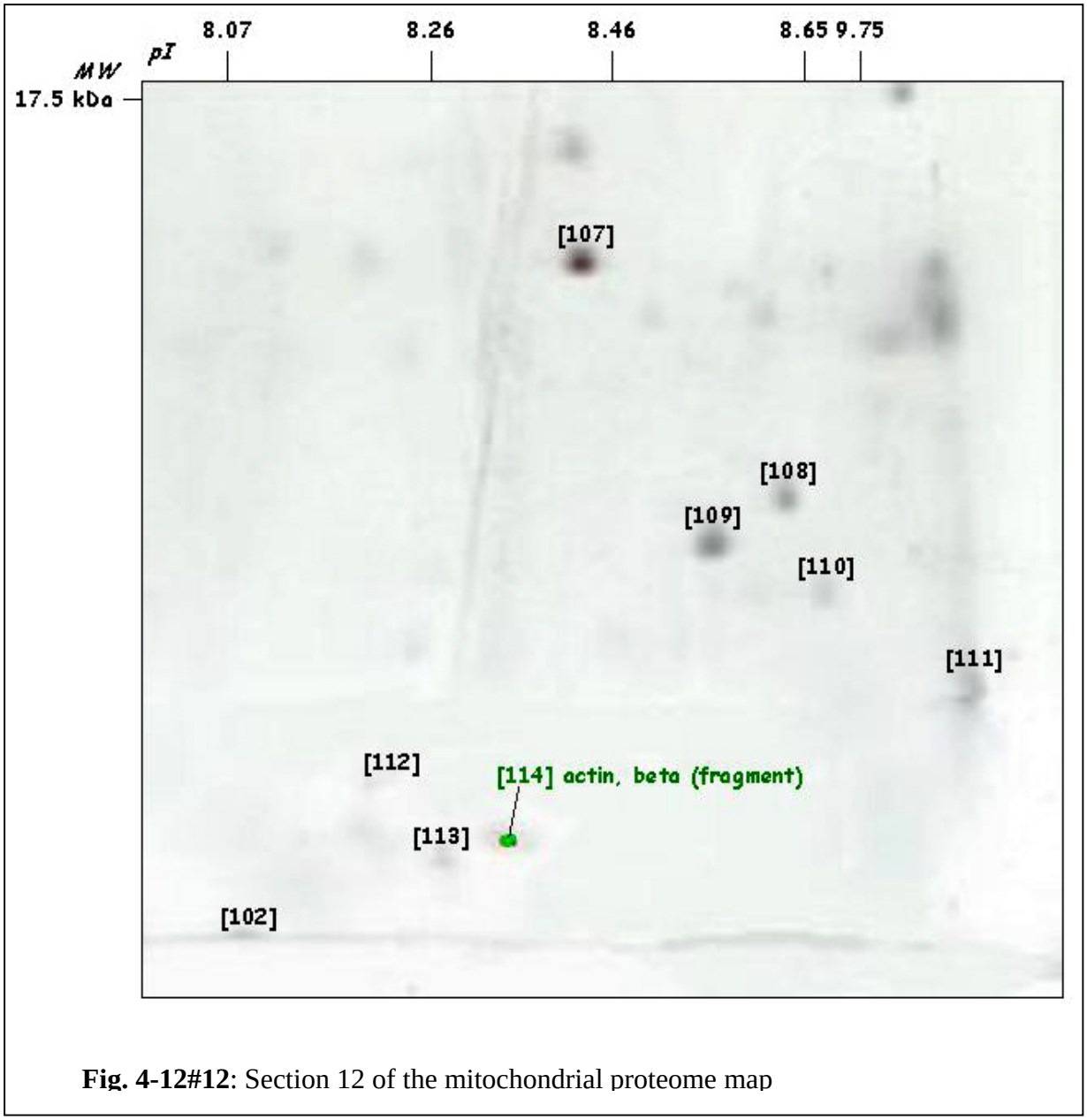

Fig. 4-12#12: Section 12 of the mitochondrial proteome map

Spot Nr.	gene name	Protein name	swiss ID	SWISS_ PROT Nr.	OMIM No.	gi	E.C.	MW(S)	pI (S)	MW(m)	pI(m)	Seq.	matched peptide (total peptide)	sequence coverage %	probability based Mowse score	Function	location
1	HSPA5	BiP protein. (HSP 70kDa protein 5) (glucose regulated protein 78 kDa, precusor) (GRP78)	GR78_ HUMAN	P11021	138120	6470150		70478,57	5,01	59100	5,20	19 - 654	10(17)	17	105	*HSP(assembly)*	*endoplasmic reticulum lumen*
2	TUBB5	tubulin, beta 5.	TBBX_ HUMAN	P04350	602662	18088719		49630,87		51200	5,00		7(15)	16	67	?	?
3	ATP5B	ATP synthase, beta chain, mitochondrial precursor.	ATPB_ HUMAN	P06576	102910	114549	3.6.3.14	51769,25		47900	5,20	48 - 529	28(60)	58	215	Complex V	M
4		**not identified**															
5	COX5A	cytochrome C oxidase, subunit Va.	COXA_ HUMAN	P20674	603773	18999392	1.9.3.1	12513,23		13000	4,80	42 - 150	8(45)	28	64	Complex IV	MIM
6	NDUFS1	NADH-ubiquinone dehydrogenase, Fe-S protein 1. (75kDa) (NADH-ubiquinone oxidoreductase 75 kDa subunit, mitochondrial precursor) (Complex I-75kDa) (CI-75kDa) (NADH-coenzyme Q)	NUAM_ HUMAN	P28331	157655	13637608	1.6.5.3 1.6.99.3	77053,44		59100	5,80	24-727	16(29)	30	147	Complex I	MIM
7	HSPA9B	heat shock 70kDa protein 9B. (mortalin-2) (stress-70 protein, mitochondrial precursor) (75 kDa glucose regulated protein) (GRP 75) (Peptide-binding protein 74) (PBP74) (Mortalin) (MOT)	GR75_ HUMAN	P38646	600548	4758570		68759,00		57900	5,90	47-679	23(44)	36	215	HSP (apoptosis and chaperone)	M
8	HSPA8	heat shock 70kDa protein 8. (HSP73) (heat shock cognate 71 kDa protein)	HS7C_ HUMAN	P11142	600816	5729877		70898,09		56400	5,70		14(20)	24	135	HSP	?
9	HSPD1	heat shock 60kDa protein 1,mitochondrial precursor. (chaperonin) (Hsp60) (CPN60) (heat shock protein 60) (HSP-60) (Mitochondrial matrix protein P1) (P60 lymphocyte protein) (HuCHA60)	CH60_ HUMAN	P10809	118190	14603309		57962,86		51400	5,70	27-573	33(99)	64	228	HSP (mitochondrial protein import and assembly)	MM
10	HSPD1	heat shock 60kDa protein 1,mitochondrial precursor. (chaperonin) (Hsp60) (CPN60) (heat shock protein 60) (HSP-60) (Mitochondrial matrix protein P1) (P60 lymphocyte protein) (HuCHA60)	CH60_ HUMAN	P10809	118190	14603309		57962,86		51400	5,80	27-573	17(53)	36	124	HSP (mitochondrial protein import and assembly)	MM
11	ACTB	actin, beta. (actin, cytoplasmic 1)	ACTB_ HUMAN	P02570	102630	14250401		41605,54		42700	5,60	2 - 375	16(63)	44	92		*cytoplasmic*
12	ACTB	actin, beta. (actin, cytoplasmic 1)	ACTB_ HUMAN	P02570	102630	14250401		41605,54		42900	5,70	2 - 375	9(30)	23	70		*cytoplasmic*
13	SUCLG2	GTP-specific succinyl-CoA synthetase, beta subunit. (Succinyl-CoA ligase [GDP-forming] beta-chain, mitochondrial precursor) (Succinyl-CoA synthetase, betaG chain) (SCS-betaG)	SCB2_ HUMAN	Q96I99	603922	3766199	6.2.1.4	42564,92		42200	5,80	38-432	6(24)	15	MS-FIT	citric Cycle	M (membrane protein)
14	---	HSPC108	Q9P042	Q9P042	---	6841440		37145,40		41000	5,80		6(20)	28	68	HSP	?
15	PDHB	pyruvate dehydrogenase, E1-beta subunit mitochondrial precursor. (PDHE1-B)	ODPB_ HUMAN	P11177	179060	387010	1.2.4.1	35890,39		35800	5,90	31 - 359	9(29)	30	72	Pyruvate complex	MM
16	PHB	prohibitin	PHB_ HUMAN	P35232	176705	4505773		29804,10		29000	5,80		11(43)	58	119	regulation proliferation	*cytoplasmic*
17		**not identified**															
18	ATP5H	ATP synthase H+ transporting,mitochondrial F0 complex, subunit d. (ATP synthase D chain, mitochondrial)	ATPQ_ HUMAN	O75947	---	5453559	3.6.3.14	18360,02		23100	5,50		16(39)	77	201	Complex V	M
19		**not identified**															
20	PRSS15	lon protease-like protein. (Lon protease homolog, mitochondrial precursor) (LONP) (LONHs)	LONM_ HUMAN	P36776	605490	414046	3.4.21.-	102825,51		67200	6,20	?-959	11(47)	15	70	AA metabolism	MM
21	HMP	inner membrane protein, mitochondrial. (mitofilin) (motor protein)	IMMT_HUMAN	Q16891	---	5803115		83626,35		62000	6,10	758	5(16)	12	ProFound 1.0e+000 (Z1.55)	TIM	MIM
22	HMP	inner membrane protein, mitochondrial. (mitofilin) (motor protein)	IMMT_HUMAN	Q16891	---	5803115		83626,35		61200	6,10	758	17(32)	28	177	TIM	MIM
23	PDIA3	glucose regulated protein, 58kDa. (protein disulfide isomerase A3 precursor) (disulfide isomerase ER-60) (ERp60) (58 kDa microsomal protein) (p58) (ERp57) (58 kDa glucose regulated protein)	PDA3_ HUMAN	P30101	602046	20127473	5.3.4.1	54265,22		51000	6,10	25-505	14(47)	26	105		*endoplasmic reticulum lumen*
24	DLST	dihydrolipoamide succinyltransferase component of 2-oxoglutarate dehydrogenase, mitochondrial precursor. (E2) (E2K).	ODO2_ HUMAN	P36957	126063	1709442	2.3.1.61	41349,64		48500	6,00	68-453	12(34)	22	73	citric cycle	M
25	UQCRC1	ubiquinol-cytochrome C reductase core protein I. (ubiquinol-cytochrome C reductase complex, core protein I, mitochondrial precursor)	UCR1_ HUMAN	P31930	191328	4507841	1.10.2.2	49101,57		44300	6,00	35-480	16(54)	27	94	complex III	MIM
26	---	unknown. (protein for MGC:9832) (actin, beta)	Q96E67	Q96E67	---	15277503		40220,13		41400	6,00	360	9(20)	28	100		*cytoplasmic*
27	IDH3A	isocitrate dehydrogenase 3 (NAD+), alpha. (isocitrate dehydrogenase [NAD], subunit alpha, mitochondrial precursor) (isocitric dehydrogenase) (NAD+-specific ICDH)	IDHA_ HUMAN	P50213	601149	5031777	1.1.1.41	36640,21		38700	6,00	28-366	10(21)	22	94	citric cycle	M
28	ECHS1	mitochondrial short-chain enoly-CoA hydratase 1, precursor. (enoyl-CoA hydratase, mitochondrial precursor) (SCEH) (enoyl-CoA hydratase 1)	ECHM_ HUMAN	P30084	602292	12707570	4.2.1.17	28354,66		27600	6,00	28-290	15(34)	44	149	ß-oxidation	MM
29	NDUFV2	NADH-ubiquinone oxidoreductase 24 kDa subunit, mitochondrial precursor. (24-kDa subunit of complex I)	NUHM_ HUMAN	P19404	600532	3123721	1.6.5.3 1.6.99.3	23760.31	5,71	24500	6,00	33-249	9(19)	30	95	Complex I	MIM

Spot Nr.	gene name	Protein name	swiss ID	SWISS_ PROT Nr.	OMIM No.	gi	E.C.	MW(S)	pI (S)	MW(m)	pI(m)	Seq.	matched peptide (total peptide)	sequence coverage %	probability based Mowse score	Function	location
30	NDUFA5	NADH ubiquinone oxidoreductase 13 kDa-B subunit. (complex I-13kDa-B)(complex I subunit B13)	NUFM_HUMAN	Q16718	601677	2499316	1.6.5.3 1.6.99.3	13327,50		12100	5,80				sequence	Complex I	MIM
31	COX5A	cytochrome C oxidase, subunit Va. (cytochrome c oxidase polypeptide Va, mitochondrial precursor)	COXA_ HUMAN	P20674	603773	18999392	1.9.3.1	12513,23	4,88	11400	6,00	42-150	6(21)	28	69	Complex IV	MIM
32	OGDH	oxoglutarate (alpha-ketoglutarate) dehydrogenase. (lipoamide) (2-oxoglutarate dehydrogenase E1 component, mitochondrial precursor) (alpha-ketoglutarate dehydrogenase)	ODO1_ HUMAN	Q02218	203740	20541592	1.2.4.2	108880,11		67000	6,50	41-1002	13(17)	16	133	citric cycle	MM
33	TRAP1	heat shock 75kDa protein, mitochondrial precursor. (HSP 75) (tumor necrosis factor type 1 receptor associated protein) (TRAP-1) (TNFR-associated protein 1)	TRAL_ HUMAN	Q12931	606219	2865466		80010,86	8,05	57500	6,40	?-704	21(47)	39	180	HSP (chaperone)	M
34	OXCT	succinyl CoA: 3-ketoacid CoA transferase, mitochondrial precursor. (succinyl CoA:3-oxoacid CoA transferase)	SCOT_ HUMAN	P55809	245050	4557817	2.8.3.5	52089,89		51300	6,10	40-520	11(19)	25	87	fat metabolism	MM
35	MCCC2	methycrotonoyl-CoA carboxylase 2 (beta) mitochondrial precursor. (non-biotin containing subunit of 3-methylcrotonyl-CoA carboxylase) (biotin carboxylase) (3-methylcrotonyl-CoA carboxylase 2) (MCCase, beta subunit) (3-methylcrotonyl-CoA:carbon dioxide ligase, beta subunit)	MCCB_ HUMAN	Q9HCC0	210210	11545863	6.4.1.4	61333,20	7,58	50000	6,60	?-563	14(42)	26	99	AA metabolism	MM
36	ATP5A1	ATP synthase, H+transporting, mitochondrial F1 complex, alpha subunit, isoform 1, cardiac muscle	ATPA_ HUMAN	P25705	164360	4757810	3.6.1.34	55209,32		47900	6,60	44-553	21(45)	43	214	complex V	MIM
37	ACADM	medium-chain acyl-CoA dehydrogenase, mitochondrial precursor.	ACDM_ HUMAN	P11310	607008 201450	2392312	1.3.99.3	43642,89		41800	6,25	26-421	17(43)	41	173	ß-oxidation	MM
38	ECH1	similar to delta3,5-delta2,4-dienoyl-CoA isomerase, mitochondrial	ECH1_ HUMAN	Q13011	600696	11433007	5.3.3.-	35994,34		31600	6,00	?-328	12(29)	44	151	ß-oxidation	M
39	ECH1	similar to delta3,5-delta2,4-dienoyl-CoA isomerase, mitochondrial	ECH1_ HUMAN	Q13011	600696	11433007	5.3.3.-	35994,34		31600	6,10	?-328	15(49)	41	112	ß-oxidation	M
40	ETFA	chain A, three-dimensional structure of human electron transfer flavoprotein. (electron transfer flavoprotein alpha-subunit, mitochondrial precursor) (alpha-ETF)	ETFA_ HUMAN	P13804	231680	2781202		35079,57		32300	6,20	?-333	10(25)	40	109	ß-oxidation	MM
41	PRDX3	peroxiredoxin 3. (thioredoxin-dependent peroxide reductase, mitochondrial precursor) (antioxidant protein 1) (AOP-1) (MER5 protein homolog) (HBC189) (PRX III)	PDX3_ HUMAN	P30048	604769	14250063		21468,45		25400	6,00	63-256	5(17)	21	MS-Fit ProFound (1.0e+000)	cell protection	M
42	HADH2	hydroxyacyl-CoA dehydrogenase, type II. (type II HADH) (endoplasmic reticulum-associated amyloid beta-peptide binding protein) (short-chain type dehydrogenase/reductase) (XH98G2)	HCD2_ HUMAN	Q99714	300256	4758504	1.1.1.35	26923,08		25500	6,10	261	11(37)	58	157	in Alzheimer' disease	*endoplasmic reticulum lumen*
43	MCCC1	methylcrotonyl-CoA carboxylase alpha chain, mitochondrial precursor. (3-methylcrotonyl-CoA carboxylase 1) (MCCase alpha subunit) (3-methylcrotonyl-CoA:carbon dioxide ligase, alpha subunit)	MCCA_ HUMAN	Q96RQ3	210200	13518228	6.4.1.4	75030,63		59400	7,00	48-725	8(14)	16	82	AA metabolism	MM
44	PDCD8	programmed cell death 8. (apoptosis-inducing factor)	PCD8_ HUMAN	O95831	300169	4757732	1.-.-.-	55699,48		58200	7,00	103-613	11(29)	25	120	Apoptosis	MIMS
45	DLD	dihydrolipoamide dehydrogenase, mitochondrial precursor	DLDH_ HUMAN	P09622	246900 238331	181575	1.8.1.4	50147,55		51500	6,90	36-509	7(19)	22	84	fat metabolism	MM
46	---	unknown. (protein for MGC 14085)	Q96I46	Q96I46	---	14043738		51905,08		49800	6,70	468	11(22)	28	118	?	?
47	ATP5A1	ATP synthase, H+transporting, mitochondrial F1 complex, alpha subunit. (ATP synthase alpha chain, mitochondrial precursor)	ATPA_ HUMAN	P25705	164360	4757810	3.6.3.14	55209,32		48100	6,80	44-553	27(39)	50	273	Complex V	MIM
48	GLUD1	chain A, structure of human glutamate dehydrogenase-Apo form. (glutamate dehydrogenase 1, mitochondrial precursor) (GDH)	DHE3_ HUMAN	P00367	138130 606762	4885281	1.4.1.3	56008,68		49500	7,00	54-558	18(30)	31	165	AA metabolism	MM
49	GLUD1	chain A, structure of human glutamate dehydrogenase-Apo form. (glutamate dehydrogenase 1, mitochondrial precursor) (GDH)	DHE3_ HUMAN	P00367	138130 606762	20151189	1.4.1.3	56008,68		49800	7,00	54-558	21(41)	33	159	AA metabolism	MM
50	TUFM	Tu translation elongation factor, mitochondrial precursor. (elongation factor Tu, mitochondrial precursor) (P43)	EFTU_ HUMAN	P49411	602389	4507733		45045,00		42700	6,80	44-452	12(23)	26	132	protein synthesis	M
51	TUFM	Tu translation elongation factor, mitochondrial precursor. (elongation factor Tu, mitochondrial precursor) (P43)	EFTU_ HUMAN	P49411	602389	4507733		45045,00		42600	6,90	44-452	23(41)	50	242	protein synthesis	M
52	ACAT1	mitochondrial acetoacetyl-CoA thiolase. (acetyl-CoA acetyltransferase, mitochondrial precursor)	THIL_ HUMAN	P24752	203750	499158	2.3.1.9	41386,02		41450	6,90	34-427	11(23)	31	109	ß-oxidation	M
53	VDAC1	voltage-dependent anion channel 1. (voltage-dependent anion-selective channel protein 1) (VDAC-1) (hVDAC1) (outer mitochondrial membrane protein porin 1) (plasmalemmal porin) (Porin 31HL) (Porin 31HM)	POR1_ HUMAN	P21796	604492	4507879		30641,40		35300	6,70	282	16(28)	67	226	VDAC	MOM
54	ETFB	electron-transfer-flavoprotein, beta polypeptide. (Beta-ETF)	ETFB_ HUMAN	P38117	130410	4503609		27843,61		29100	6,40	255	7(24)	28	81	ß-oxidation	MM
55	UQCRFS1	ubiquinol-cytochrome C reductase iron-sulfur subunit, mitochondrial precursor. (rieske iron-sulfur polypeptide 1) (rieske iron-sulfur protein) (RISP)	UCRI_ HUMAN	P47985	191327	5174743	1.10.2.2	21616,58		28300	6,30	79-274	6(24)	27	79	complex III	MIM
56	COX5B	cytochrome c oxidase polypeptide Vb, mitochondrial precursor.	COXB_ HUMAN	P10606	123866	117103	1.9.3.1	10613,04	6,33	14500	6,40	32-129	6(17)	50	ProFound 1.0e+00	complex IV	MIM

Spot Nr.	gene name	Protein name	swiss ID	SWISS_ PROT Nr.	OMIM No.	gi	E.C.	MW(S)	pI (S)	MW(m)	pI(m)	Seq.	matched peptide (total peptide)	sequence coverage %	probability based Mowse score	Function	location
57		**not identified**															
58	HSPE1	chaperonin 10-related protein. (10 kDa heat shock protein, mitochondrial) (HSP10) (10 kDa chaperonin)	CH10_ HUMAN	Q04984	600141	4028622		10800,50		11700	6,50	101	8(17)	71	150	HSP (mito protein biogenesis)	MM
59		**not identified**															
60	ACO2	aconitate hydratase, mitochondrial precursor. (aconitate hydratase) (citrate hydrolyase) (aconitase 2) (aconitase)	ACON_ HUMAN	Q99798	100850	5304852	4.2.1.3	82425,78		64100	7,20	28-780	28(55)	36	229	citric cycle	M
61	SHMT2	mitochondrial serine hydroxymethyltransferase.	GLYM_ HUMAN	P34897	138450	746436	2.1.2.1	52559,86		50300	7,30	30-504	24(52)	42	187	nucleotide metabolism	M
62	FH	fumarate hydratase, mitochondrial precursor. (fumarase)	FUMH_ HUMAN	P07954	136850 150800 605839 606812	68293	4.2.1.2	50081,55		46100	7,20	45-510	12(29)	31	125	citric cycle	M
63	UQCRC2	ubiquinol-cytochrome C reductase core protein II, mitochondrial precursor. (complex III, subunit II)	UCR2_ HUMAN	P22695	191329	12653427	1.10.2.2	46811,05		46100	7,20	15-453	13(41)	35	114	complex III	MIM
64	FDXR	adrenodoxin reductase. (NADPH: adrenodoxin oxidoreductase, mitochondrial precursor) (AR) (Ferredoxin-NADP(+) reductase)	ADRO_ HUMAN	P22570	103270	178209	1.18.1.2	49967,33		48000	7,30	33-491	17(30)	37	203	fat metabolism	MM
65	ACAA2	acetyl-CoA acyltransferase 2. (mitochondrial 3-oxoacyl-CoA) (3-ketoacyl-CoA thiolase, mitochondrial) (Beta-ketothiolase) (T1)	THIM_ HUMAN	P42765	604770	12804931	2.3.1.16	42039,29		47200	7,20	397	18(45)	49	187	ß-oxidation	M
66	UQCRC2	ubiquinol-cytochrome C reductase core protein II, mitochondrial precursor. (complex III, subunit II)	UCR2_ HUMAN	P22695	191329	12653427	1.10.2.2	46811,05		46200	7,20	15-453	12(35)	32	105	complex III	MIM
67	ACAT1	mitochondrial acetoacetyl-CoA thiolase. (acetyl-CoA acetyltransferase, mitochondrial precursor)	THIL_ HUMAN	P24752	203750	499158	2.3.1.9	41386,02		42800	7,00	34-427	11(45)	36	114	ß-oxidation	M
67/2	TOM40	probable mitochondrial import receptor, subunit TOM40 homolog. (translocase of outer membrane 40 kDa subunit homolog) (Haymaker protein) (p38.5)	OM40_ HUMAN	O96008	---	5174723		37893,10		43500	7,00	361	8(48)	27	72	TOM	MOM
68	CPO	coprpoprphyrinogen III oxidase, mito precursor. (coproporphyrinogenase) (coprogen oxidase) (COX)	HEM6_ HUMAN	P36551	121300	547615	1.3.3.3	36853,89		41300	7,00	32-354	12(21)	32	145	heme biosynthesis	M
69	VDAC1	voltage-dependent anion channel 1. (voltage-dependent anion-selective channel protein 1) (VDAC-1) (hVDAC1) (outer mitochondrial membrane protein porin 1) (plasmalemmal porin) (Porin 31HL) (Porin 31HM))	POR1_ HUMAN	P21796	604492	4507879		30641,40		35900	7,00	282	10(21)	43	141	VDAC	MOM
70	AK2	adenylate kinase 2 isoform A, mitochondrial. (adenylate kinase isoenzyme 2, mitochondrial) (ATP-AMP transphosphorylase)	KAD2_ HUMAN	P54819	103020	7524346	2.7.4.3	26346,55		30300	7,00	238	10(26)	37	135	maintenance and cell growth	MIMS
71	C21ORF33	anti-sigma cross-reacting protein homolog I beta precursor of human. (ES1 protein homolog, mitochondrial precursor) (Protein KNP-I) (GT335 protein)	ES1_ HUMAN	P30042	601659	2134764		24016,57		27200	6,90	42-268	5(31)	43	64	?	M
72	SOD2	superoxide dismutase [Mn], mitochondrial precursor. (chain A,kinetic analysis of product inhibition in human manganese superoxide dismutase)	SODM_ HUMAN	P04179	147460	134665	1.15.1.1	22204,14		25300	6,70	25-222	9(15)	44	148	cell protection	MM
73	---	cDNA FLJ20420 fis, clone KAT02462. (hypothetical 26.2 kDa protein) (similar to hypothetical protein, FLJ20420)	Q9NX63	Q9NX63	---	8923390		26152,36		28500	7,00	227	6(20)	26	75	function? Skin?	?
74	SSBP1	single-stranded DNA-binding protein, mitochondrial precursor. (Mt-SSB) (MtSSB) (PWP1-interacting protein 17)	SSB_ HUMAN	Q04837	600439	2624694		15195,14		15700	6,70	17-148	10(28)	70	138	nucleotide metabolism	M
75	GRIM19	NADH-ubiquinone oxidoreductase, B16.6 subunit. (complex I-B16.6) (CI-B16.6) (cell death-regulatory protein GRIM19) (CGI-39 protein) (gene associated with retinoic-interferon-induced mortality 19 protein) (GRIM-19) (CDA016)	NB6M_ HUMAN	Q9P0J0	---	16923946	1.6.5.3 1.6.99.3	16567,12		16600	6,80	143	11(21)	66	166	Complex I	MIM (membrane protein)
76		**not identified**															
77		**not identified**															
78		**not identified**															
79	HADHA	long-chain-fatty-acid beta-oxidation multienzyme complex, alpha chain, mitochondrial precursor. (trifunctional enzyme alpha subunit, mitochondrial precursor [includes: long-chain enoyl-CoA hydratase (EC 4.2.1.17); long chain 3-hydroxyacyl-CoA dehydrogenase(EC 1.1.1.35)]) (TP-alpha) (78 kDa gastrin-binding protein)	ECHA_ HUMAN	P40939	600890	543064	4.2.1.17 1.1.1.35	79009,87		62100	7,60	37-763	25(37)	34	225	ß-oxidation	MM
80	CS	citrate synthase, mitochondrial precursor.	CISY_ HUMAN	O75390	118950	15302936	4.1.3.7	49000,22		47050	7,20	28-466	14(21)	22	126	citric cycle	MM
81	IDH2	isocitrate dehydrogenase [NADP] mitochondrial precursor. (oxalosuccinate decarboxylase) (IDH) (NADP+-specific ICDH) (IDP) (ICD-M)	IDHP_ HUMAN	P48735	147650	20141568	1.1.1.42	46614,35		47100	7,40	40-452	15(23)	35	197	citric cycle	M
82	IDH2	isocitrate dehydrogenase [NADP] mitochondrial precursor. (oxalosuccinate decarboxylase) (IDH) (NADP+-specific ICDH) (IDP) (ICD-M)	IDHP_ HUMAN	P48735	147650	20141568	1.1.1.42	46614.35	8,32	47100	7,00	40-452	15(30)	38	173	citric cycle	M

Spot Nr.	gene name	Protein name	swiss ID	SWISS_ PROT Nr.	OMIM No.	gi	E.C.	MW (S)	pI (S)	MW(m)	pI(m)	Seq.	matched peptide (total peptide)	sequence coverage %	probability based Mowse score	Function	location
83	IDH3B	isocitrate dehydrogenase 3 (NAD+) beta, mitochondrial precursor. (isocitric dehydrogenase) (NAD+-specific ICDH)	IDHB_ HUMAN	O43837	604526	5901982	1.1.1.41	38793,79		46100	7,20	35-385	10(21)	28	95	citric cycle	M
84	BCAT2	branched chain aminotransferase 2, mitochondrial. (branched-chain amino acid aminotransferase, mitochondrial precursor) (BCAT(m)) (placental protein 18) (PP18)	BCAM_ HUMAN	O15382	113530	4502375	2.6.1.42	39915,56		43900	7,00	352	11(22)	24	108	AA metabolism	M
85	MDH2	malate dehydrogenase 2, NAD, mitochondrial.	MDHM_ HUMAN	P40926	154100	5174541	1.1.1.37	33000,45		40800	7,00	25-338	8(25)	30	76	citric cycle	MM
86	CRYZ	crystallin, zeta. (quinone oxidoreductase) (NADPH:quinone reductase)	QOR_ HUMAN	Q08257	123691	13236495	1.6.5.5	35206,63		41900	7,00	329	6(26)	29	70	detoxication	Cytoplasmic
87	MDH2	malate dehydrogenase 2, NAD, mitochondrial.	MDHM_ HUMAN	P40926	154100	5174541	1.1.1.37	33000,45		42400	7,00	25-338	14(36)	39	139	citric cycle	MM
88	GAPD	glyceraldehyde-3-phosphate dehydrogenase.	G3P2_ HUMAN	P04406	138400	31645	1.2.1.12	35922,02		43500	7,00	334	10(17)	35	2.43 (1.0e+000)		Cytoplasmic
89	GAPD	glyceraldehyde-3-phosphate dehydrogenase.	G3P2_ HUMAN	P04406	138400	7669492	1.2.1.12	35922,02		44100	7,10	334	11(27)	27	70		Cytoplasmic
90	IDH3G	isocitrate dehydrogenase. (isocitrate dehydrogenase [NAD] subunit gamma, mitochondrial precursor) (isocitric dehydrogenase) (NAD+-specific ICDH)	IDHG_ HUMAN	P51553	300089	12804901	1.1.1.41	38814,53		47100	7,20	40-393	5(21)	17	MS-Fit	citric cycle	M (membrane protein)
91	GOT2	aspartate aminotransferase 2, mitochondrial precursor. (transaminase A) (glutamate oxaloacetate transaminase-2)	AATM_ HUMAN	P00505	138150	12739307	2.6.1.1	44695,28		43100	7,60	30-430	12(32)	27	97	AA transporter	MM
92	HADHSC	short chain 3-hydroxyacyl-CoA dehydrogenase, mitochondrial precursor. (HCDH) (medium and short chain L-3-hydroxyacyl-CoA dehydrogenase)	HCDH_ HUMAN	Q16836	601609	2078329	1.1.1.35	32822,73		37700	7,00	13-314	12(24)	50	140	ß-oxidation	MM
93	AK3	adenylate kinase 4, mitochondrial. (adenylate kinase-4) (AK4) (ATP:AMP phosphotransferase)	KAD4_ HUMAN	P27144	103030	8051579	2.7.4.3	25268,00		32800	7,00	223	11(19)	34	153	nucleotide metabolism	MM
94		**not identified**															
95		**not identified**															
96	HBA1	hemoglobin, alpha chain.	HBA_ HUMAN	P01922	141800 141850 141860	996122		15126,36		12700	7,10	141	5(10)	35	64		Cytoplasmic
97		**not identified**															
98		**not identified**															
99		**not identified**															
100		**not identified**															
101	HBB	hemoglobin, beta chain.	HBB_ HUMAN	P02023	141900 603903	122615		15867,22		10200	7,00	146			von sequence		Cytoplasmic
102		**not identified**															
103	HBAP or REA	B-cell associated protein. (B-cell receptor associated protein) (D-prohibitin)	Q99623	Q99623	---	6005854		33296,38		35700	8,10	299	14(26)	51	161		*B-cell*
104		**not identified**															
105	NIPSNAP1	NIPSNAP homolog 1. (4-nitrophenylphosphatase domain and non-neutonal SNAP25-like 1)	NPS1_ HUMAN	Q9BPW8	603249	4505399		33309,98		29900	8,00	284	9(22)	23	86	?	?
106	ATP5O	ATP synthase H+ transporting, mitochondrial F1 complex, o subunit. (oligomycin sensitivity conferring protein) (human ATP synthase OSCP subunit, oligomycin sensitivity conferring protein)	ATPO_ HUMAN	P48047	600828	4502303	3.6.3.14	20875,49		26100	8,40	24-213	12(34)	47	110	Complex V	MM
107		**not identified**															
108		**not identified**															
109		**not identified**															
110		**not identified**															
111		**not identified**															
112		**not identified**															
113		**not identified**															
114	ACTB	actin, beta. (actin, cytoplasmic 1) (fragment)	ACTB_ HUMAN	P02570	102630	16359158		41605,54		10200	8,10	2 - 375			von sequence	von sequence	Cytoplasmic
115		**not identified**															
116		**not identified**															
117	PNPASE	polynucleotide phosphorylase-like protein	Q8TCS8	Q8TCS8	---	20372922	2.7.7.8	85936,59		60500	6,50	783	14(20)	18	124	nucleotide metabolism	?
118	OXCT	succinyl CoA: 3-ketoacid CoA transferase, mitochondrial precursor. (succinyl CoA:3-oxoacid CoA transferase)	SCOT_ HUMAN	P55809	245050	4557817	2.8.3.5	52089,89	6	51200	6,10	40-520	5(29)	16	MS-Fit	fat metabolism	MM
119	PMPCA or MPPA or KIAA0123	mitochondrial processing peptidase alpha subunit, mitochondrial precursor. (alpha-MPP) (P-55) (HA1523)	MPPA_ HUMAN	Q10713	---	1709089	3.4.24.64	54624,57		50100	6,30	34-525	7(22)	16	MS-Fit and ProFound 1.0e+000 (Z1,77)	regulation and assembly(Aa metabolism)	MM

Spot Nr.	gene name	Protein name	swiss ID	SWISS_ PROT Nr.	OMIM No.	gi	E.C.	MW (S)	pI (S)	MW(m)	pI(m)	Seq.	matched peptide+N106	sequence coverage %	probability based Mowse score	Function	location
120	LAP3 orLAPEP	cytosol aminopeptidase. (leucine aminopeptidase) (LAP) (leucyl aminopeptidase) (proline aminopeptidase) (prolyl aminopeptidase)	AMPL_ HUMAN	P28838	---	12643394	3.4.11.1 3.4.11.5	52640,08		49400	6,20	488	9(15)	18	101	regulation and assembly(Aa metabolism)	*Cytoplasmic*
121	ALDH1B1	aldehyde dehydrogenase X, mitochondrial precursor. (ALDH class 2)	DHA5_ HUMAN	P30837	100670	399363	1.2.1.3	55292,03		48500	6,00	18-517	10(20)	27	105	detoxication of alcohol	MM
122	PMPCB	mitochondrial processing peptidase beta subunit, mitochondrial precursor. (beta-MPP) (P-52)	MPPB_ HUMAN	O75439	603131	4758734	3.4.24.64	49487,50		44200	6,00	46-489	7(27)	17	63	protein regulation	MM
123	ACADM	medium-chain acyl-CoA dehydrogenase, mitochondrial precursor.	ACDM_ HUMAN	P11310	607008 201450	17440754	1.3.99.3	43642,89		41700	6,00	26-421	9(13)	20	131	ß-oxidation	MM
124	ACADM	medium-chain acyl-CoA dehydrogenase, mitochondrial precursor.	ACDM_ HUMAN	P11310	607008 201450	17440754	1.3.99.3	43642,89		41900	6,50	26-421	10(17)	25	121	ß-oxidation	MM
125	MRPS22	mitochondrial ribosomal protein S22. (gibt protein) (chromosome 3 open reading frame 5) (mitochondrial 28S ribosomal protein S22) (S22mt) (MRP-S22) (GK002)	RT22_ HUMAN	P82650	605810	9910244		41280,38		39400	6,10	360	11(27)	23	97	ribosomal protein	M
126	NDUFS3	NADH-ubiquinone oxidoreductase 30 kDa subunit, mitochondrial precursor. (30-kDa subunit of complex I) (Complex I-30KD) (CI-30KD)	NUGM_ HUMAN	O75489	603846	5138999	1.6.5.3 1.6.99.3	26414,92		26500	5,90	37-264	15(26)	48	222	Complex I	MIM
127	TSFM	elongation factor Ts, mitochondrial precursor. (EF-Ts) (EF-TsMt)	EFTS_HUMAN	P43897	604723	12644268		30503,99		33200	6,30	46-325	3(38)		sequence	protein synthesis	M
128	ETFA	chain A, three-dimensional structure of human electron transfer flavoprotein. (electron transfer flavoprotein alpha-subunit, mitochondrial precursor) (alpha-ETF)	ETFA_ HUMAN	P13804	231680	2781202		35079,57		33200	6,40	?-333	6(25)	28	66	ß-oxidation	MM
129	---	hypothetical protein FLJ113428. (cDNA FLJ11342 fis) (clone PLACE10108009)	Q9NUJ1	Q9NUJ1	---	8923001		33932,51		30600	6,60	306	6(20)	20	71	?	?
130	PYCR1	pyrroline-5-carboxylate reductase. (pyrroline-5-carboxylate reductase 1) (P5CR) (P5C reductase)	PROC_ HUMAN	P32322	179035	5902036	1.5.1.2	33374,65		34700	7,00	319	11(35)	31	84	Proline biosynthesis	M
131	---	similar to hypothetical protein FLJ10709. (hypothetical 72.6 kDa protein)	Q9BUK4	Q9BUK4	---	8922609		72600,98		57500	7,50	586	23(39)	40	258	?	?
132	SQRDL	sulfide:quinone oxidoreductase, mitochondrial precursor	SQRD_HUMAN	Q9Y6N5	---	10864011	1.-.-.-	49960,71		55700	7,60	?-450	21(43)	47	218	mitochondrial sulfide oxidation	M
133	HADHB	trifunctional enzyme beta subunit, mitochondrial precursor, [Includes: 3-ketoacyl-CoA thiolase; acetyl-CoA acyltransferase; beta-ketothiolase]. (TP-beta)	ECHB_ HUMAN	P55084	143450	4504327	2.3.1.16	47484,90		53700	7,50	34-474	18(29)	31	154	ß-oxidation	MM
134	AFXN1	sideroflexin 1	SFX1_ HUMAN	Q9H9B4	---	20140250		35619,42		39600	7,30	322	7(17)	20	87	iron transport	M (membrane protein)
135	AKL3L	adenylate kinase-3,mitochondrial. (adenylate kinase 3) (AK3) (AK3-alpha) (GTP:AMP phosphotransferase)	KAD3_ HUMAN	Q9UIJ7	---	11130641	2.7.4.10	25434,22		30100	7,50	226	10(21)	50	154	nucleotide metabolism	MM
136	GBAS	NIPSNAP2 protein. (glioblastoma amplified sequence)	NPS2_ HUMAN	O75323	603004	2769254		33742,64		30100	7,40	286	6(11)	16	70	?	?
137	NDUFB9	NADH-ubiquinone oxidoreductase, B22 subunit. (Complex I-B22) (CI-B22)	NI2M_ HUMAN	Q9Y6M9	601445	6274550	1.6.5.3 1.6.99.3	21699,72		28900	7,20	178	10(29)	46	109	complex I	MIM
138	NDUFB10	NADH-ubiquinone oxidoreductase, PDSW subunit. (Complex I-PDSW) (CI-PDSW)	NIDM_ HUMAN	O96000	603843	4758774	1.6.5.3 1.6.99.3	20645,48		27300	7,80	171	13(21)	47	145	complex I	MIM
139		**not identified**															
140	PPIF	peptidyl-prolyl cis-trans isomerase, mitochondrial precursor. (PPIase) (rotamase) (peptidyl-prolyl isomerase F) (cyclophilin F)	PPIF_ HUMAN	P30405	604486	5031987	5.2.1.8	18897,38		20500	8,00	30-207	4(19)	33	sequence	assembly protein	MM

Tab. 7-1: *The identified proteins of my study.* Proteins from the mitochondrial fraction of human lymphoblastiod cells were extracted and separated by 2D-electrophoresis. The identification of proteins was carried out with MALDITOF and MALDI-QTOF mass spectrometry. The database search was performed with several search engines such as Mascot, ProFound, and MS-Fit. Information about a specific protein contains the spot number, the full name, the accession ID and SWISS-PROT number, the E.C. and gi numbers, the theoreticalMW and pI values from SWISS-PROT database [MW(S) and pI(S)] and the measuredMW and pI values [MW(m) and pI(m)].The data from the MS analysis i.e. the numbers of matching peptides and the probability of assignment of a random identity are listed here as well.
M: mitochondrial; MM: mitochondrial matrix; MIM: mitochondrial inner membrane; MOM: mitochondrial outer membrane; MIMS: mitochondrial inter membrane space.

REFERENCES

[Abbott, 1999] Abbott A. A post-genomic challenge: learning to read patterns of protein synthesis. *Nature* 1999, **402**: 715-720

[Alberts *et al.*, 1994] Alberts B, Bray D, Lewis J, Raff M, Roberts K and Watson JD. Molecular biology of the cell. (3rd ed.) New York, London Garland science Publishing, 1994

[Almeida *et al.*, 1997] Almeida A and Medina JM. Isolation and characterisation of tightly coupled mitochondria from neurons and astrocytes in primary culture. *Brain Res* 1997, **764**: 167-172

[Anderson *et al.*, 1981] Anderson S, Bankier AT, Barrell BG, de Bruijn MH, Coulson AR, Drouin J, Eperon IC, Nierlich DP, Roe BA, Sanger F, Schreier PH, Smith AJ, Staden R and Young IG. Sequence and organization of the human mitochondrial genome. *Nature* 1981, **290**: 457-465

[Annan *et al.*, 1996] Annan RS and Carr SA. Phosphopeptide analysis by matrix-assisted laser desorption time-of-flight mass spectrometry. *Anal Chem* 1996, **68**: 3413-3421

[Bauer *et al.*, 1999] Bauer MF, Gempel K, Hofmann S, Jaksch M, Philbrook C and Gerbitz KD. Mitochondrial Disorders: A diagnostic challenge in clinical chemistry. *Clin Chem Lab Med* 1999, **37**: 855-876

[Bjellqvist *et al.*, 1993] Bjellqvist B, Hughes GJ, Pasquali C, Paquet N, Ravier F, Sanchez JC, Frutiger S and Hochstrasser D. The focussing positions of polypeptides in immobilized pH gradients can be predicted from their amino acid sequences. *Electrophoresis* 1993, **14**: 1023-1031

[Boles *et al.*, 1998] Boles RG, Roe T, Senadheera D, Mahnovski V and Wong LJ. Mitochondrial DNA deletion with Kearns Sayre syndrome in a child with Addison disease. *Eur J Pediatr* 1998, **157**: 643-647

[Boucherie *et al.*, 1995] Boucherie H, Dujardin G, Kermorgant M, Monribot C, Slonimski P and Perrot M. Two-dimensional protein map of Saccharomyces cerevisiae: construction of a gene-protein index. *Yeast* 1995, **11**: 601-613

[Bourgeron *et al.*, 1992] Bourgeron T, Chretien D, Rötig A, Munnich A and Rustin P. Isolation and characterisation of mitochondria from human B lymphoblastoid cell lines. *Biochem Biophys Res Commun* 1992, **186**: 16-23

[Bourgeron *et al.*, 1993] Bourgeron T, Chretien D, Amati P, Rotig A, Munnich A and Rustin P. Expression of respiratory chain deficiencies in human cultured cells. *Neuromuscul Disord* 1993, **3**: 605-608

[Bradford, 1976] Bradford MM. A rapid and sensitive method for the quantitation of microgram quantities of protein utilising the principle of protein-dye binding. *Anal Biochem* 1976, **72**: 248-254

[Bronfman *et al.*, 1998] Bronfman M, Loyola G and Koenig CS. Isolation of intact organelles by differential centrifugation of digitonin treated hepatocytes using a table Eppendorf centrifuge. *Anal Biochem* 1998, **255**: 252-256

[Carroll *et al.*, 2002] Carroll J, Shannon RJ, Fearnley IM, Walker JE and Hirst J. Definition of the nuclear encoded protein composition of bovine heart mitochondrial complex I. *J Biol Chem* 2002, **277**: 50311-50317

[Claros *et al.*, 1996] Claros MG and Vincens P. Computational method to predict mitochondrially imported proteins and their targeting sequences. *Eur J Biochem* 1996, **241**: 779-786

[DiMauro, 2000] DiMauro S. Introduction: Mitochondrial Encephalomyopathies. *Brain Pathol* 2000, **10**: 419-421

[de Duve *et al.*, 1955] de Duve C, Pressman BC, Gianetto R, Wattiaux R and Appelmans F. Tissue fraction studies: intracellular distribution patterns of enzymes in rat liver tissue. *Biochem J* 1955, **60**: 604-617

[Fernandez *et al.*, 1998] Fernandez J, Gharahdaghi F and Mische SM. Routine identification of proteins from sodium dodecyl sulfate-polyacrylamide gel electrophoresis (SDS-PAGE) gels or polyvinyl difluoride membranes using matrix assisted laser desorption/ionization time-of-flight mass spectrometry (MALDI-TOF-MS). *Electrophoresis* 1998, **19**: 1036-1045

[Folgero *et al.*, 1993] Folgero T, Bertheussen K, Lindal S, Torbergsen T and Oian P. Mitochondrial disease and reduced sperm motility. *Hum Reprod* 1993, **8**: 1863-1868

[Frey *et al.*, 2000] Frey TG and Mannella CA. The internal structure of mitochondria. *Trends Biochem Sci.* 2000, **25**: 319-324

[Fountoulakis *et al.*, 2003] Fountoulakis M and Schlaeger EJ. The mitochondrial proteins of the neuroblastoma cell line IMR-32. *Electrophoresis* 2003, **24**: 260-275

[Garrels *et al.*, 1997] Garrels JI, McLaughlin CS, Warner JR, Futcher B, Latter GI, Kobayashi R, Schwender B, Volpe T, Anderson DS, Mesquita-Fuentes R and Payne WE. Proteome studies of Saccharomyces cerevisiae: identification and characterisation of abundant proteins. *Electrophoresis* 1997, **18**:1347-1360

[Giles *et al.*, 1980] Giles RE, Blanc H, Cann HM, Wallace DC. Maternal inheritance of human mitochondrial DNA. *Proc Natl Acad Sci USA* 1980, **77**: 6715-6719

[Gobom *et al.*, 2001] Gobom J, Schuerenberg M, Mueller M, Theiss D, Lehrach H and Nordhoff E. α-cyano-4-hydroxycinnamic acid affinity sample preparation: A protocol for MALDI-MS peptide analysis in proteomics. *Anal Chem* 2001, **73**: 434-438

[Gottlieb *et al.*, 2000] Gottlieb RA and Adachi S. Nitrogen cavitation for cell disruption to obtain mitochondria from cultured cells. *Methods Enzymol* 2000, **322**: 213-221

[Gray *et al.*, 1999] Gray MW, Burger G and Lang BF. Mitochondrial evolution. *Science* 1999, **283**: 1476-1481

[Green *et al.*, 1998] Green DR and Reed JC. Mitochondria and apoptosis. *Science* 1998, **281**: 1309-1312

[Grossman *et al.*, 1996] Grossman LI and Shoubridge EA. Mitochondrial genetics and human disease. *Bio Essays* 1996, **18**: 983-991

[Gustafson *et al.*, 2002] Gustafson AW, Heckerling PS, Vissing J and Schwartz M. Paternal inheritance of mitochondrial DNA. *N Engl J Med* 2002, **347**: 2081-2082

[Grivell, 1988] Grivell LA. Protein import into mitochondria. *Int Rev Cytol* 1988, **111**: 107-141

[Gygi *et al.*, 2000] Gygi SP, Corthals GL, Zhang Y, Rochon Y and Aebersold R. Evaluation of two-dimensional gel electrophoresis-based proteome analysis technology. *Proc Natl Acad Sci USA* 2000, **97**: 9390-9395

[Hanson *et al.*, 1996] Hanson B, Nuttal S and Hoogenraad N. A receptor for the import of proteins into human mitochondria. *Eur J Biochem* 1996, **235**: 750-3

[Harvey *et al.*, 1999] Harvey L, Arnold B, Lawrence ZS, Paul M, David B and James DE. Molecular cell biology (4th edition). New York, WH Freeman and Company, 1999

[Henningsen *et al.*, 2002] Henningsen R, Gale BL, Straub KM and DeNagel DC. Application of zwitterionic detergents to the solubilisation of integral membrane proteins for two-dimensional gel electrophoresis and mass spectrometry. *Proteomics* 2002, **2**: 1479-1488

[Holt *et al.*, 1988] Holt IJ, Harding AE and Morgan-Hughes JA. Deletions of muscle mitochondrial DNA in patients with mitochondrial myopathies**.** *Nature* 1988, **331**: 717-719

[Jha *et al.*, 1998] Jha KK, Banga S, Palejwala V and Ozer HL. SV40-mediated immortalisation. *Exp Cell Res* 1998, **245**: 1-7

[Jensen *et al.*, 1996] Jensen ON, Vorm O and Mann M. Sequence patterns produced by incomplete enzymatic digestion or one-step Edman degradation of peptide mixtures as probes for protein database searches. *Electrophoresis* 1996, **17**: 938-944

[Jung *et al.*, 2000] Jung E, Hoogland C, Chiappe D, Sanchez JC, Hochstrasser DF. The establishment of a human liver nuclei two-dimensional electrophoresis reference map. *Electrophoresis* 2000, **21**: 3483-3487

[Karas *et al.*, 1988] Karas M and Hillenkamp F. Laser desorption ionization of proteins with molecular masses exceeding 10,000 daltons. *Anal Chem* 1988, **60**: 2299-2301

[Katunuma *et al.*, 1966] Katunuma N, Okada M and Nishii Y. Regulation of the urea cycle and TCA cycle by ammonia. *Adv Enzyme Regul* 1966, **4**: 317-36

[Kerner *et al.*, 2000] Kerner J and Hoppel C. Fatty acid import into mitochondria. *Biochim Biophys Acta* 2000, **1486**: 1-17

[Klose, 1975] Klose J. Protein mapping by combined isoelectric focussing and electrophoresis of mouse tissues, a novel approach to testing for induced point mutations in mammals. *Humangenetik* 1975, **26**: 231-243

[Klose *et al.*, 1995] Klose J and Kobalz U. Two-dimensional electrophoresis of proteins: an updated protocol and implications for a functional analysis of the genome. *Electrophoresis* 1995, **16**: 1034-1059

[Klose, 1999a] Klose J. Fractionated extraction of total tissue proteins from mouse and human for 2-D electrophoresis. *Methods Mol Biol* 1999, **112**: 67-85

[Klose, 1999b] Klose J. Large-Gel 2-D electrophoresis. *Methods Mol Biol* 1999, **112**: 147-172

[Klose *et al.*, 2002] Klose J, Nock C, Herrmann M, Stuhler K, Marcus K, Bluggel M, Krause E, Schalkwyk LC, Rastan S, Brown SD, Bussow K, Himmelbauer H and Lehrach H. Genetic analysis of the mouse brain proteome. *Nat Genet* 2002, **30**: 385-393

[Koehler, 2000] Koehler CM. Protein translocation pathways of the mitochondrion. *FEBS Lett* 2000, **476**: 27-31

[Krebs, *et al.*, 1932] Krebs HA and Henseleit K. Untersuchungen über die Harnstoffbildung im Tierkörper. *Hoppe-Seylers Z Physiol Chem* 1932, **210**: 33-66

[Laemmli, 1970] Laemmli UK. Cleavage of structural proteins during the assembly of the head of Bacteriophage T4. *Nature* 1970, **227**: 680-685

[Leonard *et al.*, 2000a] Leonard JV and Schapira AHV. Mitochondrial respiratory chain disorders I: Mitochondrial DNA defects. *Lancet* 2000, **355**: 299-304

[Leonard *et al.*, 2000b] Leonard JV and Schapira AHV. Mitochondrial respiratory chain disorders II: Neurodegenerative disorders and nuclear gene defects. *Lancet* 2000, **355**: 389-394

[Lestienne, 1992] Lestienne P. Mitochondrial DNA mutations in human diseases: a review. *Biochimie* 1992, **74**: 123-130

[Letellier *et al.*, 2000] Letellier T, Durrieu G, Malgat M, Rossignol R, Antoch J, Deshouillers JM, Coquet M, Lacombe D, Netter JC, Pedespan JM, Redonnet-Vernhet I and Mazat JP. Statistical analysis of mitochondrial pathologies in childhood: identification of deficiencies using principal component analysis. *Lab Invest* 2000**, 80**: 1019-1030

[Lopez, 1999] Lopez MF. Advantages of carrier ampholyte IEF. *Methods Mol Biol* 1999, **112**: 109-110

[Lopez *et al.*, 2000] Lopez MF, Kristal BS, Chernokalskaya E, Lazarev A, Shestopalov AI, Bogdanova A and Robvinson M. High-throughput profiling of the mitochondrial proteome using affinity fractionation and automation. *Electrophoresis* 2000, **21**: 3427-3440

[Lopez *et al.*, 2002] Lopez MF and Melov S. Applied proteomics: mitochondrial proteins and effect on function. *Circ Res* 2002, **90**: 380-389

[Lowry *et al.*, 1951] Lowry OH, Rosebrough NJ, Farr AL and Randall RJ. Protein measurement with the folin phenol reagent. *J Biol Chem* 1951, **193**: 265-275

[Madden *et al.*, 1987] Madden EA and Storrie B. The preparative isolation of mitochondria from Chinese hamster ovary cells. *Anal Biochem* 1987, **163**: 350-357

[Maillet *et al.*, 1996] Maillet I, Lagniel G, Perrot M, Boucherie H and Labarre J. Rapid identification of yeast proteins on two-dimensional gel. *J Biol Chem* 1996, **271**: 10263-10270

[Margulis, 1974] Margulis L. On the evolutionary origin and possible mechanism of colchicine-sensitive mitotic movements. *Biosystems* 1974, **6**: 16-36

[Martin *et al.*, 1998] Martin H, Eckerskorn C, Gartner F, Rassow J, Lottspeich F and Pfanner N. The yeast mitochondrial intermembrane space: purification and analysis of two distinct fractions. *Anal Biochem* 1998, **265**: 123-128

[Millar *et al.*, 1994] Millar DG and Shore GC. Mitochondrial Mas70p signal anchor sequence. Mutations in the transmembrane domain that disrupt dimerization but not targeting or membrane insertion. *J Biol Chem* 1994, **269**: 12229-12232

[Navarre *et al.*, 2002] Navarre C, Degand H, Bennett KL, Crawford JS, Mørtz E and Boutry M. Subproteomics: identification of plasma membrane proteins from the yeast Saccharomyces cerevisiae. *Proteomics* 2002, **2**: 1706-1714

[Neitzel, 1986] Neitzel H. A routine method for the establishment of permanent growing lymphoblastoid cell lines. *Hum Genet* 1986, **73**: 320-326

[Nielsen *et al.*, 2002] Nielsen ML, Bennett KL, Larsen B, Moniatte M and Mann M. Peptide end sequencing by orthogonal MALDI tandem mass spectrometry. *Journal of Proteome Research* 2002, **1**: 63-71

[Nordhoff *et al.*, 2001] Nordhoff E, Egelhofer V, Giavalisco P, Eickhoff H, Horn M, Przewieslik T, Theiss D, Schneider U, Lehrach H and Gobom J. Large-gel two-dimensional electrophoresis-matrix assisted laser desorption/ionization-time of flight-mass spectrometry: an analytical challenge for studying complex protein mixtures. *Electrophoresis* 2001, **22**: 2844-2855

[O'Farrell, 1975] O'Farrell PH. High resolution two-dimensional electrophoresis of proteins. *J Biol Chem* 1975, **250**: 4007-4021

[Orth *et al.*, 2001] Orth M and Schapira AHV. Mitochondria and degenerative disorders. *Am J Med Genet* 2001, **106**: 27-36

[Osiewacz, 1997] Osiewacz HD. Genetic regulation of aging. *J Mol Med* 1997, **75**: 715-727

[Osiewacz, 2002] Osiewacz HD. Mitochondrial functions and aging. *Gene* 2002, **286**: 65-71

[Papadopoulou *et al.*, 1999] Papadopoulou LC, Sue CM, Davidson MM, Tanji K, Nishino I, Sadlock JE, Krishna S, Walker W, Selby J, Glerum DM, Coster RV, Lyon G, Scalais E, Lebel R, Kaplan P, Shanske S, De Vivo DC, Bonilla E, Hirano M, DiMauro S and Schon EA. Fatal infantile cardioencephalomyopathy with COX deficiency and mutations in SCO2, a COX assembly gene. *Nat Genet* 1999, **23**: 333-337

[Parker, 2000] Parker JC. Commentary: human mitochondrial cytopathies. *Ann Clin Lab Sci* 2000, **30**: 159-162

[Pennisi, 1997] Pennisi E. Laboratory workhorse decoded. *Science* 1997, **277**: 1432-1434

[Perrot *et al.*, 1999] Perrot M, Sagliocco F, Mini T, Monribot C. Schneider U, Shevchenko A, Mann M, Jenö P and Boucherie H. Two-dimensional gel protein database of Saccharomyces cerevisiae (update 1999). *Electrophoresis* 1999, **20**:2280-2298

[Pesole *et al.*, 2000] Pesole G, Gissi C, Catalano D, Grillo G, Licciulli F, Liuni S, Attimonelli M and Saccone C. MitoNuc and MitoAln: two related databases of nuclear genes coding for mitochondrial proteins. *Nucleic Acids Res* 2000, **28**: 163-165

[Petruzzella *et al.*, 1998] Petruzzella V, Tiranti V, Fernandez P, Ianna P, Carrozzo R and Zeviani M. Identification and characterization of human cDNAs specific to BCS1, PET112, SCO1, COX15 and COX11, five genes involved in the formation and function of the mitochondrial respiratory chain. *Genomics* 1998, **54**: 494-504

[Polyak *et al.*, 1998] Polyak K, Li YB, Zhu H, Lengauer C, Willson JK, Markowitz SD, Trush MA, Kinzler KW and Vogelstein B. Somatic mutations of the mitochondrial genome in human colorectal tumours. *Nat Genet* 1998, **20**: 291-293

[Rabilloud, 1990] Rabilloud T. Mechanisms of protein silver staining in polyacrylamide gels: a 10 year synthesis. *Electrophoresis* 1990, **11**: 785-794

[Rabilloud, 1992] Rabilloud T. A comparison between low background silver diammine and silver nitrate protein stains. *Electrophoresis* 1992, **13**: 429-439

[Rabilloud, 1996] Rabilloud T. Solubilization of proteins for electrophoretic analyses. *Electrophoresis* 1996, **17**: 813-829

[Rabilloud *et al.*, 1998] Rabilloud T, Kieffer S, Procaccio V, Louwagie M, Courchesne PL, Patterson SD, Martinez P, Garin J and Lunardi J. Two-dimensional electrophoresis of human placental mitochondria and protein identification by mass spectrometry: toward a human mitochondrial proteome. *Electrophoresis* 1998, **19**: 1006-1014

[Rabilloud *et al.*, 1999] Rabilloud T, Blisnick T, Heller M, Luche S, Aebersold R, Lunardi J and Braun-Breton C. Analysis of membrane proteins by two-dimensional electrophoresis: comparison of the proteins extracted from normal or Plasmodium falciparum- infected erythrocyte ghosts. *Electrophoresis* 1999, **20**: 3603-3610

[Rabilloud *et al.*, 2002] Rabilloud T, Strub JM, Carte N, Luche S, Van Dorsselaer A, Lunardi J, Giegé R and Florentz C. Comparative proteomics as a new tool for exploring human mitochondrial tRNA disorders. *Biochemistry* 2002, **41**: 144-150

[Rajapakse *et al.*, 2001] Rajapakse N, Shimizu K, Payne M and Busija D. Isolation and characterization of intact mitochondria from neonatal rat brain. *Brain Res Brain Res Protoc* 2001, **8**: 176-83

[Roberti *et al.*, 1997] Roberti M, Musicco C, Loguercio Polosa P, Gadaleta MN, Quagiariello E and Cantatore P. Purification and characterisation of a mitochondrial, single-stranded-DNA-binding protein from paracentrotus lividus eggs. *Eur J Biochem* 1997, **247**: 52-58

[Rohr *et al.*, 1976] Rohr HP, Luthy J, Gudat F, Oberholzer M, Gysin C, Stalder G and Bianchi L. Stereology: a new supplement to the study of human liver biopsy specimens. *Prog Liver Dis* 1976, **5**: 24-34

[Schapira *et al.*, 1999] Schapira AH and Cock HR. Mitochondrial myopathies and encephalomyopathies. *Eur J Clin Invest* 1999, **29**: 886-898

[Shevchenko *et al.*, 1996a] Shevchenko A, Wilm M, Vorm O and Mann M. Mass spectrometric sequencing of proteins from silver-stained polyacrylamide gels. *Anal Chem* 1996, **68**: 850-858

[Shevchenko *et al.*, 1996b] Shevchenko A, Jensen ON, Podtelejnikov AV, Sagliocco F, Wilm M, Vorm O, Mortensen P, Shevchenko A, Boucherie H and Mann M. Linking genome and proteome by mass spectrometry: Large-scale identification of yeast proteins from two-dimensional gels. *Proc Natl Acad Sci USA* 1996, **93**: 14440-14445

[Shore *et al.*, 1995] Shore GC, McBride HM, Millar DG, Steenaart NA and Nguyen M. Import and insertion of proteins into the mitochondrial outer membrane. *Eur J Biochem* 1995, **227**: 9-18

[Sims, 1990] Sims NR. Rapid isolation of metabolically active mitochondria from rat brain and subregions using Percoll density gradient centrifugation. *J Neurochem* 1990, **55**: 689-707

[Smeitink *et al.*, 2001] Smeitink J, van den Heuvel L and DiMauro S. The genetics and pathology of oxidative phosphorylation. *Nat Rev Genet* 2001, **2**: 342-352

[Smith *et al.*, 1985] Smith PK, Krohn RI, Hermanson GT, Mallia AK, Gartner FH, Provenzano MD, Fujimoto EK, Goeke NM, Olson BJ and Klenk DC. Measurement of protein using bicinchoninic acid. *Anal Biochem* 1985, **150**: 76-85

[Smithies *et al.*, 1956] Smithies O and Poulik MD. Two-dimensional Electrophoresis of serum proteins. *Nature* 1956, **177**: 1033

[Stoscheck, 1990] Stoscheck CM. Increased uniformity in the response of the Coomassie blue G protein assay to different proteins. *Anal Biochem* 1990, **184**: 111-116

[Strack *et al.*, 2001] Strack A, Duffy CF, Malvey M and Arriaga EA. Individual mitochondrion characterization: a comparison of classical assays to capillary electrophoresis with laser-induced fluorescence detection. *Anal Biochem* 2001, **294**: 141-147

[Stryer, 1995] Stryer L. Biochemistry (4th edition). New York, WH Freeman and Company,1995

[Sue *et al.*, 2000] Sue CM and Schon EA. Mitochondrial respiratory chain diseases and mutations in nuclear DNA: a promising start? *Brain Pathol* 2000, **10**: 442-450

[Swain *et al.*, 1995] Swain M and Ross NW. A silver stain protocol for proteins yielding high resolution and transparent background on sodium dodecyl sulfate-polyacrylamide gels. *Electrophoresis* 1995, **16**: 948-951

[Switzer, 1979] Switzer RC, Merril CR and Shifrin S. A highly sensitive silver stain for detecting proteins and peptides in polyacrylamide gels. *Anal Biochem* 1979, **98**: 231-237

[Tiranti *et al.*, 1998] Tiranti V, Hoertnagel K, Carrozzo R, Galimberti C, Munaro M, Granatiero M, Zelante L, Gasparini P, Marzella R, Rocchi M, Bayona-Bafaluy MP, Enriquez JA, Uziel G, Bertini E, Dionisi-Vici C, Franco B, Meitinger T and Zeviani M. Mutations of SURF-1 in Leigh disease associated with cytochrome c oxidase deficiency. *Am J Hum Genet* 1998, **63**: 1609-1621

[Wallace *et al.*, 1988] Wallace DC, Singh G, Lott MT, Hodge JE, Schur TG, Lezza AMS, Elsas LJ and Nikoskelainen EK. Mitochondrial DNA mutation associated with Leber's hereditary optic neuropathy. *Science* 1988, **242**: 1427-1430

[Wallace *et al.*, 1999] Wallace DC, Brown MD and Lott MT. Mitochondrial DNA variation in human evolution and disease. *Gene* 1999, **238**: 211-230

[Weber *et al.*, 1969] Weber K and Osborn M. The reliability of molecular weight determinations by dodecyl sulfate-polyacrylamide gel electrophoresis. *J Biol Chem* 1969, **244**: 4406-4412

[Wilichowski *et al.*, 1997] Wilichowski E, Grüters A, Kruse K, Rating D, Beetz R, Korenke GC, Ernst BP, Christen HJ and Hanefeld F. Hypoparathyroidism and deafness associated with pleioplasmic large scale rearrangements of the mitochondrial DNA: a clinical and molecular genetic study of four children with Kearns-Sayre syndrome. *Pediatr Res* 1997, **41**, 193-200

[Wilkins *et al.*, 1996] Wilkins MR, Sanchez JC, Williams KL and Hochstrasser DF. Current challenges and future applications for protein maps and post-translational vector maps in proteome projects. *Electrophoresis* 1996, **17**: 830-838

[Wilkins *et al.*, 1999] Wilkins MR, Gasteiger E, Bairoch A, Sanchez JC, Williams KL, Appel RD and Hochstrasser DF. Protein identification and analysis tools in the ExPASy Server. *Methods Mol Biol* 1999, **112**: 531-552

[Zeviani *et al.*, 1998] Zeviani M, Tiramti V and Piantadosi C. Mitochondrial disorders. *Medicine* 1998,**77**: 59-72

[Zeviani *et al.*, 1999] Zeviani M, Corona P, Nijtmans L and Tiranti V. Nuclear gene defects in mitochondrial disorders. *Ital J Neurol Sci* 1999, **20**: 401-408

ACKNOWLEDGMENTS

The present dissertation project has been performed at the “Klinik für Pädiatrie mit Schwerpunkt Neurologie” (Director: Prof. Dr. C. Hübner) of the Medical Faculty Charité of the Humboldt-University Berlin and in collaboration with the SFB 577 (Partial project TP4 *Genetic variability of mitochondrial disorders*) at the “Institut für Humangenetik der Charité” (Director: Prof. Dr. K. Sperling). I thank both directors for the opportunity to work and study in their laboratories.

I would like to express my gratitude to the Friedrich-Ebert-Stiftung and to Ms Holona who provided the opportunity for me to come to Germany and supported me financially for the last three years.

I would also like to show my sincere respect and thankfulness to PD Dr. Markus Schuelke for the supervision of this work. His kindness, patience, thoughtfulness, continuous support and encouragement made this work a reality. Moreover, under his guidance I also comprehended the spirit of research and discovery, which I will benefit my future work.

I thank Dipl. Ing. Sandra Techritz for the introduction into the field of MALDI-TOF mass spectrometry and her kind co-operation for protein identification. I thank for her patience and warm-hearted help, especially for the inspired discussions and her suggestions. My thanks also go to Dr. Sophie Häbel for the fruitful co-operation, in whose lab the MALDI-TOF-MS and MALDI-QTOF-MS measurements were performed.

Furthermore, I am grateful to all the members of Professor Dr. Dr. J. Klose’s group for their friendly help. Especially I thank Yvonne Kläre for her patient and clear introduction into the 2D-electrophoresis techniques. I would also like to show my deep respect to Professor Dr. Dr. J. Klose himself for his guidance in the field of 2D-electrophoresis and his valuable suggestions.

I would like to acknowledge the contribution of Antje Gerlach and PD Dr. Heidemarie Neitzel, who performed the cultivation of EBV-transformed lymphoblastoid cell lines.

I also like to thank Petra Schrade at Prof. Dr. S. Bachmann’s laboratory who contributed all the electron microscopic photographs presented in this work.

I like to thank Anke Horn and Angelika Zwirner for their excellent technical assistance.

I acknowledge all my colleagues and friends for their useful advice and support throughout the work. Special thanks go to my best friends Christine Gerstenfeld and Lei Mao, whose warm-hearted help and support are never forgot through my life.

Finally, I would like to show my deep love and gratitude to my family, my parents and parents-in-law. Their immense love, encouragement and support animated me to finish this work.

CURRICULUM VITAE

PERSONAL DATA

Family name	Xie	**Address**	"Klinik für Pädiatrie m. S. Neurologie" of
First name	Jing		the Charité, Humboldt-University Berlin
Birthday	06, Jan, 1970		Augustenburger Platz 1
Place of birth	Beijing, China		13353 Berlin Germany
Citizenship	Chinese	**E-mail**	cxjing@yahoo.com

EDUCATION

- **1999 – 2002** Dissertation project at the Neuropediatric Department of the Charité, Humboldt University Berlin
  Subject: Proteome analysis of mitochondrial disorders.
  Thesis: Establishment of a two-dimensional electrophoresis map of human mitochondrial proteins
  Supervisor: PD Dr. Markus Schuelke
- **1988-1995** Master of clinical medicine of Beijing Medical University, Beijing, P. R. China
  Specialization: Pediatric Neurology
  Thesis: The Neuropsychological evaluation of children with epilepsy by using human drawing tests
  Advisor: Prof. Dr. Qing Lin (Clinical Medicine, Neuropediatrics), Prof. Dr. Shi Cheng (Basic Medicine, Cell Biology)

RESEARCH EXPERIENCE

- **2000-present** Establishment of a 2D electrophoresis map of human mitochondrial proteins — a new strategy to diagnose mitochondrial disorders.
- **1998-1999** Epileptic children with attention-deficit-hyperkinetic-disease — Analysis with computerized T.O.V.A. (Test of Variable Attention)
- **1996-1999** Research in pseudo seizures of children
- **1996-1998** The prognosis of cured epileptic children (100 cases)
- **1993-1995** The neuropsychological evaluation of epileptic children
- **1992-1993** Research on protective function of metal sulfur protein on murine myocardial cells

CLINICAL EXPERIENCE

- **1998-1999** Pediatrician in charge of neonatology at the Pediatric Department of the First Teaching Hospital of Beijing Medical University
- **1997-1998** Chief of residents at the same Department
- **1993-1997** Residency at the at the same Department
- **1992-1993** Internship

PUBLICATIONS

Xie J, Kläre Y, Neitzel H, Klose J, Schuelke M. Towards a novel strategy to identify mitochondrial diseases. *Neuropediatrics* 2002, **33**: A11 **This Poster has won a poster prize at the 28th Annual Meeting of the Gesellschaft für Neuropädiatrie**

Xie J, Lin Q. Nonepileptic tonicoid spasm (case report of 15 children). *Chinese Pediatrics Journal* 1999, **37**: 240

Xie J, Lin Q. The prognosis of epilepsy of cured epileptic children. *Chinese Pediatrics Journal* 1999, **37**: 166-168

Xie J, Lin Q. The neuropsychological state of epileptic children and human figure drawing tests. pp445-466, in: *Modern Diagnosis and Therapy of Children with Epilepsy*, Tianjin Science and Technology Publishing House, 1996

Xie J, Lin Q. The neuropsychological evaluation of epileptic children by using human figure drawing tests. *Chinese Pediatrics Journal* 1996, **34**: 77-80. **This paper has won the award as "Excellent Paper" by the Chinese Medical Association**

Xie J, Bao XH. Analysis of misdiagnosis of botulism (case report of two children). *Clinical Applied Pediatrics Journal* 1995,**10**:178.

Cheng S, **Xie J** *et al*. Initial research on protective function of metal sulfur protein on murine myocardial cells. *Beijing Medical University Transactions* 1994.

ERKLÄRUNG

Hiermit erkläre ich, Jing XIE, geboren am 06.01.1970 in Beijing (China), an Eides Statt, daß meine Dissertation mit dem Thema *"Establishment of a two-dimensional electrophoresis map of human mitochondrial proteins"* von mir selbst und ohne Hilfe Dritter verfaßt wurde, auch in Teilen keine Kopie anderer Arbeiten darstellt und die benutzten Hilfsmittel sowie die Literatur vollständig angegeben sind. Ich habe mich anderwärtig nicht um einen Doktorgrad beworben und besitze einen entsprechenden Doktorgrad nicht. Ich erkläre die Kenntnisnahme der dem Verfahren zugrunde liegenden Promotionsordnung der Medizinischen Fakultät Charité der Humboldt-Universität zu Berlin.

Berlin, den _____

_____

Unterschrift